LIITE 1

Labtium/Aalto-yliopisto, Mustalipeän ei-Newtonilaisuus ja pisaroituminen – projektin tulokset

Mustalipeän ei-Newtonilaisuus

Ari Kankkunen, Jorma Torniainen, Mika Järvinen

Aalto-yliopisto, Insinööritieteiden korkeakoulu,
Energiatekniikan laitos
Labtium Oy

1 Johdanto
1.1 Tausta
1.2 Viskositeetti
1.3 Mustalipeän viskositeettiin vaikuttavat tekijät
1.4 Mustalipeän ei-Newtonilaisuutta kuvaavat yhtälöt
2 Kokeet
2.1 Näytteenotto
2.2 Viskositeettinmittausmenetelmä
2.3 Koelipeät
2.4 Viskositeetit leikkausnopeuden muuttuessa
2.5 Viskositeettimittauksen kalibrointi
2.6 Kapillaariviskometri
2.7 Kapillaariviskometrin kalibrointi
3 Mustalipeän käsittelyn vaiheet
3.1 Haihdutin
3.2 Pumput
3.3 Putkistot
3.4 Suutinputki
3.5 Lusikka
3.6 Kalvo, rihmat ja pisarat
4 Pisaran muodonmuutos
4.1 Simulointi OpenFoam-ohjelmalla
5 Johtopäätökset
5.1 Ei-Newtonilainen viskositeetti
5.2 Tulosten merkitys
5.3 Jatkotutkimustarpeita
Lähdeluettelo
Liite 1 Havulipeän viskositeettikäyrät
Liite 2 Lehtipuulipeän viskositeettikäyrät
Liite 3 Sekalipeän viskositeettikäyrät
Liite 4 Eukalyptuslipeän viskositeettikäyrät
Liite 5 Kemialliset analyysit
Liite 6 Kalibrointiöljyn N4000 ominaisuudet
Liite 7 Kalibrointiöljyn N75 ominaisuudet

Mustalipeä on yleensä Newtonilainen neste, joskus leikkausoheneva

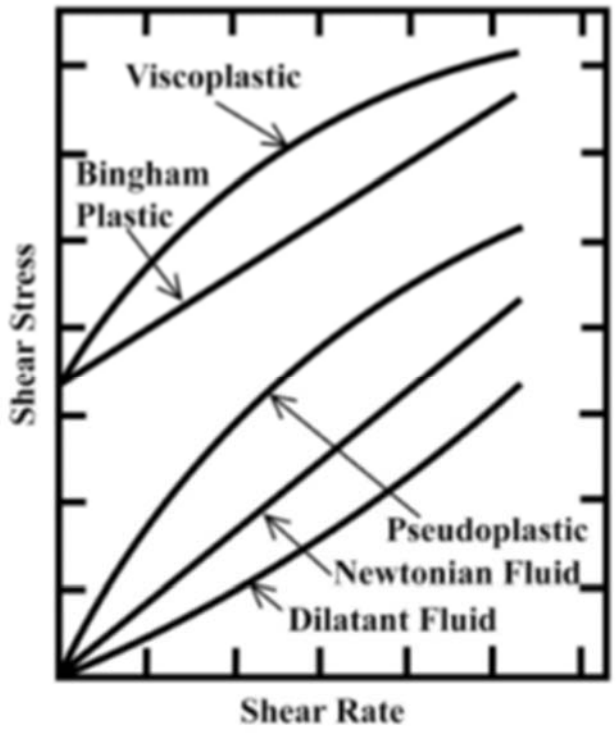

$$\tau = K\dot{\gamma}^n$$

Ei-Newtonilaisen polymeerin viskositeetti

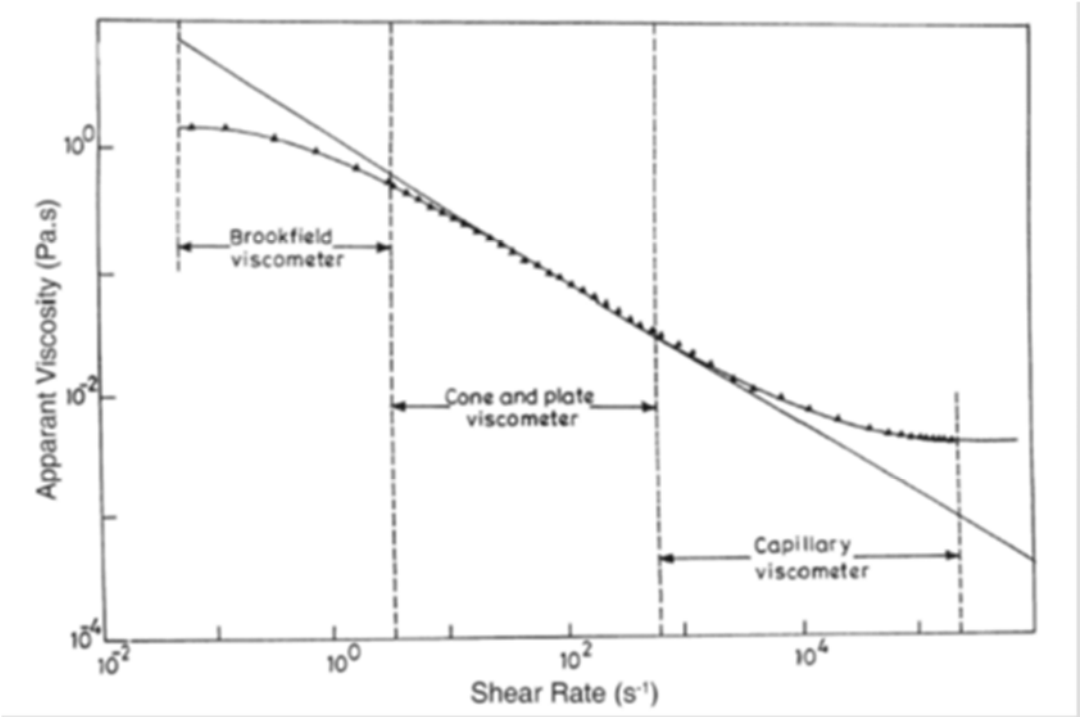

Leikkausohenemisen syyt

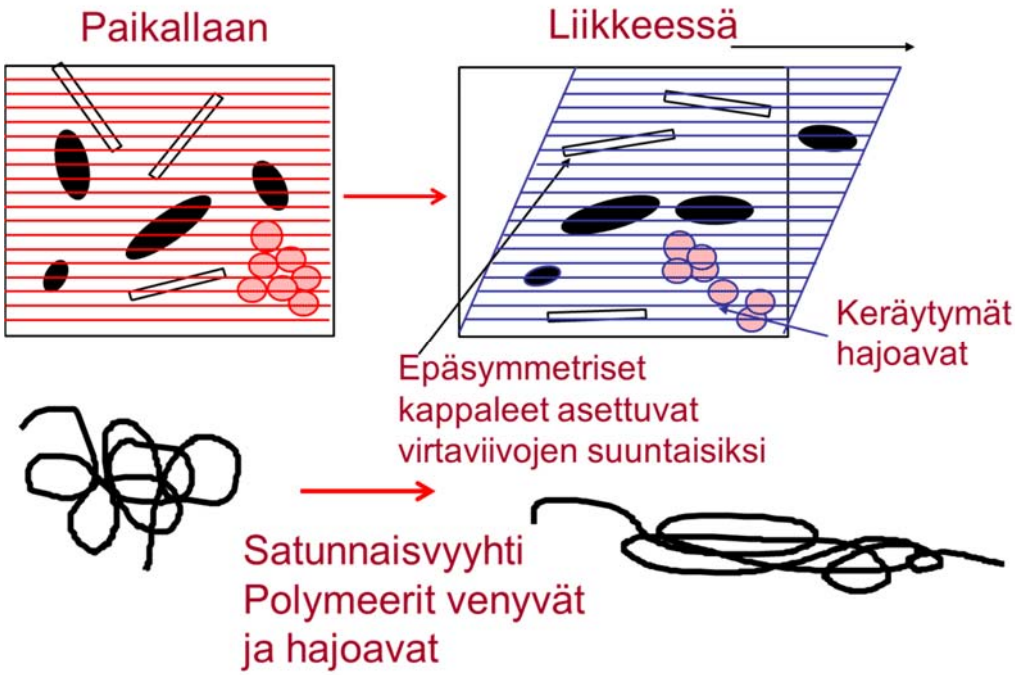

Mustalipeän viskositeetti Newtonilainen

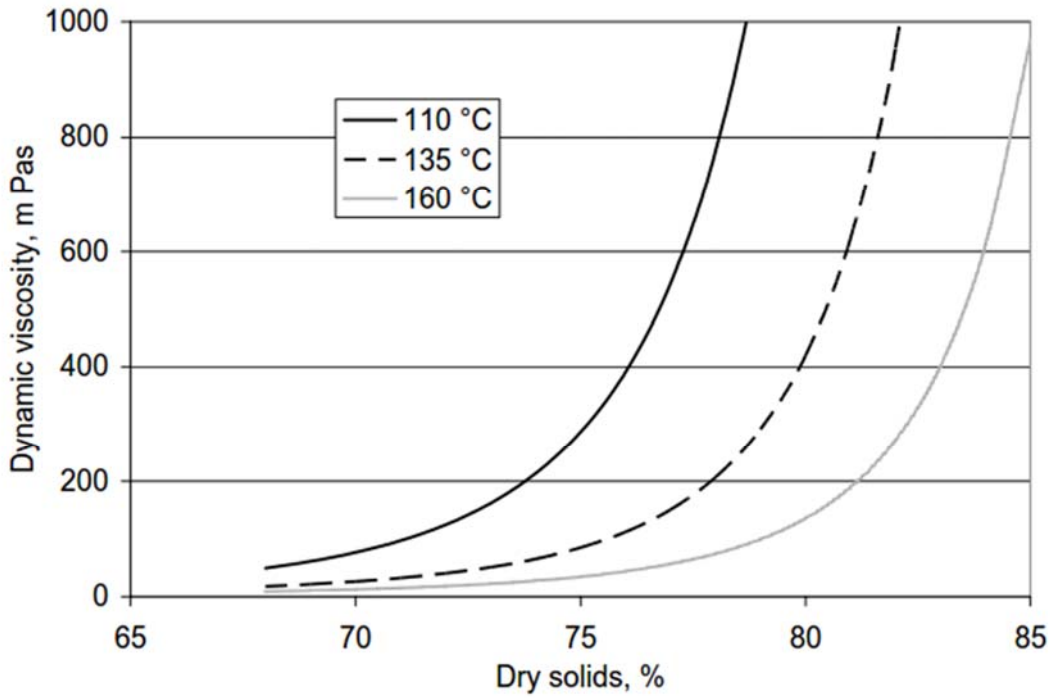

Mustalipeän viskositeetti Zaman&Fricke 1991

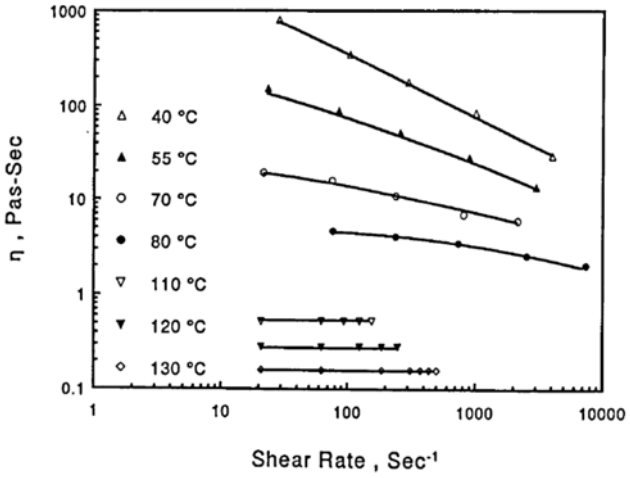

Kuiva-ainepitoisuudella 75.4 %

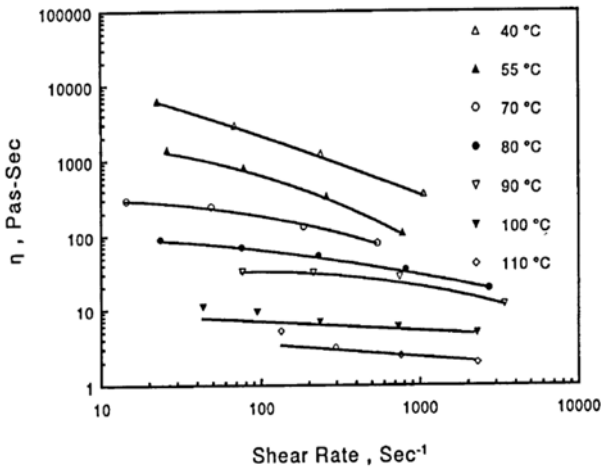

Kuiva-ainepitoisuudella 84.1 %

Mustalipeän viskositeetti

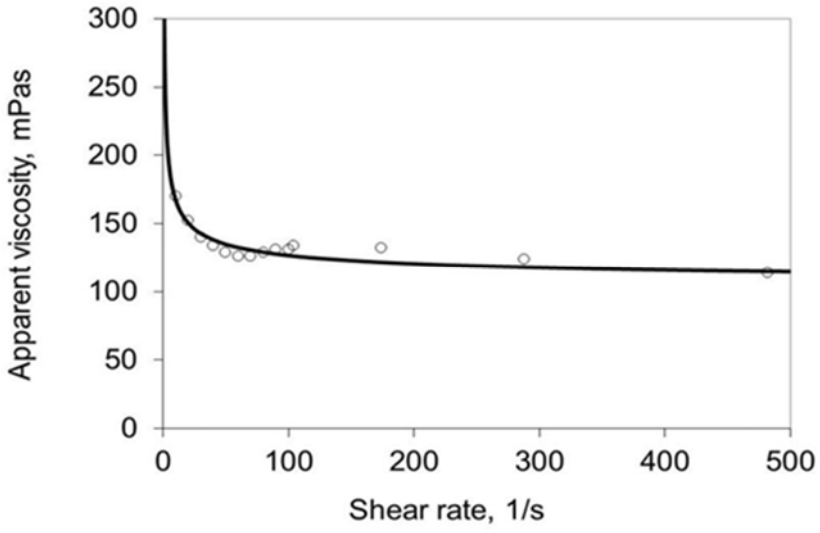

$$\mu = \mu_{\infty}\left(1 + a\dot{\gamma}^{-0.5}\right)^2$$

Järvinen, M., Kankkunen, A., Virtanen, R., Miikkulainen, P., Heikkilä,. V.P, A One-Dimensional 2-Phase Flow Model and Experimental Validation for a Flashing Viscous Liquid in a Splash Plate Nozzle, Atomization and Sprays, to be published 2015.

Koelipeät

Lipeälaatu	Ruiskutus	Kuiva-ainepitoisuus			Kiehumis pisteen
	lämpötila	Tehdas	Lab. Normaali	Lab. Paineistettu	nousu
	°C	%	%	%	°C
Havu	134.6	75.7	73.7	73.1	18.3
Lehtipuu	126	70	73.1	71.2	15
Seka	144	81.8	81.8	82.7	28
Eukalyptus	-	-	77.8	-	-

				Rauma 20.2.2014	*Kymi 26.3.2014*	*Äänekoski 25.4*
Kuiva-aine		%	SCAN-N 22:77	73.1	82.7	71.2
Kuiva-aineen						
tuhka		%	KCL 59:83	56.3	58.2	56.3
hiili	C	%	ASTM D 5373	31.1	28.9	30.5
vety	H	%	ASTM D 5373	4.4	3.4	3.7
typpi (Kjeldahl)	N	%	SFS 5505 modif.	0.062	0.073	0.116
natrium	Na	%	SCAN-N 37:98	21.7	22.1	21.6
kalium	K	%	SCAN-N 37:98	2.7	3.4	2.8
alumiini	Al	mg/kg	SCAN-N 38:10	32	23	22
barium	Ba	mg/kg	SCAN-N 38:10	4.4	8.0	5.6
kalsium	Ca	mg/kg	SCAN-N 38:10	360	230	120
kupari	Cu	mg/kg	SCAN-N 38:10	2.5	< 1	< 1
rauta	Fe	mg/kg	SCAN-N 38:10	17	12	8.7
magnesium	Mg	mg/kg	SCAN-N 38:10	390	160	190
mangaani	Mn	mg/kg	SCAN-N 38:10	63	60	66
fosfori	P	mg/kg	SCAN-N 38:10	89	120	130
pii	Si	mg/kg	SCAN-N 38:10	290	260	180
vanadiini	V	mg/kg	SCAN-N 38:10	15	< 5	15
sinkki	Zn	mg/kg	SCAN-N 38:10	15	29	24
rikki	S	%	SCAN-N 38:10			
kloori	Cl	%	AOX-laite	0.2	0.2	0.2
karbonaatti	$CO_3^=$	%	SCAN-N 32:98	5.2	6.2	6.1
sulfaatti	$SO_4^=$	%	KCL 71:81	7.2	7.0	6.3
sulfidi	$S^=$	%	SCAN-N 31:94	3.6	2.7	2.3
jäännösalkali	NaOH	%	SCAN-N 33:94	4.6	4.3	3.2
polysakkaridit		%	HPAEC-PAD	1.2	1.6	4.0
epäorg./org.-suhde			KCL 61:83	0.67	0.71	0.64
kalorimetrinen lämpöarvo		MJ/kg	Autom. kalorimetri	13.18	12.20	12.73
tehollinen lämpöarvo		MJ/kg				
Näytteen tehollinen lämpöarvo		MJ/kg				
Dynaaminen viskositeetti		mPa*s				

Viskometri

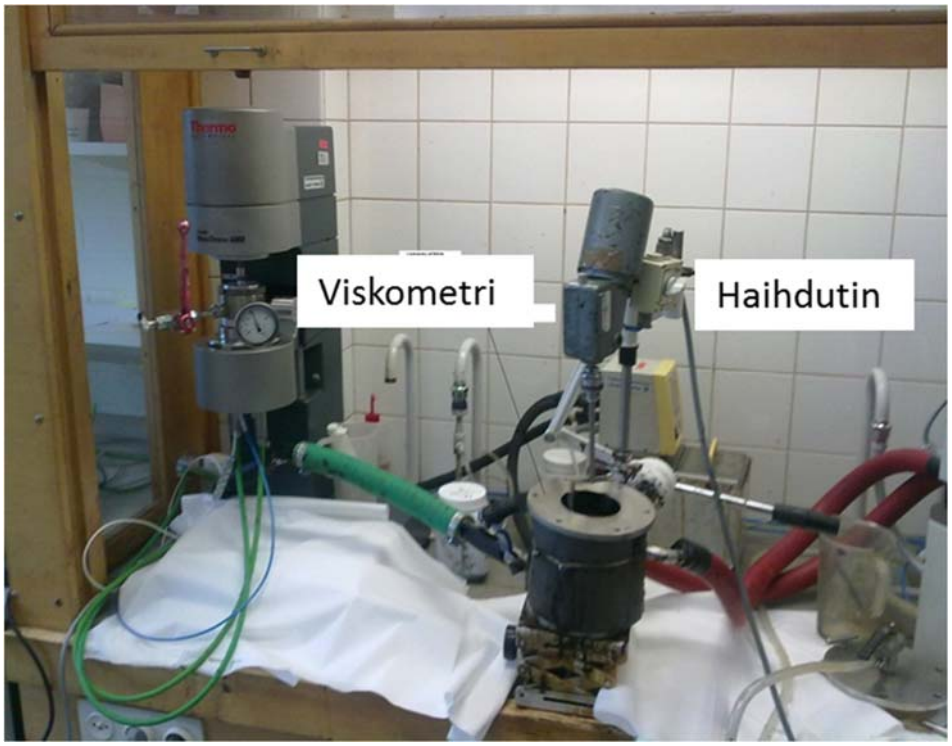

Mustalipeän viskositeetti leikkausnopeuden muuttuessa

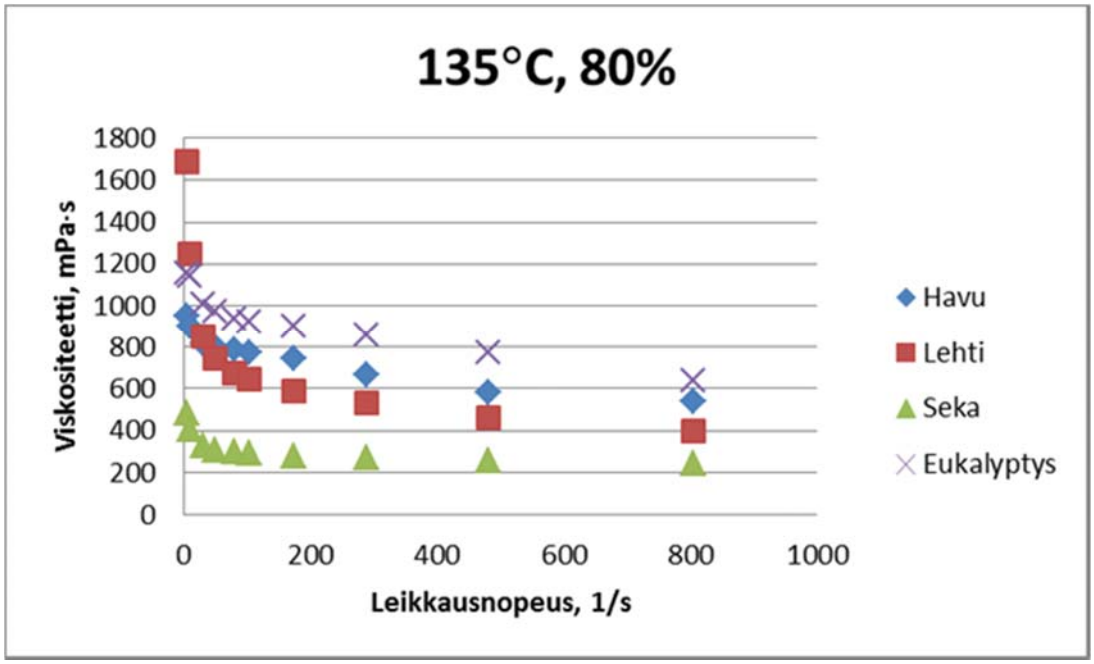

Kalibrointi

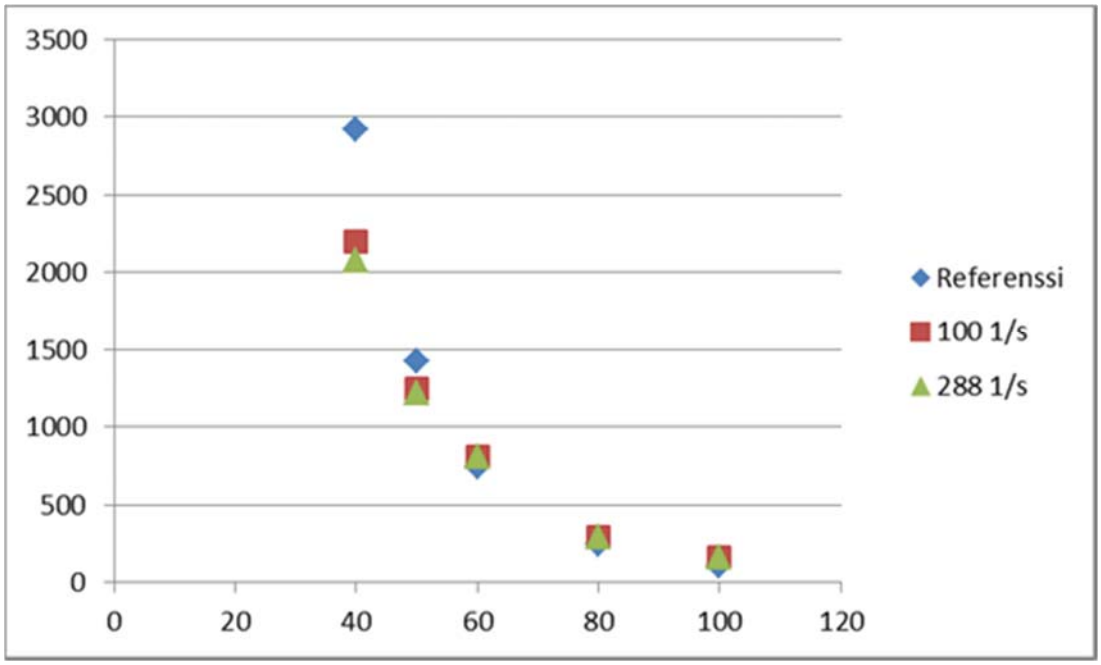

Viskositeetti lämpötilan muuttuessa

Lämpötila, °C	Sertifioitu arvo mPas	Mitattu arvo, 100 1/s mPas	Mitattu arvo, 288 1/s mPas	Ero 100 1/s mPas	Ero 288 1/s mPas	Ero 100 1/s %	Ero 288 1/s %
40	2921	2195	2080	-726	-841	-24.9	-28.8
50	1423	1245	1218	-178	-205	-12.5	-14.4
60	744.7	810	802	65.3	57.3	8.8	7.7
80	247.6	290	288	42.4	40.4	17.1	16.3
100	102.1	165	158	62.9	55.9	61.6	54.8

Kapillaariviskometri

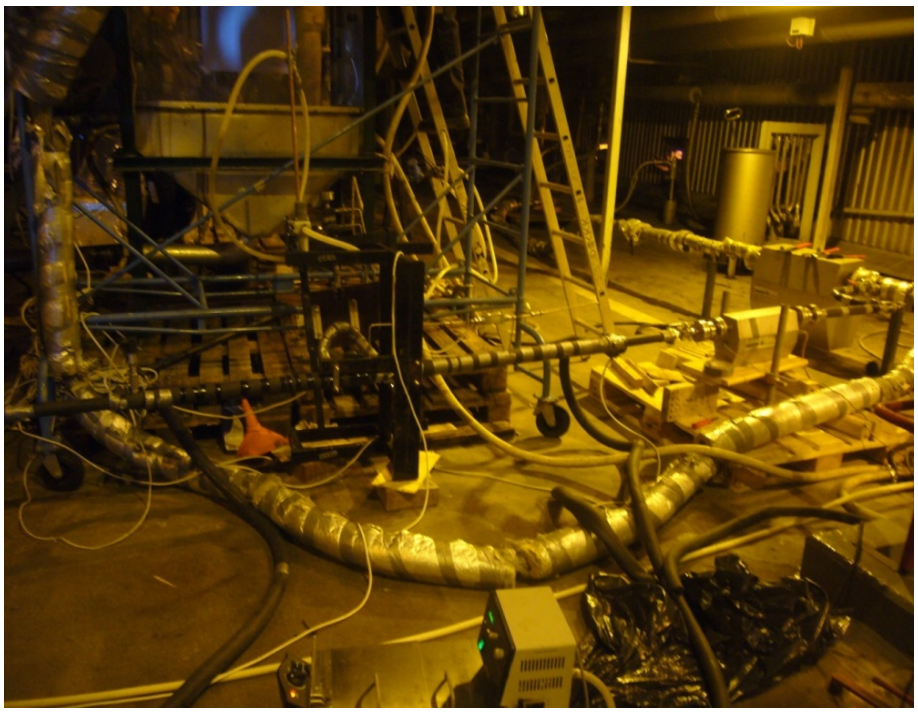

Mustalipeän viskositeetti

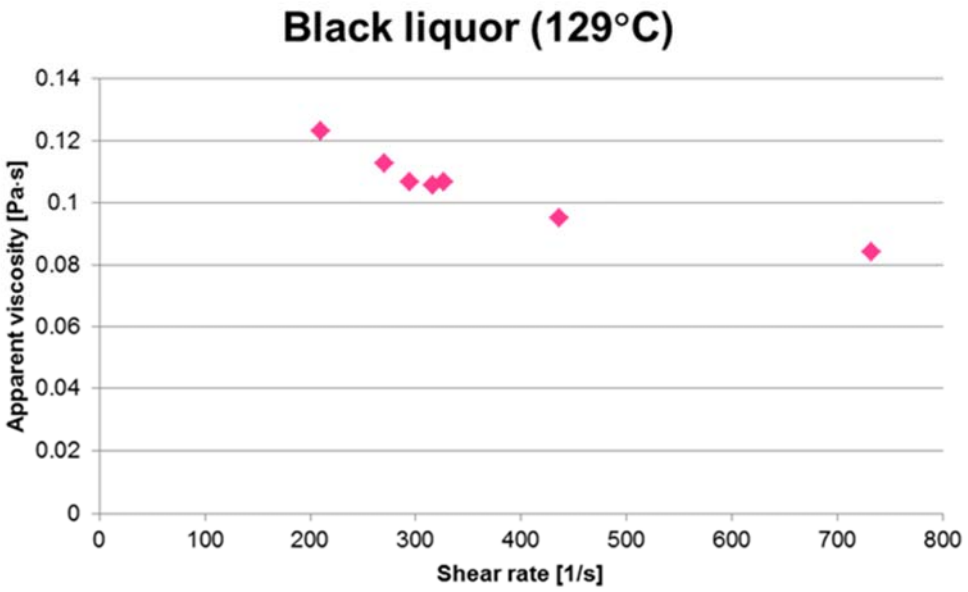

Havulipeä, kuiva-ainepitoisuus 73.1 %

8 mm pisarat 300 mPas 0-0.6 s

- 8 mm ei suurta eroa
- 15 m/s nopeudella pisarat valmiit 9 m päässä

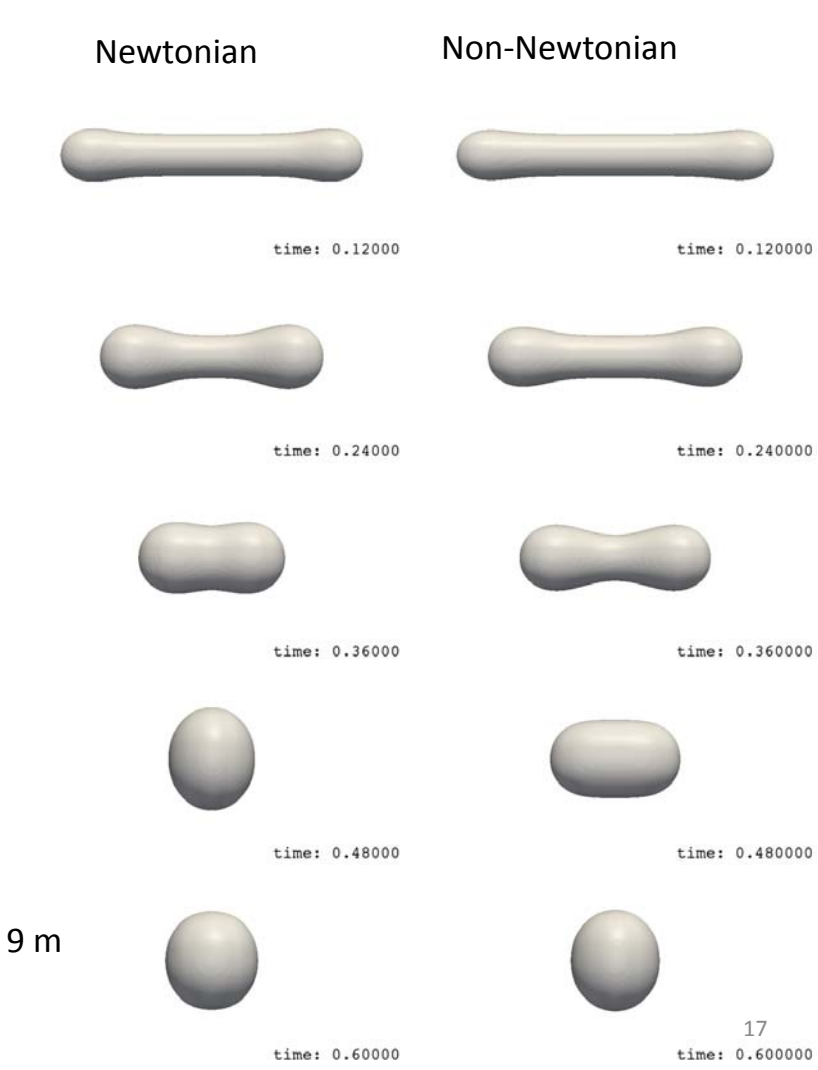

Aalto University
School of Engineering

8 mm pisaran muodostuminen, vertailu numeroina

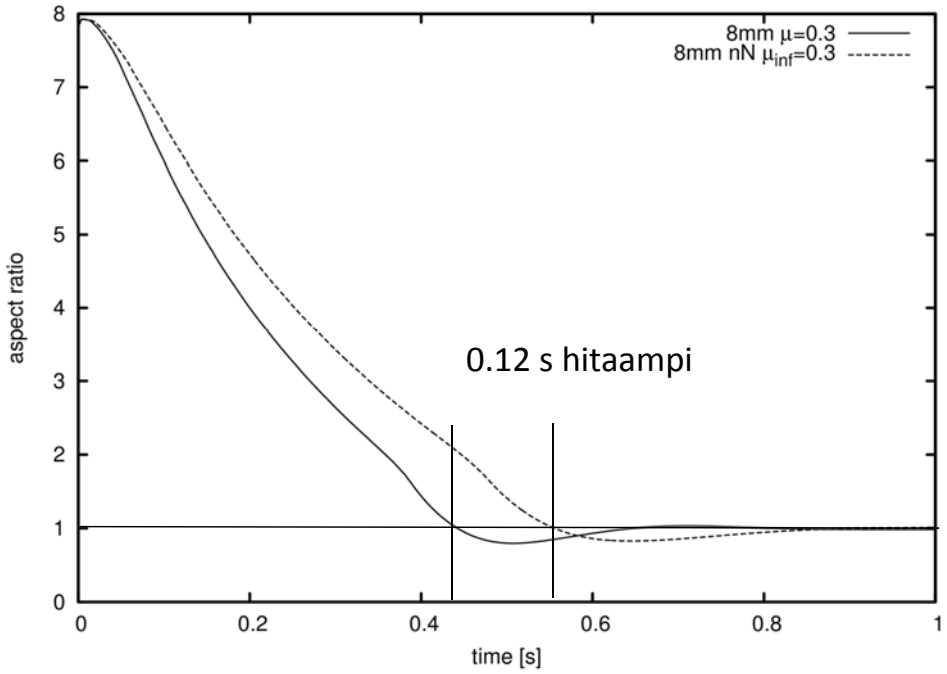

Aalto University
School of Engineering

Johtopäätökset

- Kaikki lipeät ei-Newtonilaisia pienillä leikkausnopeuksilla
- Ei merkitystä pumpuissa tai putkistoissa
- Haihduttimen loppuosissa ja etenkin pisaroitumiselle tulipesässä ei-Newtonilaisuus tärkeää

Jatkotutkimus

- Viskometrin toiminta varmistettava
- Pisaran muodonmuutoksen mallinnusta jatkettava
- Malli validoitava

LIITE 2

ÅA, CFD Modeling of Reduced Lignin Black Liquor Combustion – projektin tulokset

Executive Summary and Conclusions – CFD Modeling of Reduced Lignin Black Liquor Combustion

Markus Engblom, Nikolai DeMartini

21 January 2015

Lignin removal by precipitation using CO_2 is a technology that is commercially available, and mills are starting to implement it. They are doing this either to obtain the lignin or as a means of reducing the load to the recovery boiler. Lignin removal will affect both the heating value of the black liquor and the amount of char carbon in the black liquor during combustion. The heating value was calculated to change from 13.2 MJ/kg d.s. for the original black liquor to 11.6 MJ/kg d.s. for the 20% reduced lignin case. Thus the HHRR was calculated to be 2.9, 2.6 and 2.3 MW/m^2 on a LHV basis for the base case, 10% reduced lignin and 20% reduced lignin cases respectively. The calculated adiabatic temperatures are 1240, 1170 and 1130 °C respectively. The amount of fixed carbon (combustible carbon in the char) was found to decrease in combustion experiments with three reduced lignin black liquors and the fraction of fixed carbon to the model was 14.3, 10.3 and 7.4% of the total dry solids for the base case, 10% reduced lignin and 20% reduced lignin cases respectively, while the volatile fraction (kg volatiles/kg d.s.) was assumed to remain the same. This is a key assumption because in addition to reducing the amount of organic material to the boiler, the fraction of that material that forms char is reduced, thus the amount of char to the walls and bed is reduced both because of the reduction in organics to the boiler and the reduction in the amount of char formed. From a practical perspective, the firing changes needed are more significant than if the removal of lignin only affected the total amount of organics to the boiler.

Thus, spraying conditions and/or air distribution will need to be adjusted to maintain the lower furnace temperature and to maintain carbon on the bed, which are needed for high reduction efficiency and low SO_2. Seven different cases were run for a CFD model of the WisaForest recovery boiler. The seven cases were:

- Case 1. Base case at 100% MCR, 3% excess O_2 (wet gases)
- Cases 2 & 3. 10% and 20% lower lignin with the same air distribution, but total air reduced to maintain 3% excess O_2 (wet gases). These runs provide information about carbon distribution in the boiler.
- Cases 4 & 5. 10% and 20% lower lignin with the same total air as cases 2 & 3, but with air redistributed to balance the carbon distribution.
- Cases 6 & 7. 10% and 20% lower lignin with the mean droplet size increased to increase the carbon to the lower furnace to balance the air in cases 2 & 3.

Without changing the air distribution or firing conditions (same droplet size distribution), the removal of lignin was calculated to result in a significant deficit in carbon delivery to the lower furnace. The calculated deficit was 13% and 37% (carbon that would be converted compared to carbon fed) for 10% and 20% lignin removal respectively (cases 2 & 3). To balance the carbon by changing the air distribution (less air to lower furnace, cases 4 & 5) or droplet size distribution (larger droplets, cases 6 & 7) alone required significant changes to these parameters, Table 1.

Table 1. Air distribution and average droplet size distribution for cases 1 and 4-7. In 4&5 the air distribution was adjusted and in 6-7 the air distribution was maintained, but the mean droplet size was adjusted.

Parameter	Case 1	Case 4	Case 5	Case 6	Case 7
Lignin reduction	0%	10%	20%	10%	20%
Primary Air	22	20	15	22	22
Secondary Air	43	40	30	43	43
Tertiary Air	35	40	55	35	35
Mean droplet size (mm)	5.7	5.7	5.7	12.5	23
Excess Temperature (°C)	18.4	18.4	18.4	13.7	6.5

Even for a 10% reduction in lignin, the calculations indicate that both air distribution and spraying conditions will need to be adjusted. To get more carbon to the lower furnace, spraying angle or nozzle will likely need to be changed, especially at lignin removal levels higher than 10%. It does not appear that adjusting black liquor firing temperature alone will be sufficient to maintain the carbon to the bed.

The calculation of additional cases would help clarify how to adjust firing conditions to maintain carbon to the lower furnace and thus maintain the lower furnace temperature. Specifically:

- Reduced lignin 10% and 20%, but with 100% MCR (runs so far have been 97% MCR and 94% MCR respectively)
- Spray tilt (10% and 20% reduced lignin)
- Combination of changes to spray (T or tilt) and air distribution
- Sensitivity analysis – Impact of distribution of carbon between volatiles and char & impact of swelling

PROCESS CHEMISTRY CENTRE

ÅBO AKADEMI UNIVERSITY

CFD Modeling of Reduced Lignin Black Liquor Combustion

Markus Engblom, Niko DeMartini
Åbo Akademi

SKY Lipeätyöryhmä meeting 21.1.2015

Objective and CFD runs 1-7

- CFD modeling for studying what operational changes may be needed when firing reduced lignin black liquor
- CFD modeling of Wisaforest recovery boiler
  - **Run 1:** Base Case, 100% MCR, flue gas O_2 3% (wet)
  - **Runs 2 and 3:** 10% and 20% lignin removed, total air adjusted for flue gas O_2 3% (wet), other variables unchanged
  - **Runs 4-7:** 10% & 20% lignin removed, modifications to air distribution (Runs 4&5) and liquor spraying (Runs 6&7)

Modeled Black Liquors (1/3)

	Original Black Liquor (wt% d.s.)	Lignin [1] (wt% d.s.)
C	32.2	64.5
H	3.3	6
N	0.09	0.1
Na	21.4	0.3
K	2.4	0.05
Cl	0.3	0
Tot. S	6.4	2.5
SO4	5.4	0
OH	1.74	0
HHV (MJ/kg d.s.)	13.2	26.5

Composition of reduced lignin BL based:

- Lignin content of BL: 36 wt-%
- 175 kg H_2SO_4/ton lignin precipitated [1]

1 Tomani, P. The lignoboost process. In Proceedings to The 2nd Nordic Wood Biorefinery Conf., 2-4 Sept. 2009, Helsinki, Finland, pp. 181-188.

Modeled Black Liquors (2/3)

	Original Black Liquor (wt% d.s.)	10% lower lignin (wt% d.s.)	20% lower ligning (wt% d.s.)
C	32.2	30.9	28.9
H	3.3	3.2	3.03
N	0.09	0.09	0.09
Na	21.4	22.8	23.9
K	2.4	2.6	2.7
Cl	0.3	0.32	0.34
Tot. S	6.4	7.0	7.5
SO_4	5.4	6.7	7.87
OH	1.74	1.4	1.1
HHV (MJ/kg d.s.)	13.2	12.4	11.6

Modeled Black Liquors (3/3)

	Original Black Liquor	10% lower lignin	20% lower lignin
Liquor d.s. (wt-%)	81.3	81.3	81.3
Volatiles (kg/kg d.s.)	0.337	0.337	0.337
Char-C (kg/kg d.s.)	0.143	0.103	0.074
Inorganics (kg/kg d.s.)	0.516	0.555	0.585
Na_2S (kg/kg d.s.)	0.115	0.120	0.121
Na_2SO_4 (kg/kg d.s.)	0.080	0.101	0.118
Na_2CO_3 (kg/kg d.s.)	0.320	0.335	0.345
HHV (MJ/kg d.s.)	13.2	12.4	11.6
LHV (MJ/kg liquor)	8.4	7.8	7.2

Liquor feed and combustion air (Runs 1-3)

	Original Black Liquor	10% lower lignin	20% lower ligning
Liquor feed (tds/d)	5320	5160	5000
Of MCR (%)	100	97	94
Air (kg/s)	272	256	232
Air (Nm3/s)	211	199	180
Primary	22%	22%	22%
Secondary	43%	43%	43%
Tertiary	35%	35%	35%
Target flue gas O_2 (% wet)	3.0	3.0	3.0
HHRR (MW/m^2) based on (HHV / LHV)	3.6 / 2.9	3.3 / 2.6	3.0 / 2.3
$T_{adiabatic}$	1240 °C	1150 °C	1100 °C

CFD calculation strategy

- Set up Base Case
  - Liquor and air mass flows
  - Droplet size for C-balanced situation
- Reduced lignin cases
  - liquor to 10% or 20% reduced lignin
  - total air for target 3% O_2 (wet flue gas)
  - Other variables remain the same

ÅA CFD Recovery Furnace Model

• Fluent based
•ÅA sub-models for droplets and char bed

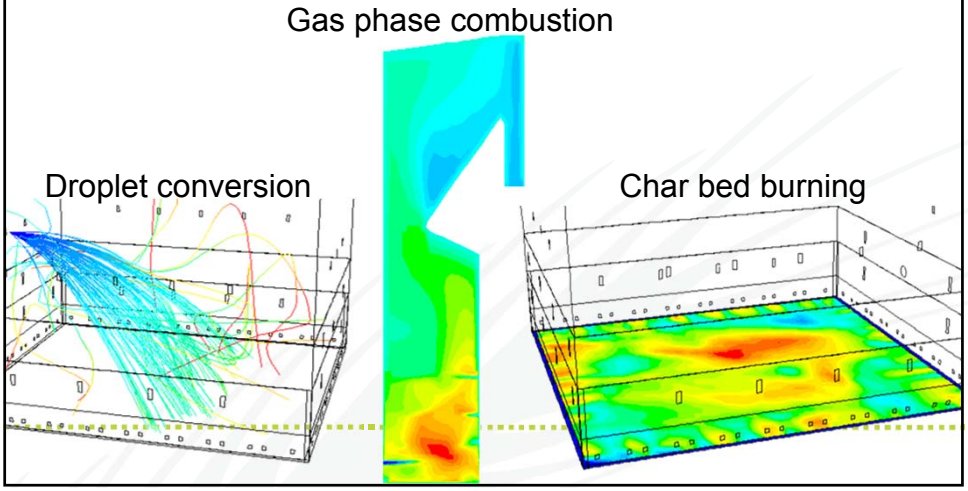

Char bed burning model

Carbon input by droplets

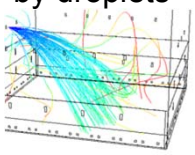

Char carbon conversion

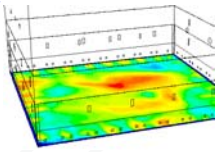

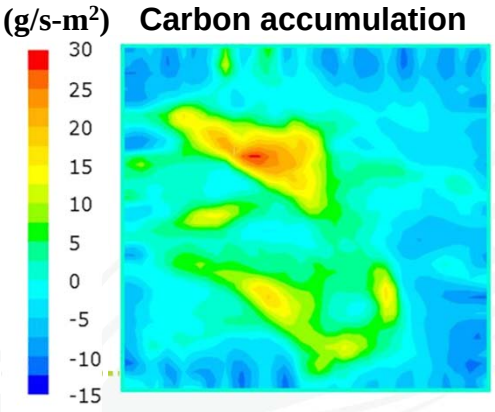

Wisa liquor gun locations

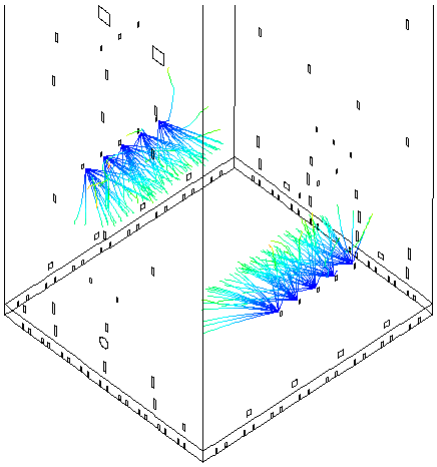

Guns on left and right wall; 5 guns/wall

CFD results

Temperature

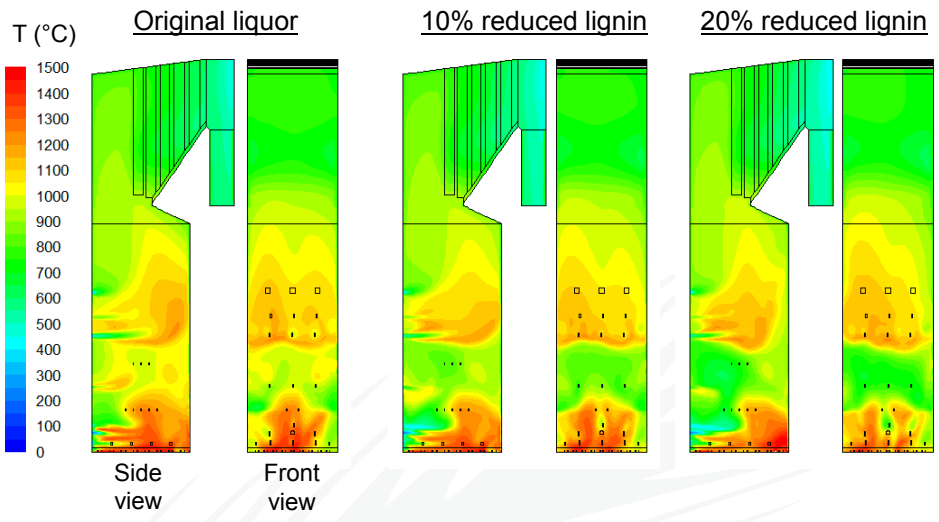

O_2 concentration

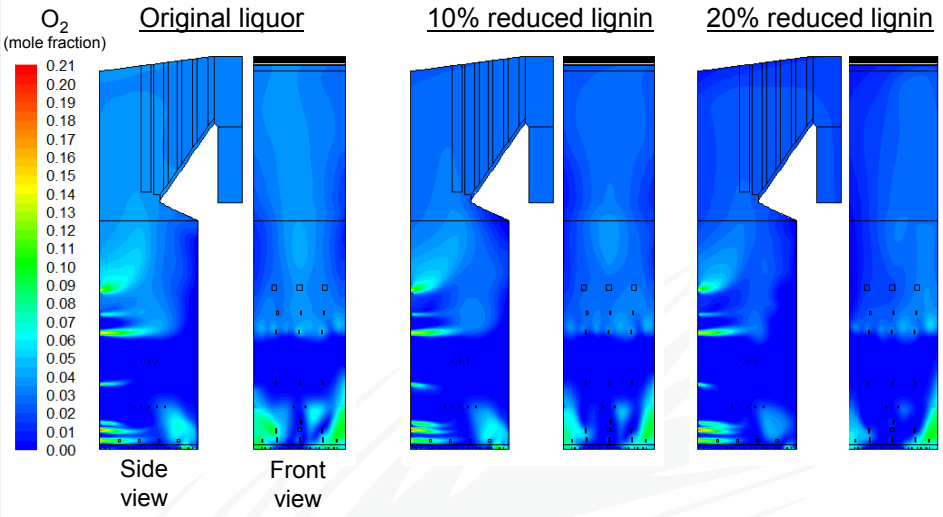

Carbon to walls/bed

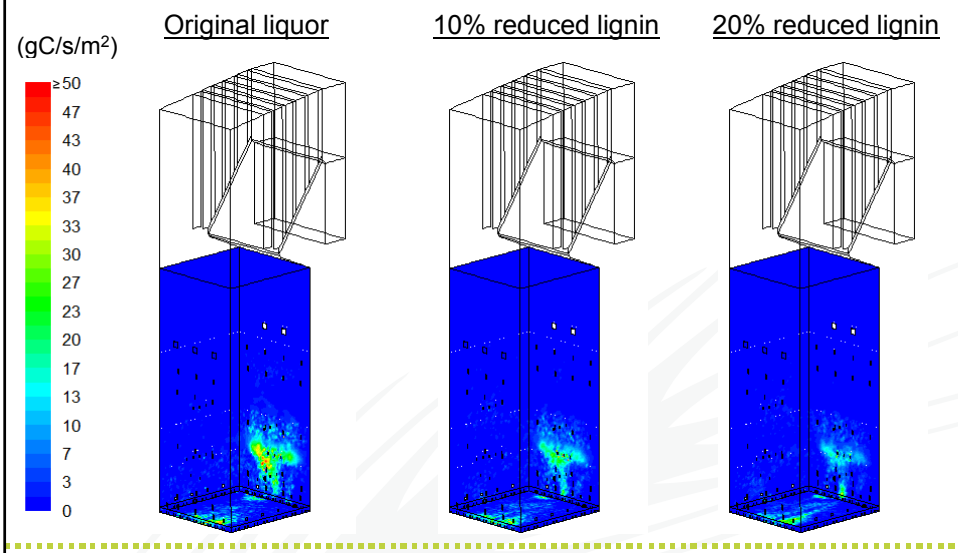

Left wall, back wall, and char bed

Carbon to walls/bed

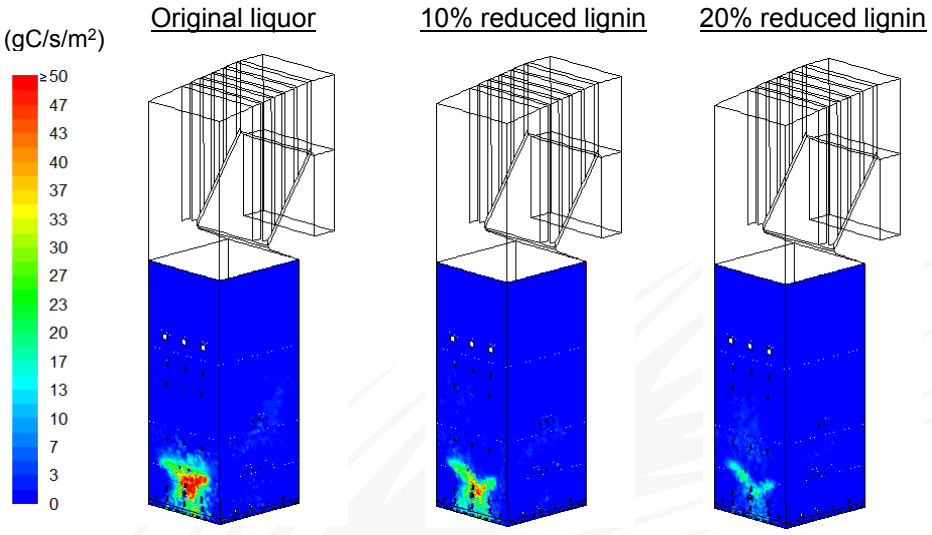

Right wall and front wall

Furnace carbon loading

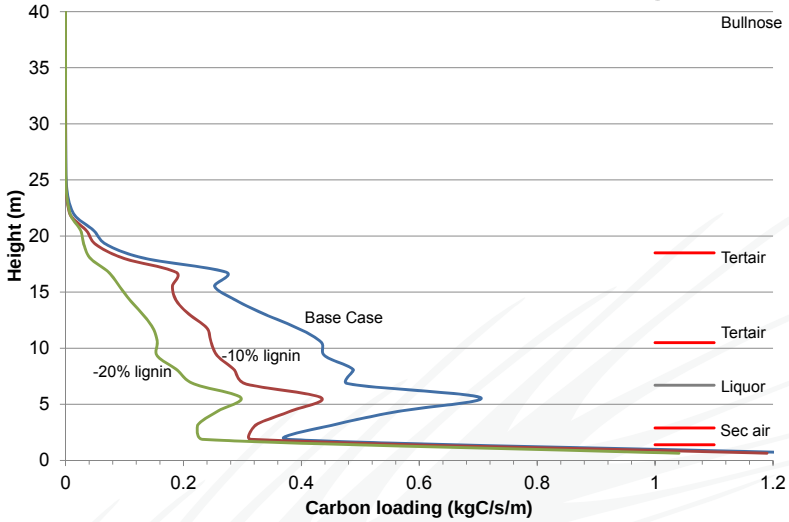

Furnace carbon conversion

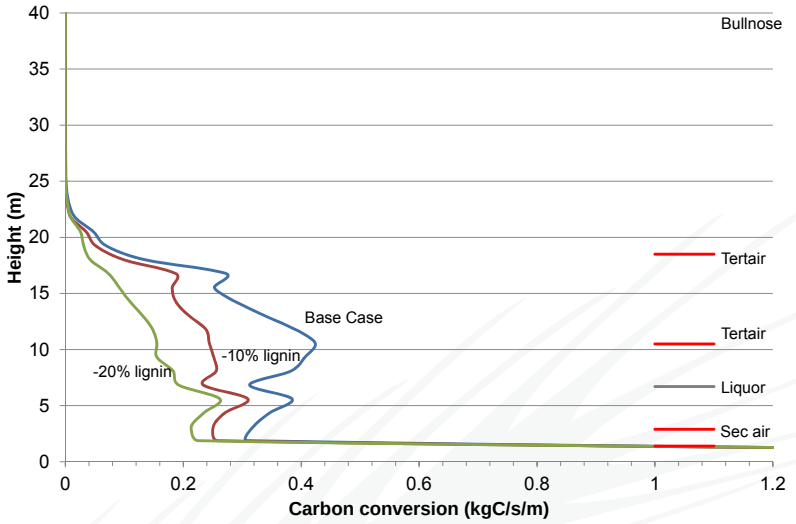

Fate of char carbon

(kg/s)	Base Case	10% reduced lignin	20% reduced lignin
In liquor feed	8.81	6.19	4.30
in-flight conversion	3.90	2.60	1.79
to bed/walls	4.91	3.59	2.51
conversion on bed/walls	4.70	4.37	4.10
carbon accumulation	0.21	-0.78	-1.59

Fate of char carbon

(%)	Base Case	10% reduced lignin	20% reduced lignin
In liquor feed	100.0	100.0	100.0
in-flight conversion	44.3	42.0	41.6
to bed/walls	55.7	58.0	58.4
conversion on bed/walls	53.4	70.5	95.5
carbon accumulation	2.3	-12.5	-37.1

Carbon accumulation and comb. air

	Base Case	10% reduced lignin	20% reduced lignin
carbon accumulation (kg/s)	0.21	-0.78	-1.59
Air to balance carbon accumulation (kg/s)	2.4	-8.9	-18.2

Conclusions - Runs 1-3

- Less char-C with lignin removal
- Lower furnace less loaded with char-C
- Dynamic situation of more carbon conversion than delivery
- Operational changes
  - Reduce prim/sec air (runs 4 & 5) and/or
  - Change spraying – larger droplets (runs 6 & 7)

Runs 4 and 5 – Reduced air

- Primary and secondary air reduced to reflect the reduced char carbon load to the lower furnace
- CFD calculation objective:
  - Reduce carbon oxidation in lower furnace until carbon balance ≈ 0
  - By reducing prim/sec air
- Run 4: 10% lignin removed
- Run 5: 20% lignin removed

Air Distribution – Runs 4 and 5

	Run 2	Run 4		Run3	Run 5
Lignin Removed	10%	10%		20%	20%
	Original Air	Modified Air		Original Air	Modified Air
Total Air (kg/s)	256	256		232	232
Primary (kg/s)	56	44		51	35
Secondary (kg/s)	110	97		100	58
Tertiary (kg/s)	90	115		81	139
Primary (%)	22	17		22	15
Secondary (%)	43	38		43	25
Tertiary (%)	35	45		35	60

Temperature (-10% lignin)

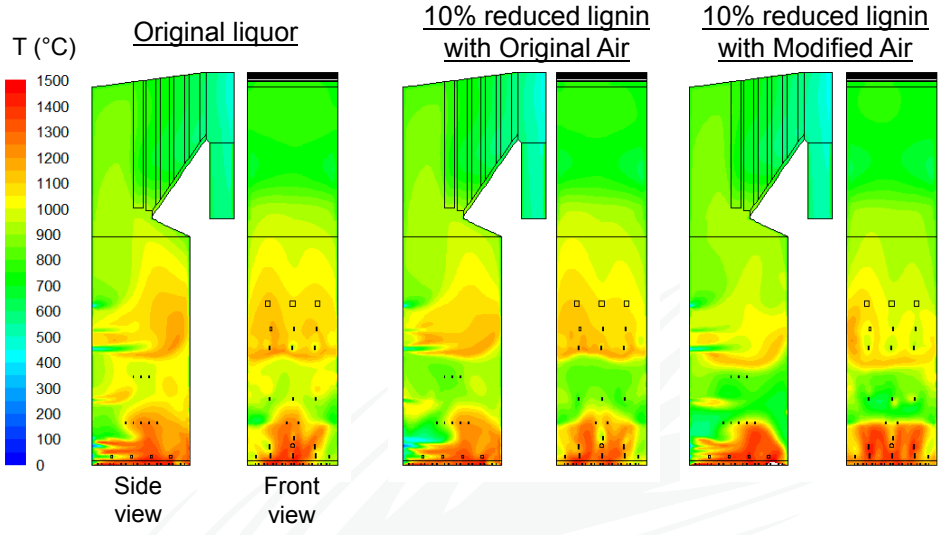

O_2 concentration (-10% lignin)

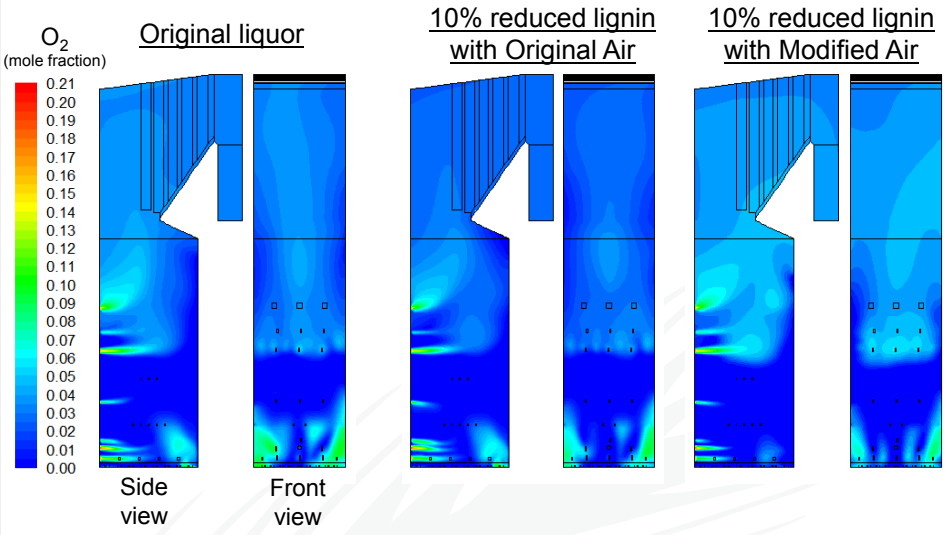

CO concentration (-10% lignin)

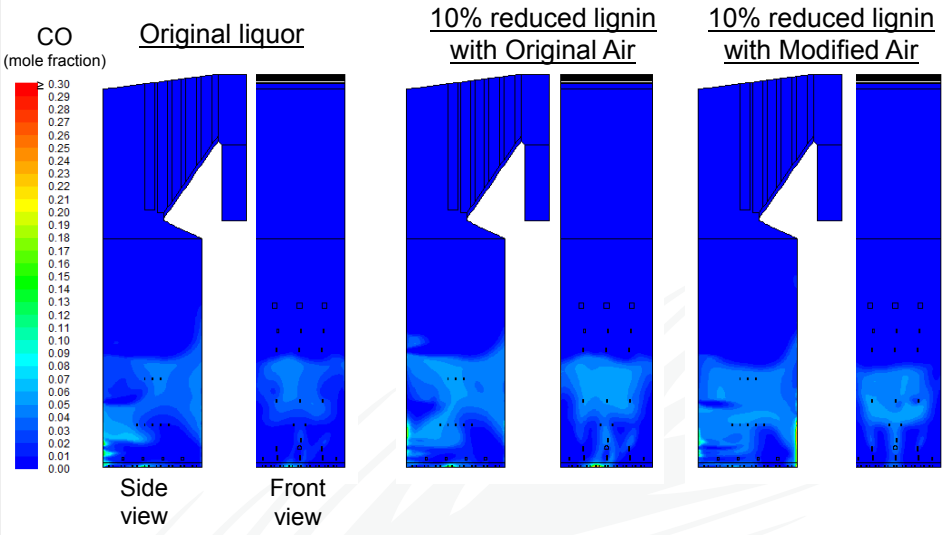

H_2 concentration (-10% lignin)

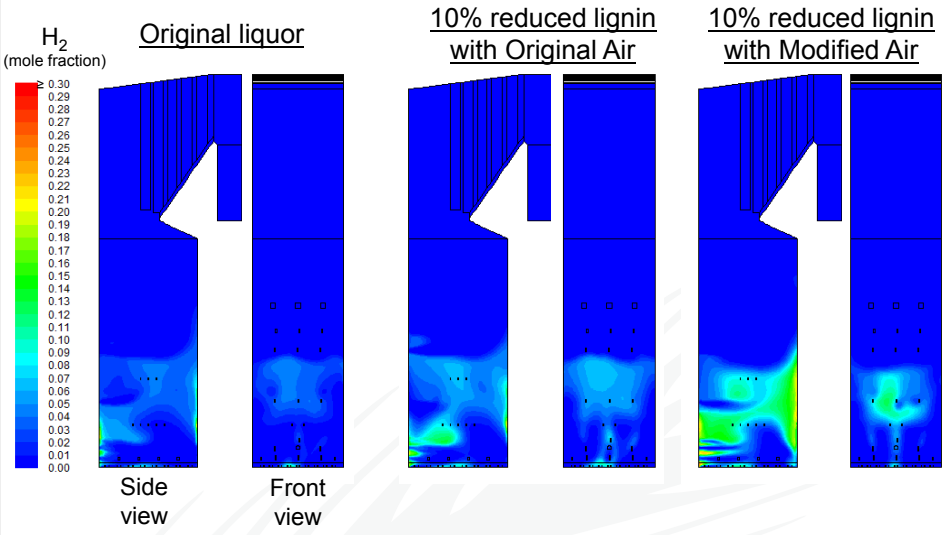

Temperature (-20% lignin)

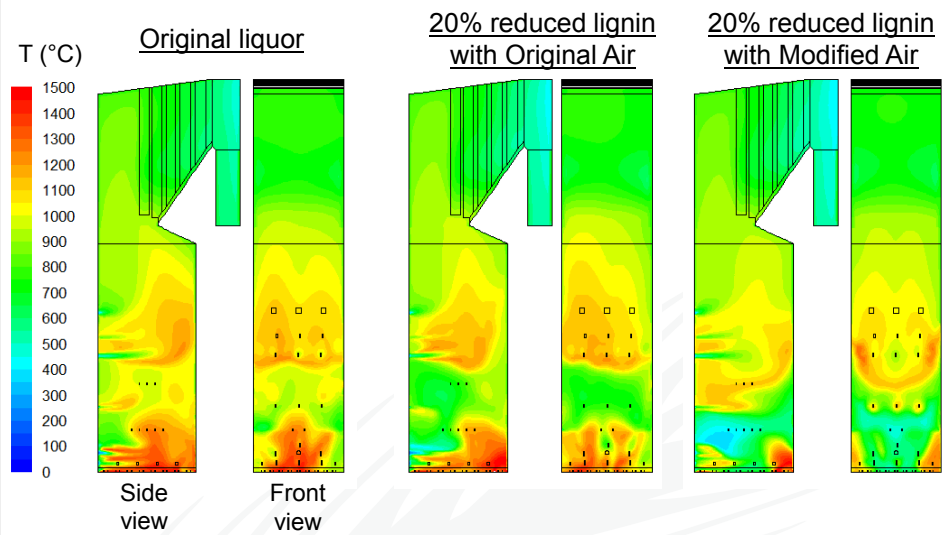

O_2 concentration (-20% lignin)

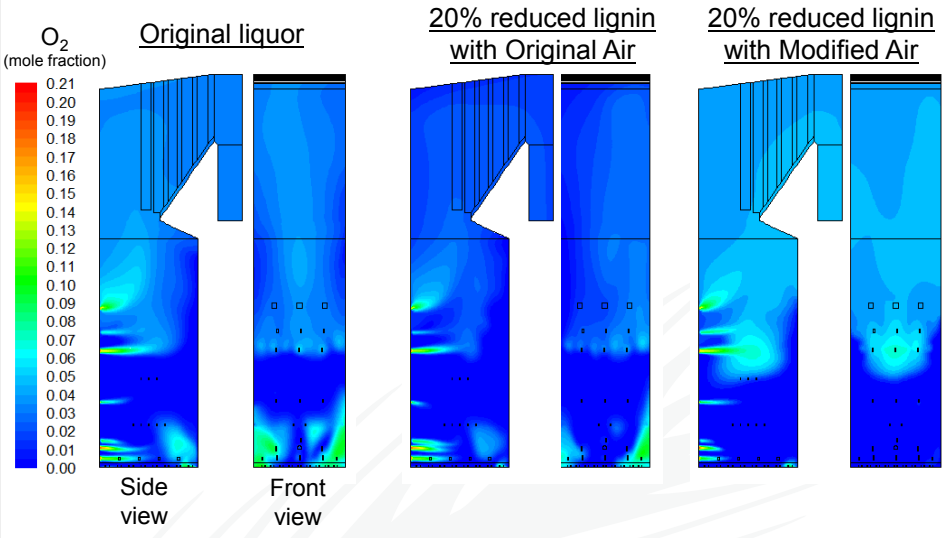

CO concentration (-20% lignin)

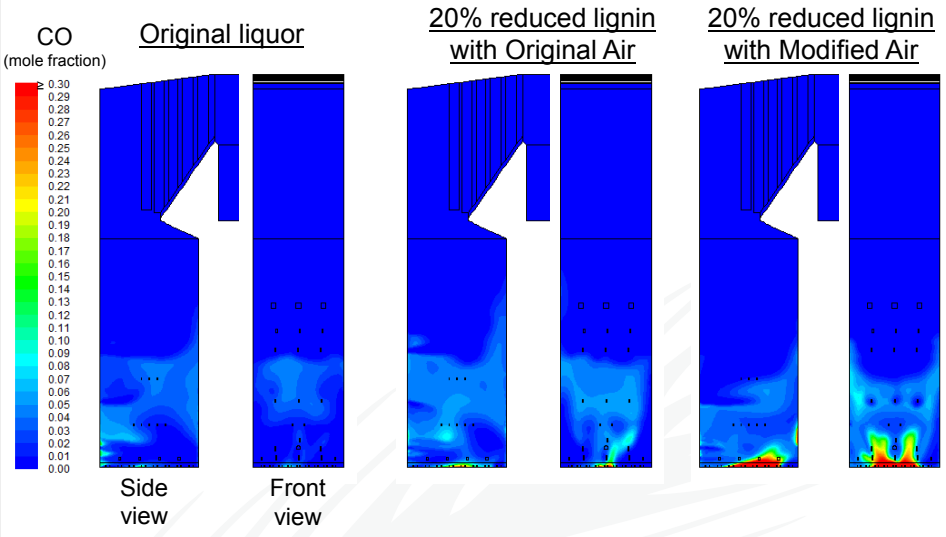

H_2 concentration (-20% lignin)

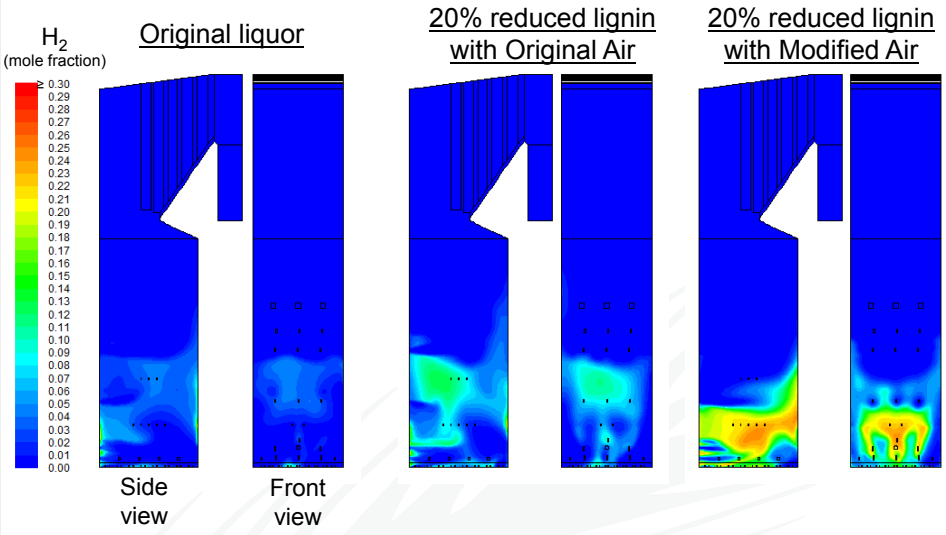

Carbon to walls/bed (-10% lignin)

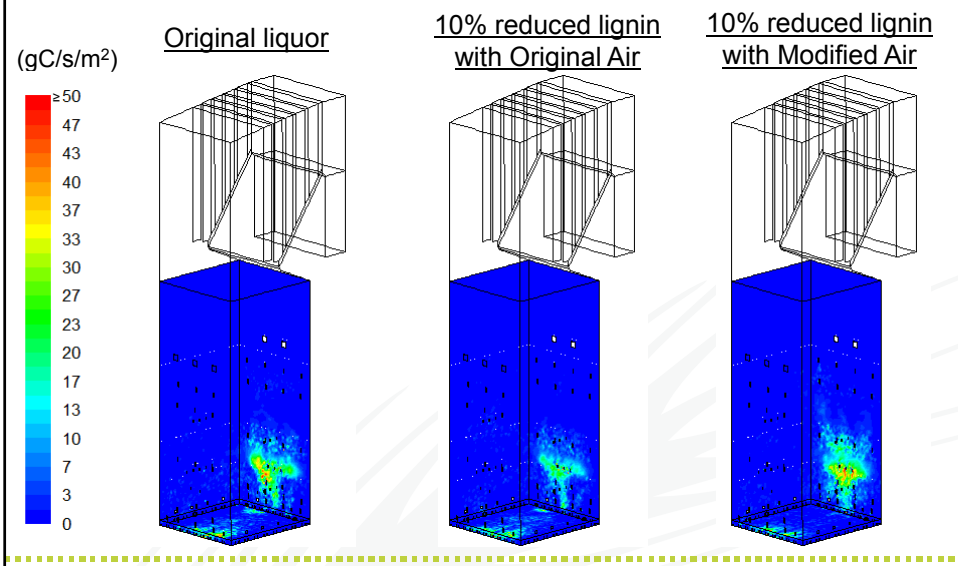

Left wall, back wall, and char bed

Carbon to walls/bed (-10% lignin)

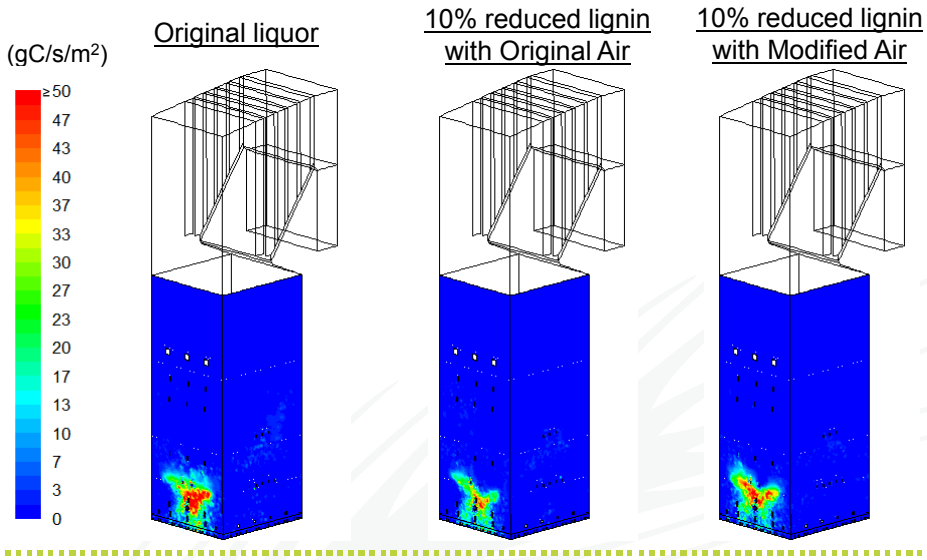

Right wall and front wall

Carbon to walls/bed (-20% lignin)

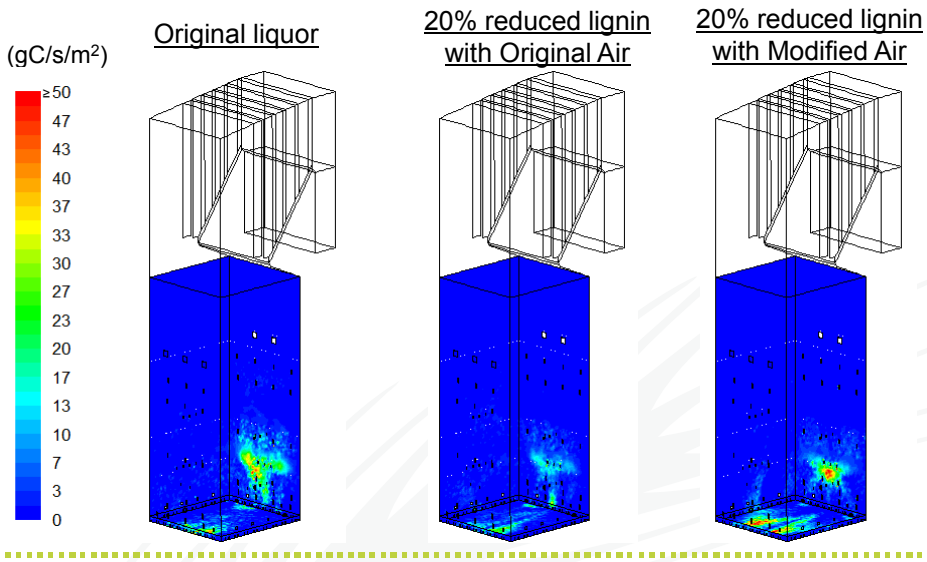

Left wall, back wall, and char bed

Carbon to walls/bed (-20% lignin)

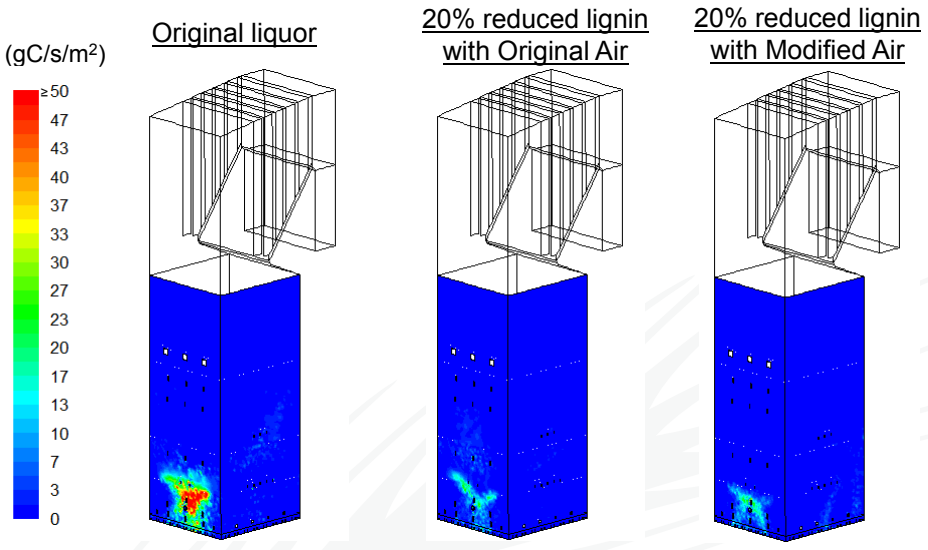

Right wall and front wall

Furnace carbon loading (-10%)

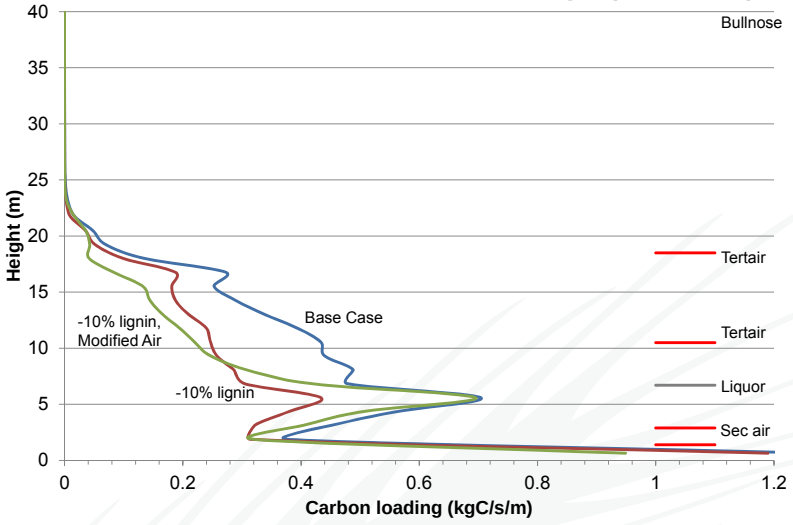

Furnace carbon conversion (-10%)

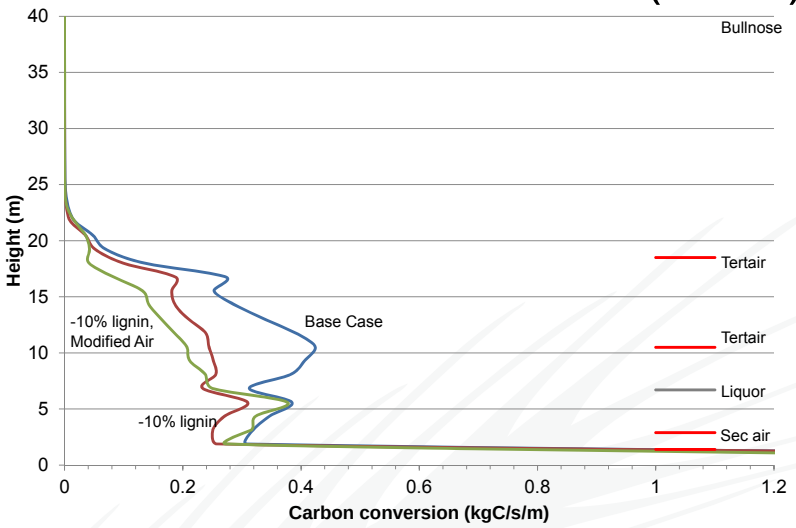

Fate of char carbon (-10%)

(kg/s)	Base Case	10% reduced lignin, Original Air	10% reduced lignin, Modified Air
In liquor feed	8.81	6.19	6.19
in-flight conversion	3.90	2.60	1.79
to bed/walls	4.91	3.59	4.40
conversion on bed/walls	4.70	4.37	4.38
carbon accumulation	0.21	-0.78	0.01

Fate of char carbon (-10%)

(%)	Base Case	10% reduced lignin, Original Air	10% reduced lignin, Modified Air
In liquor feed	100.0	100.0	100.0
in-flight conversion	44.3	42.0	28.9
to bed/walls	55.7	58.0	71.1
conversion on bed/walls	53.4	70.5	70.9
carbon accumulation	2.3	-12.5	0.2

Furnace carbon loading (-20%)

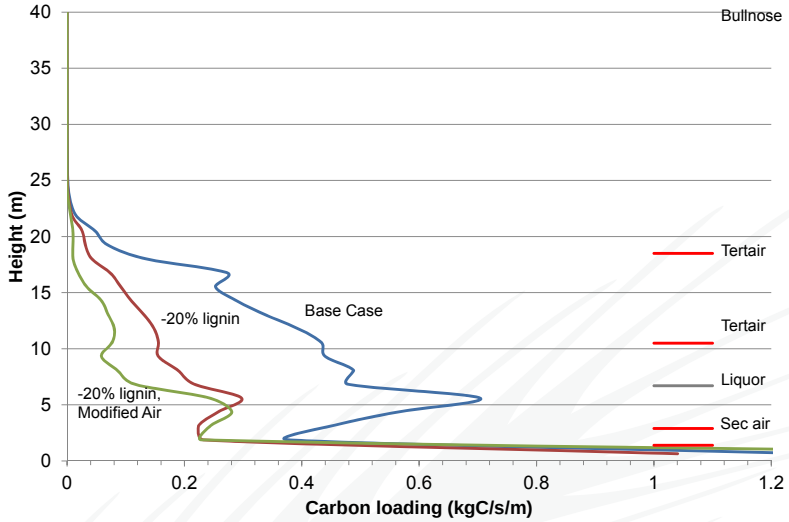

Furnace carbon conversion (-20%)

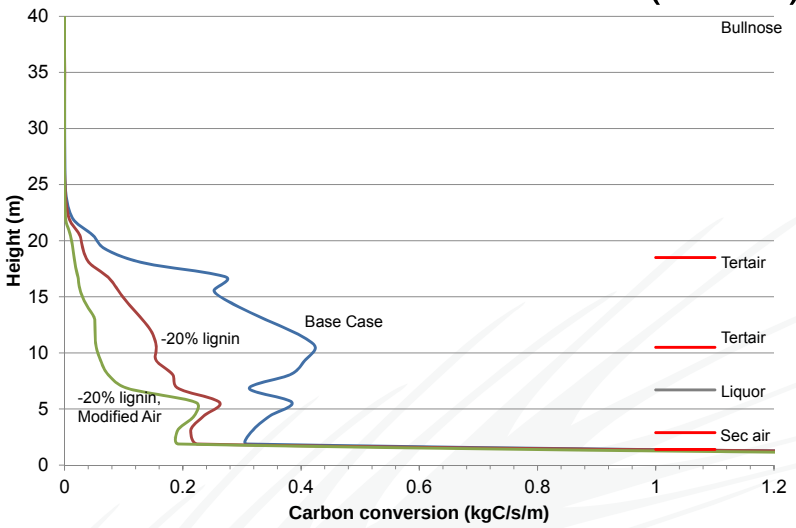

Fate of char carbon (-20%)

(kg/s)	Base Case	20% reduced lignin, Original Air	20% reduced lignin, Modified Air
In liquor feed	8.81	4.30	4.30
in-flight conversion	3.90	1.79	0.67
to bed/walls	4.91	2.51	3.63
conversion on bed/walls	4.70	4.10	3.68
carbon accumulation	0.21	-1.59	-0.05

Fate of char carbon (-20%)

(%)	Base Case	20% reduced lignin, Original Air	20% reduced lignin, Modified Air
In liquor feed	100.0	100.0	100.0
in-flight conversion	44.3	41.6	15.5
to bed/walls	55.7	58.4	84.5
conversion on bed/walls	53.4	95.5	85.7
carbon accumulation	2.3	-37.1	-1.2

Conclusions - Runs 4 and 5

- Considerable changes to lower furnace air needed to reach carbon balanced situation
  - Base Case: 22% prim / 43% sec / 35% tert
  - Run 4: 17% prim / 38% sec / 45% tert
  - Run 5: 15% prim / 25% sec / 60% tert
- Uncertain if modeled air splits could be used in reality
- Results suggest air distribution adjustment unlikely alone to be sufficient (if even possible) operational change

Conclusions - Runs 1-3

- Less char-C with lignin removal
- Lower furnace less loaded with char-C
- Dynamic situation of more carbon conversion than delivery
- Operational changes
  - Reduce prim/sec air (runs 4 & 5) and/or
  - Change spraying – larger droplets (runs 6 & 7)

Runs 6 & 7 – Larger Droplets

- Larger droplets will result in more carbon reaching the lower furnace. The droplet size distribution has been proposed to provide a carbon balance based on the original primary, secondary and tertiary air distribution
- In practice this larger particle size distribution would be achieved by reducing the firing temperature or changing the spray angle or nozzle

CFD runs 6 and 7

- Objective:
  - Increase char-carbon delivery to lower furnace until carbon balance ≈ 0
  - by increasing droplet size in liquor spray (lower liquor T)
- Run 6: 10% lignin removed
- Run 7: 20% lignin removed

CFD runs 6 and 7

- Droplet size, liquor temperature, droplet velocity, etc – freely adjustable, independent parameters in CFD model
- For Runs 6 and 7, need to link droplet size, droplet velocity, and liquor temperature to each other in CFD model
- How are droplet size and droplet velocity connected to liquor temperature?

Spray characterization (Miikkulainen et al.)

Nozzle A

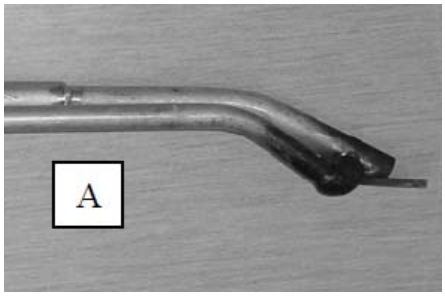

Nozzle B

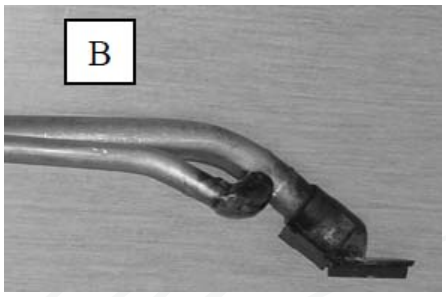

	Nozzle A	Nozzle B
Nozzle pipe diameter	27 mm	28 mm
Splash plate angle	23°	36°
Nozzle exit area reduced by plate?	Partly reduced	Not reduced

Miikkulainen, P., Kankkunen, A. & Järvinen, M. 2002, "The Effect of Excess Temperature and Flashing on Black Liquor Spray Properties", *IFRF Finnish - Swedish Flame Days 2002, Vaasa, Finland, 24-25 September*

Reprinted with permission from IFRF

Liquor T - droplet size – dependence

Nozzle A

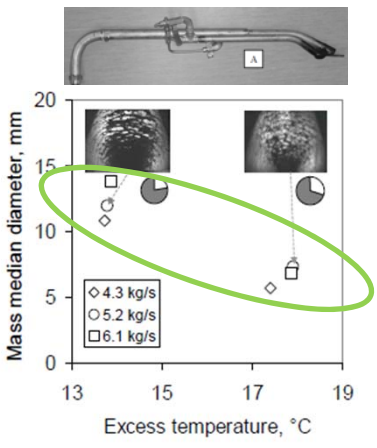

Nozzle B

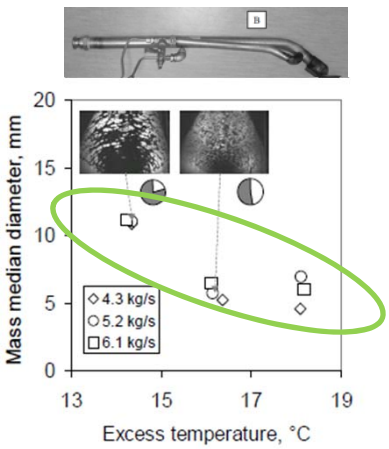

Miikkulainen, P., Kankkunen, A. & Järvinen, M. 2002, "The Effect of Excess Temperature and Flashing on Black Liquor Spray Properties", *IFRF Finnish - Swedish Flame Days 2002, Vaasa, Finland, 24-25 September*

Reprinted with permission from IFRF

Liquor T - droplet size – dependence

Generic correlation for CFD

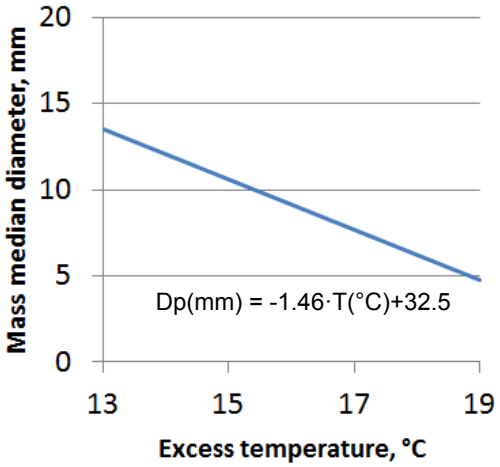

Liquor T - droplet size – dependence

Nozzle A

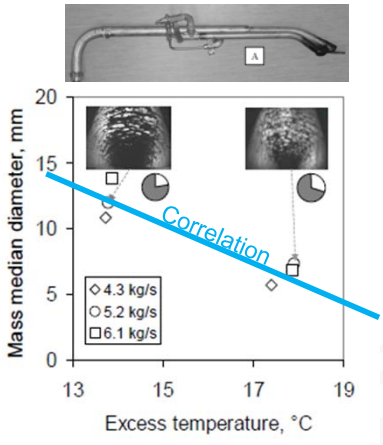

Nozzle B

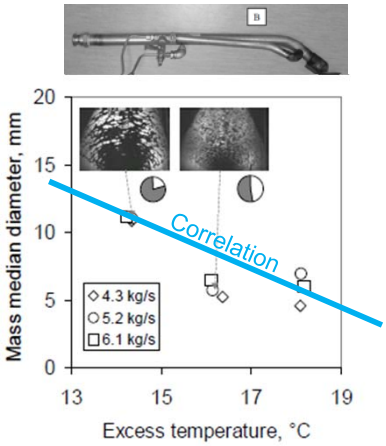

Miikkulainen, P., Kankkunen, A. & Järvinen, M. 2002, "The Effect of Excess Temperature and Flashing on Black Liquor Spray Properties", *IFRF Finnish - Swedish Flame Days 2002, Vaasa, Finland, 24-25 September*

Reprinted with permission from IFRF

Liquor T - droplet velocity – dependence

Nozzle A

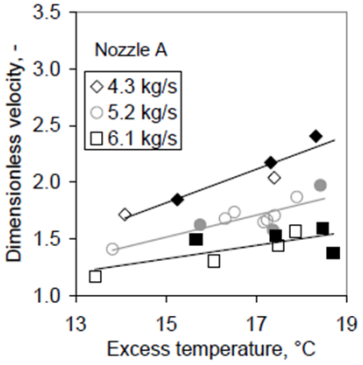

Dimensionless velocity, v(-)

$$v(-) = \frac{\text{Actual Liquor Velocity}}{\text{Liquor Velocity assuming no flashing}}$$

Miikkulainen, P., Kankkunen, A. & Järvinen, M. 2002, "The Effect of Excess Temperature and Flashing on Black Liquor Spray Properties", *IFRF Finnish - Swedish Flame Days 2002, Vaasa, Finland, 24-25 September*

Reprinted with permission from IFRF

Liquor T - droplet velocity – dependence

Nozzle A

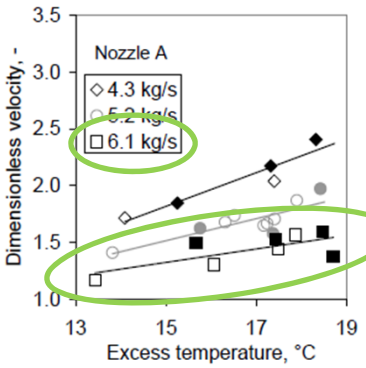

10% and 20% reduced lignin Cases, liquor mass flow ~7 kg/s

Miikkulainen, P., Kankkunen, A. & Järvinen, M. 2002, "The Effect of Excess Temperature and Flashing on Black Liquor Spray Properties", *IFRF Finnish - Swedish Flame Days 2002, Vaasa, Finland, 24-25 September*

Reprinted with permission from IFRF

Liquor T - droplet velocity – dependence

Nozzle A

Nozzle B

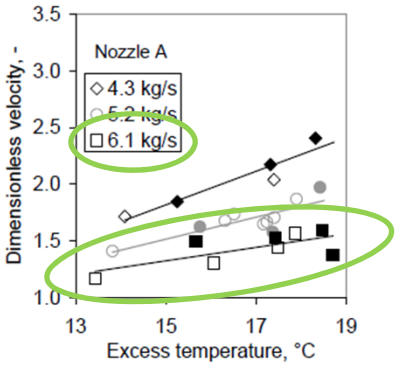

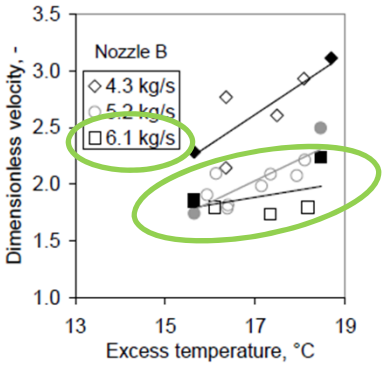

10% and 20% reduced ligning
Cases, liquor mass flow ~7 kg/s

Miikkulainen, P., Kankkunen, A. & Järvinen, M. 2002, "The Effect of Excess Temperature and Flashing on Black Liquor Spray Properties", *IFRF Finnish - Swedish Flame Days 2002, Vaasa, Finland, 24-25 September*

Reprinted with permission from IFRF

Liquor T - droplet velocity – dependence

Generic correlation for CFD

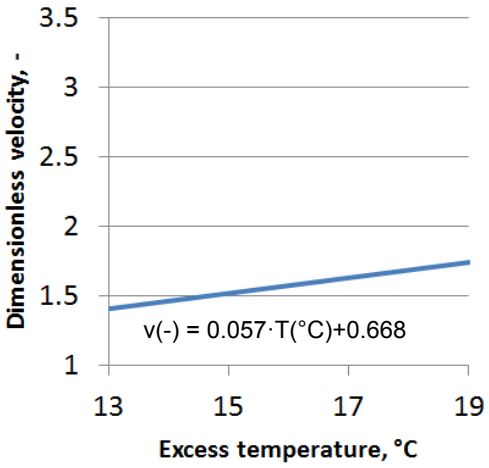

Liquor T - droplet velocity – dependence

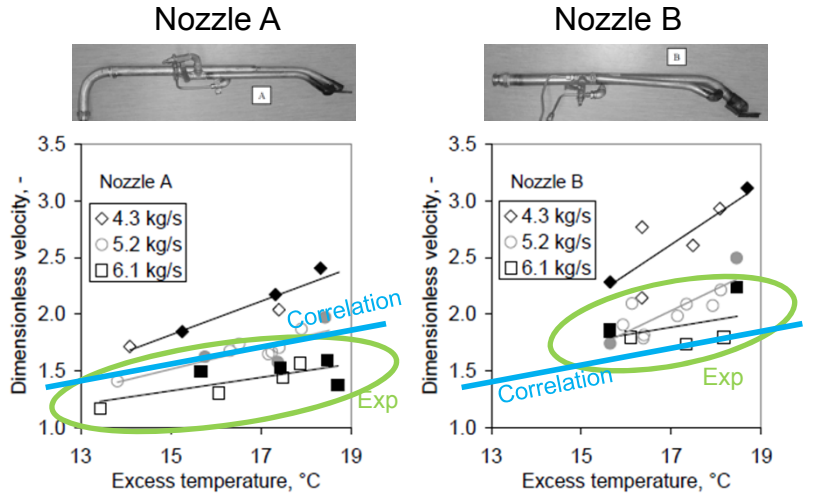

Miikkulainen, P., Kankkunen, A. & Järvinen, M. 2002, "The Effect of Excess Temperature and Flashing on Black Liquor Spray Properties", *IFRF Finnish - Swedish Flame Days 2002, Vaasa, Finland, 24-25 September*

Reprinted with permission from IFRF

CFD runs 6 and 7 vs. Base Case

	Base Case	10% reduced lignin (Run 6)	20% reduced lignin (Run 7)
Average droplet size	5.7 mm	12.5 mm	23.0 mm
Initial droplet velocity	15.0 m/s	12.7 m/s	9.2 m/s
Excess temperature	18.4 °C	13.7 °C	6.5 °C
Liquor T changed from Base Case		-4.7 °C	-11.9 °C

Temperature (-10% lignin)

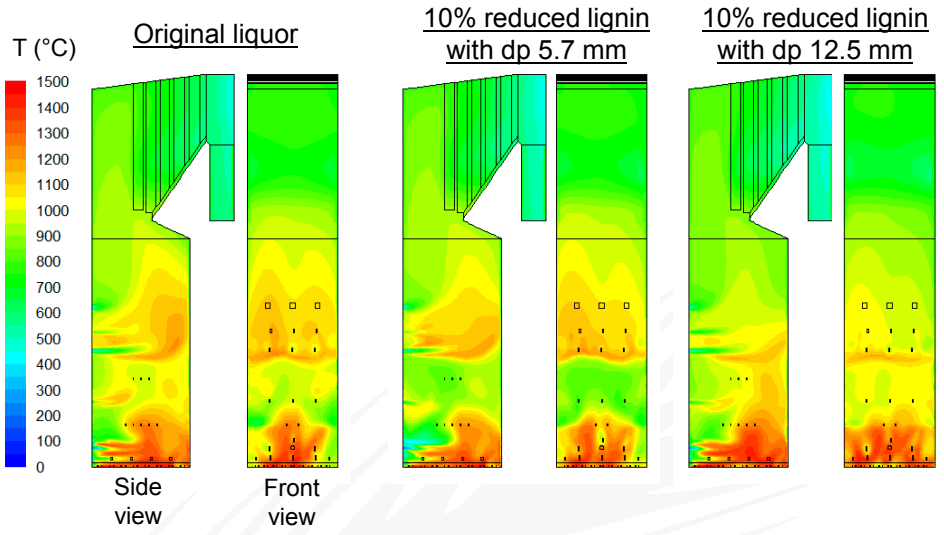

O_2 concentration (-10% lignin)

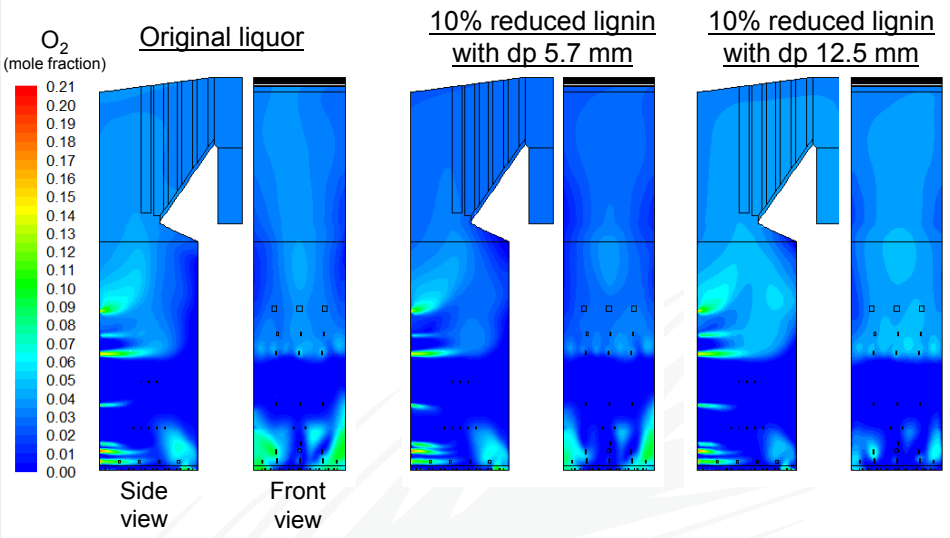

CO concentration (-10% lignin)

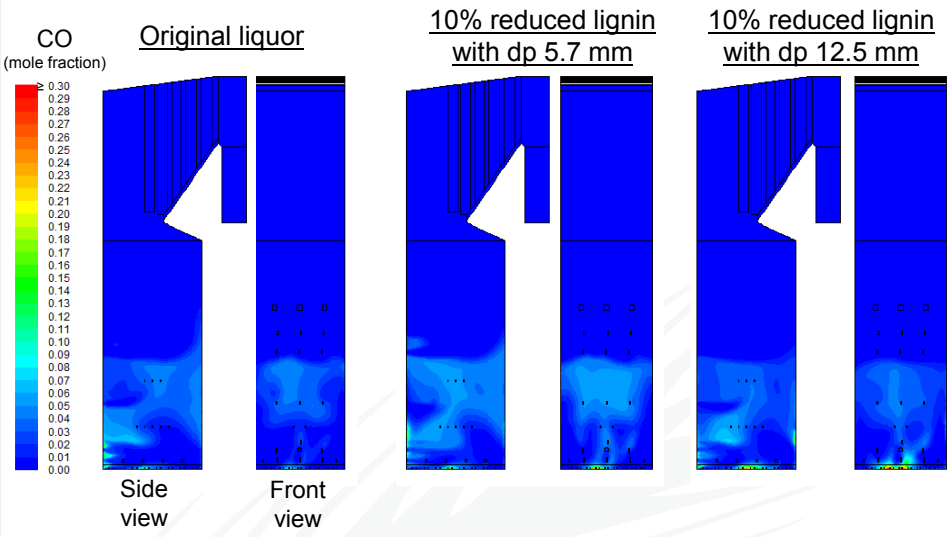

H_2 concentration (-10% lignin)

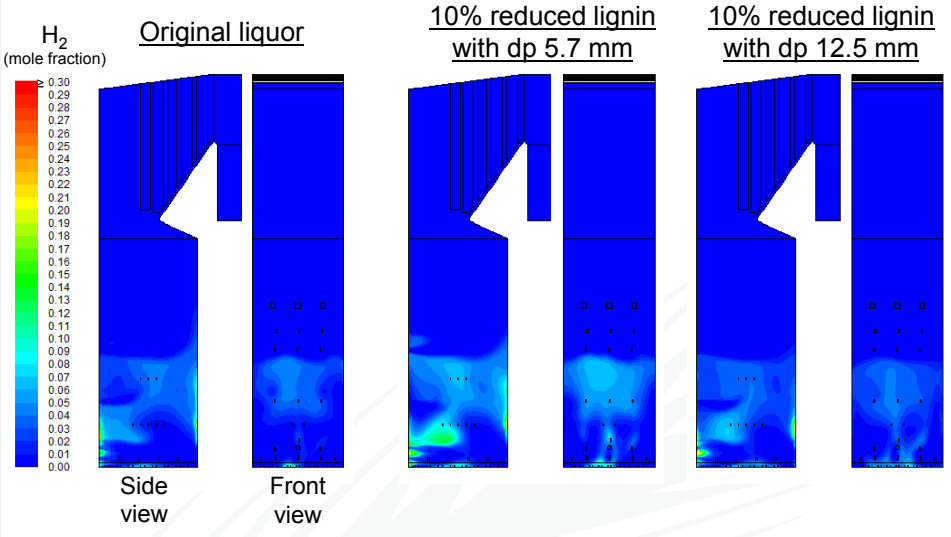

Temperature (-20% lignin)

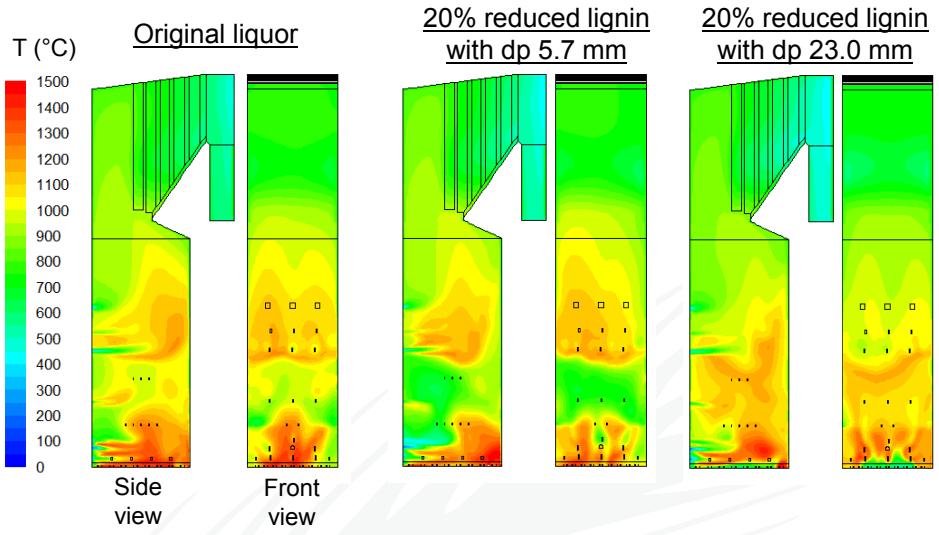

O_2 concentration (-20% lignin)

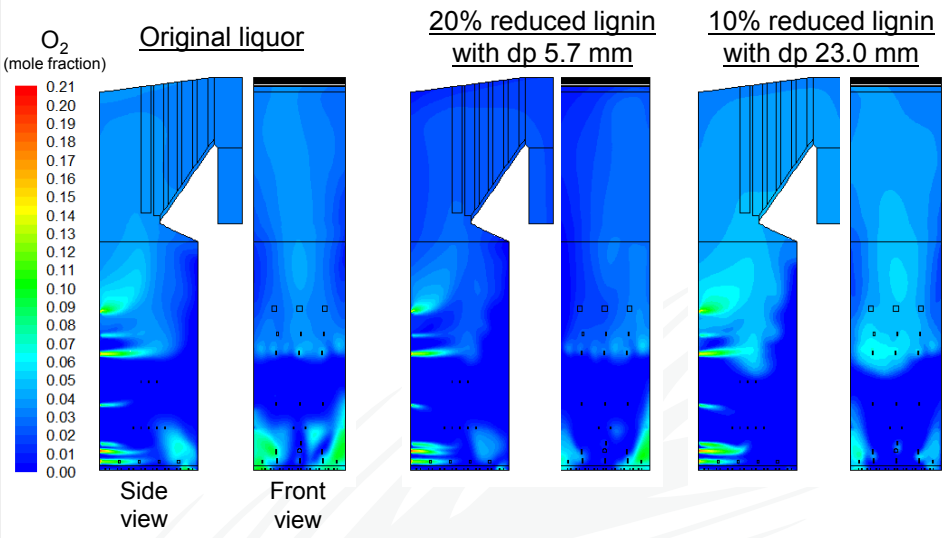

CO concentration (-20% lignin)

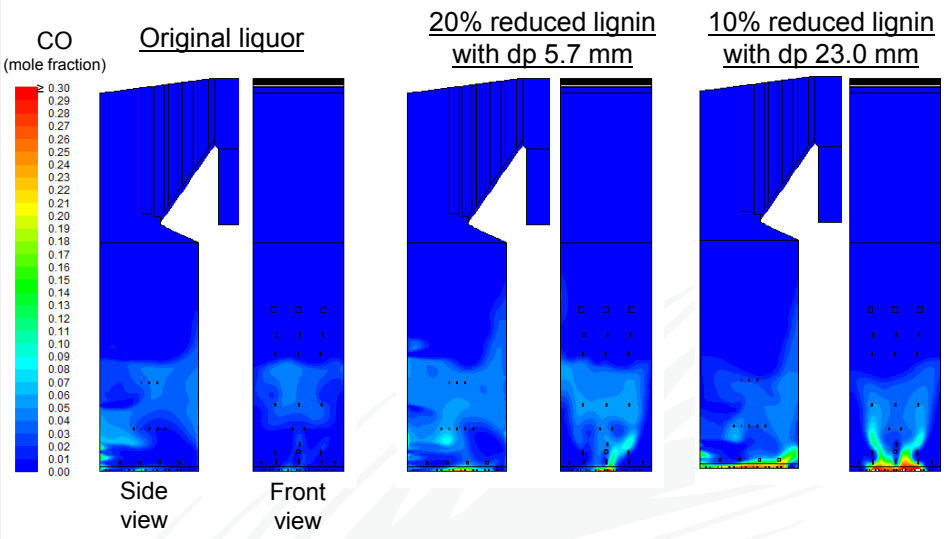

H_2 concentration (-20% lignin)

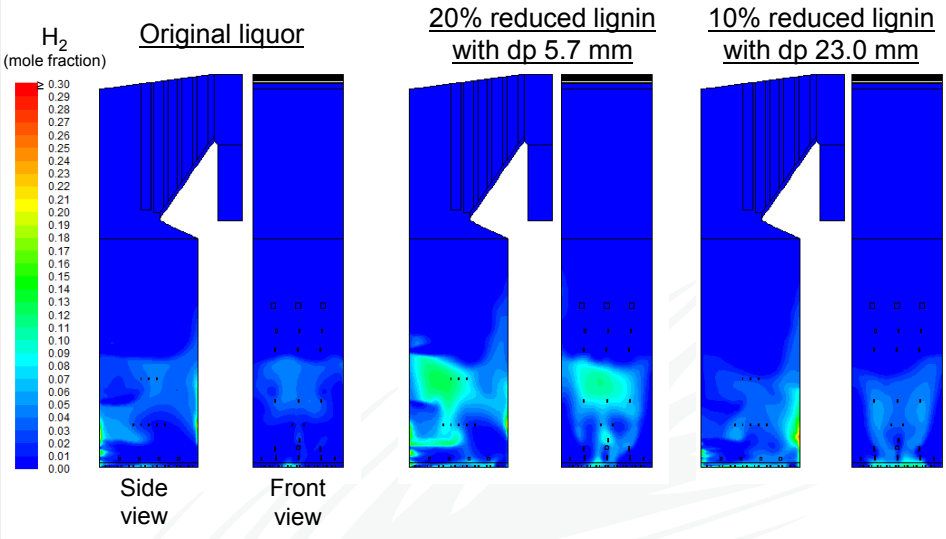

Carbon to walls/bed (-10% lignin)

(gC/s/m^2)

≥50
47
43
40
37
33
30
27
23
20
17
13
10
7
3
0

Original liquor

10% reduced lignin with dp 5.7 mm

10% reduced lignin with dp 12.5 mm

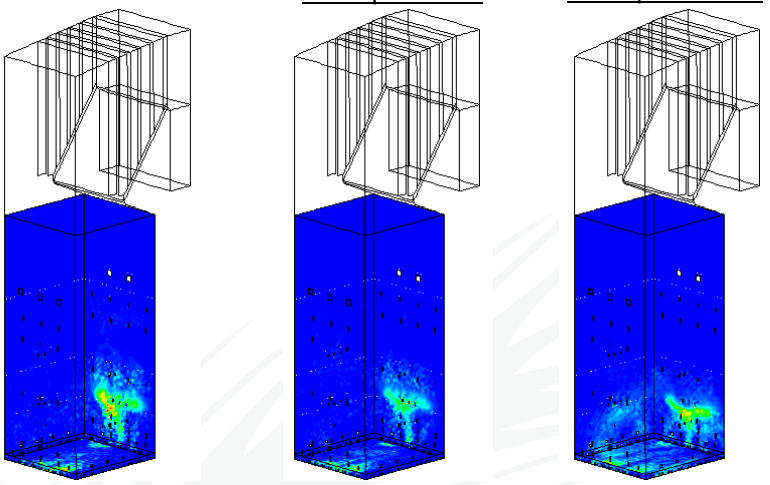

Left wall, back wall, and char bed

Carbon to walls/bed (-10% lignin)

(gC/s/m^2)

≥50
47
43
40
37
33
30
27
23
20
17
13
10
7
3
0

Original liquor

10% reduced lignin with dp 5.7 mm

10% reduced lignin with dp 12.5 mm

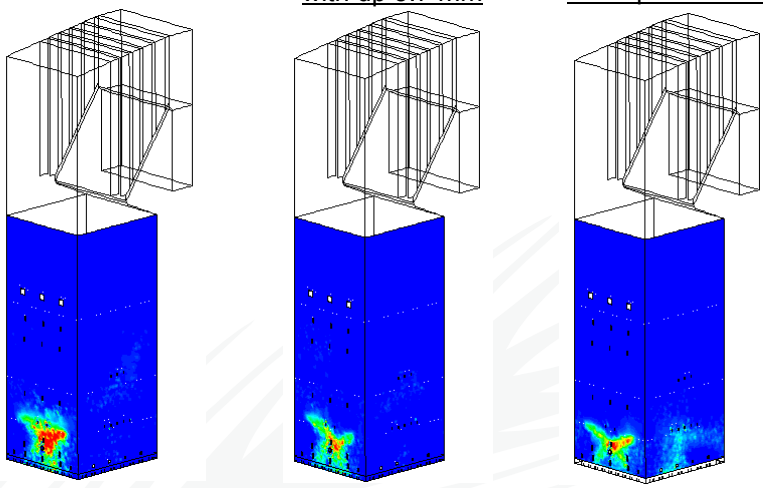

Right wall and front wall

Carbon to walls/bed (-20% lignin)

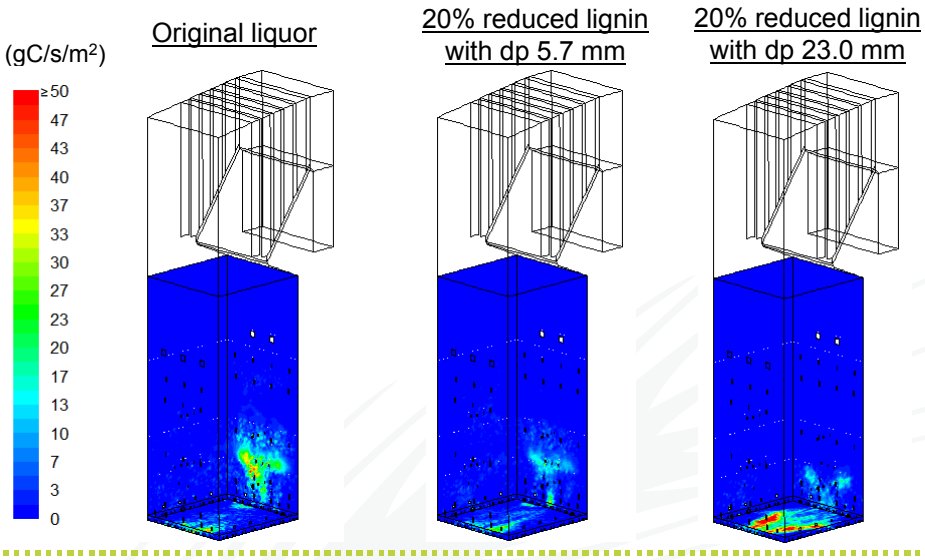

Left wall, back wall, and char bed

Carbon to walls/bed (-20% lignin)

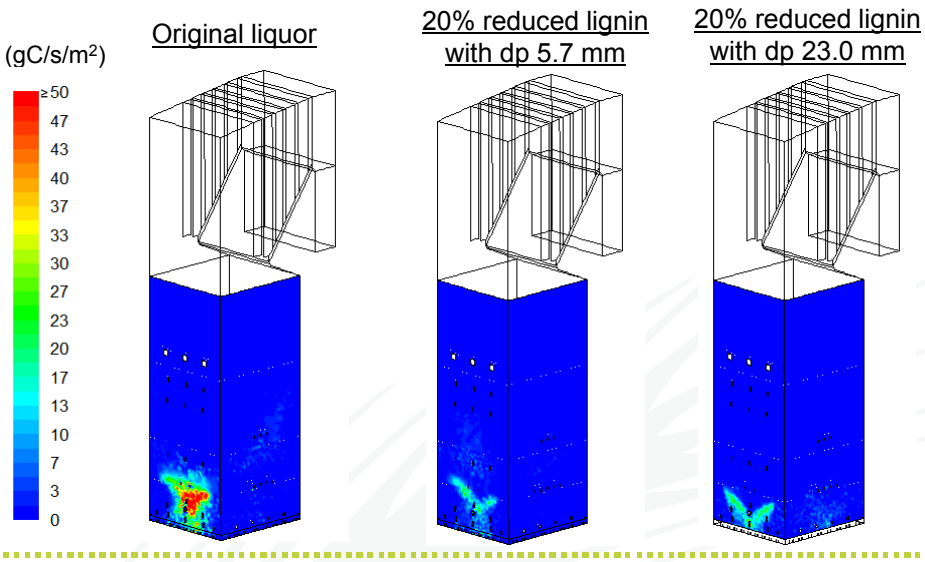

Right wall and front wall

Furnace carbon loading (-10%)

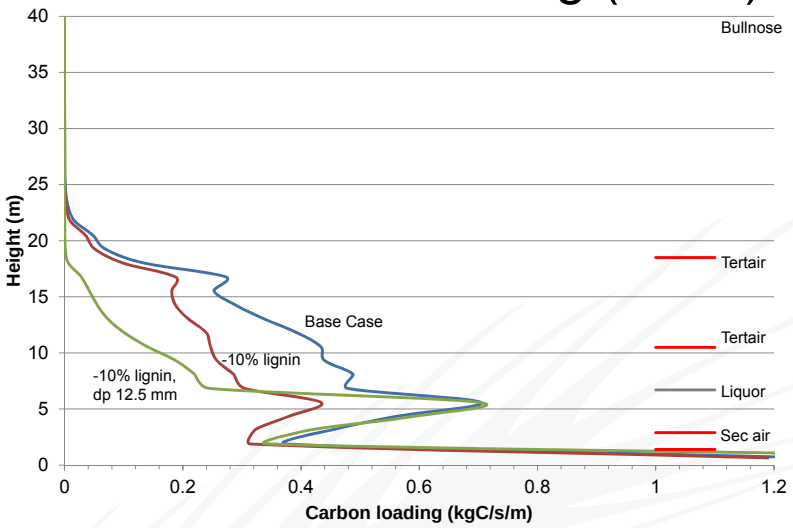

Furnace carbon conversion (-10%)

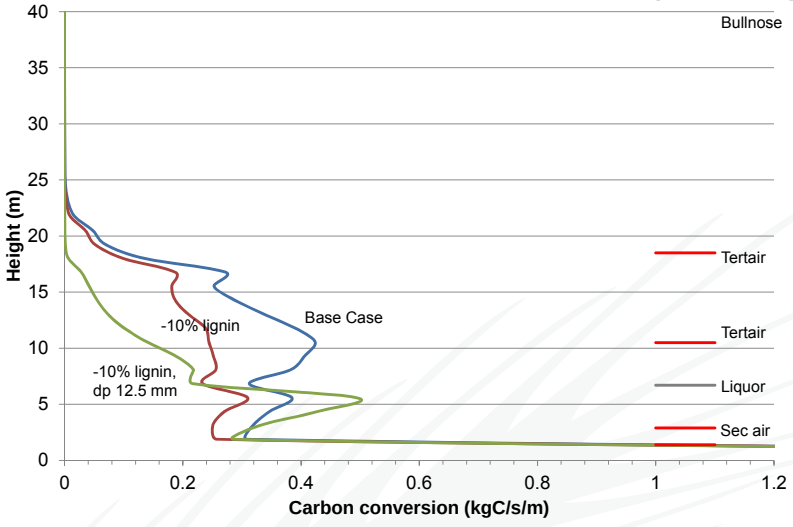

Fate of char carbon (-10%)

(kg/s)	Base Case	10% reduced lignin, dp 5.7 mm	10% reduced lignin, dp 12.5 mm
In liquor feed	8.81	6.19	6.19
in-flight conversion	3.90	2.60	1.01
to bed/walls	4.91	3.59	5.18
conversion on bed/walls	4.70	4.37	5.16
carbon accumulation	0.21	-0.78	0.02

Fate of char carbon (-10%)

(%)	Base Case	10% reduced lignin, dp 5.7 mm	10% reduced lignin, dp 12.5 mm
In liquor feed	100.0	100.0	100.0
in-flight conversion	44.3	42.0	16.3
to bed/walls	55.7	58.0	83.7
conversion on bed/walls	53.4	70.5	83.4
carbon accumulation	2.3	-12.5	0.3

Furnace carbon loading (-20%)

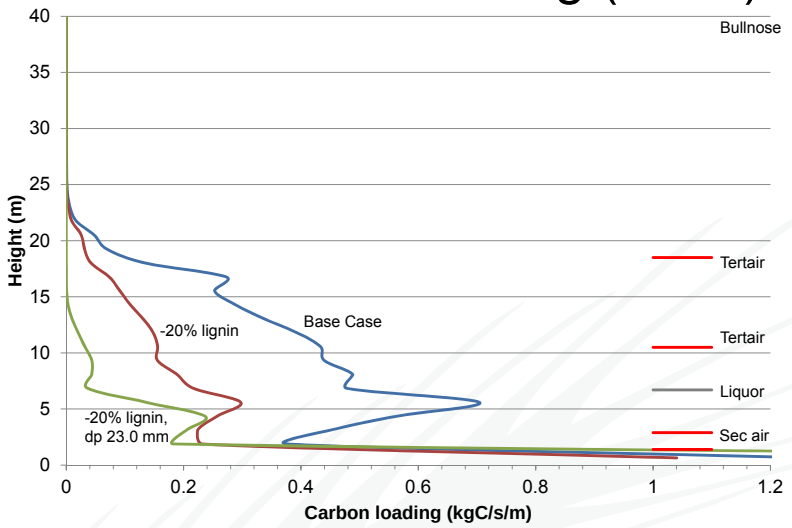

Furnace carbon conversion (-20%)

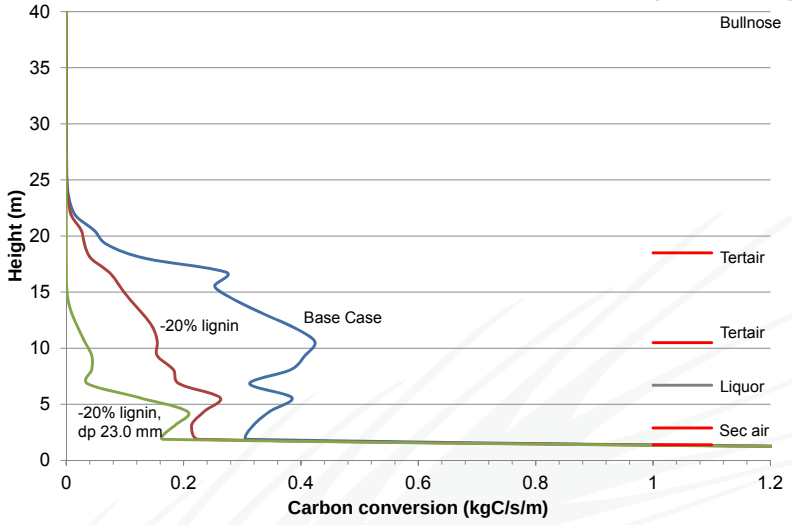

Fate of char carbon (-20%)

(kg/s)	Base Case	20% reduced lignin, dp 5.7 mm	20% reduced lignin, dp 23.0 mm
In liquor feed	8.81	4.30	4.30
in-flight conversion	3.90	1.79	0.24
to bed/walls	4.91	2.51	4.05
conversion on bed/walls	4.70	4.10	4.02
carbon accumulation	0.21	-1.59	0.03

Fate of char carbon (-20%)

(%)	Base Case	20% reduced lignin, dp 5.7 mm	20% reduced lignin, dp 23.0 mm
In liquor feed	100.0	100.0	100.0
in-flight conversion	44.3	41.6	5.7
to bed/walls	55.7	58.4	94.3
conversion on bed/walls	53.4	95.5	93.6
carbon accumulation	2.3	-37.1	0.7

Conclusions - Runs 6 and 7

- With lignin removal and air split unchanged considerably larger droplets are needed to reach carbon balanced situation (=”steady operation”)
- Estimated to correspond to a decrease in liquor temperature of 4.7 °C or 11.9 °C when 10% or 20% lignin removed respectively
- Results suggest both liquor temperature and air distribution will need to be adjusted

Conclusions - Runs 1-7

- Less char-C with lignin removal
- Lower furnace less loaded with char-C
- Operational changes
  - Reduce prim/sec air **and**
  - Change spraying – larger droplets

Conclusions – condidates for additional runs

- Reduced lignin 10% and 20%, but with 100% MCR (runs so far have been 97% MCR and 94% MCR respectively)
- Spray tilt (10% and 20% reduced lignin)
- Combination of changes to spray (T or tilt) and air distribution
- Sensitivity analysis – Impact of distribution of carbon between volatiles and char & impact of swelling

LIITE 3

ÅA, Combustion Properties of Reduced-lignin Black Liquors – tutkimus

Combustion properties of reduced-lignin black liquors

NIKLAS VÄHÄ-SAVO, NIKOLAI DEMARTINI, RUFUS ZIESIG, PER TOMANI, HANS THELIANDER, ERKKI VÄLIMÄKI, AND MIKKO HUPA

ABSTRACT: The growing interest in production of green chemicals and biofuels from biomass provides an incentive for pulp mills to identify new possibilities in recovering more wood components from the pulping process. One possibility is to use lignin, separated from black liquor. We undertook this work to determine the combustion properties of reduced-lignin black liquors—two kraft liquors and one soda liquor—in a laboratory-scale, single-particle furnace. The combustion times, maximum swollen volume, nitric oxide formation, cyanate formation, and sulfur release were measured for the original liquors, the filtrates, and intermediate levels of lignin reduction. Combustion experiments were conducted at 900°C in 10% oxygen. Cyanate formation experiments were carried out by pyrolyzing the droplets at 800°C in 100% nitrogen to form a char. The chars were then gasified at 800°C in a 13% carbon dioxide/87% nitrogen atmosphere to obtain the smelt. Sulfur release was studied by pyrolyzing the samples at temperatures ranging from 300°C to 900°C. Liquors with the lowest lignin content had a smaller maximum swollen volume than the original sample. The devolatilization time was not affected by the lignin removal to any great extent, but lignin removal did have a clear effect on the char burning time. The amount of formed nitric oxide (g N/kg black liquor solids) remained constant or decreased slightly with increasing lignin removal in the kraft liquor samples, while for the soda samples the amount of nitric oxide formed increased. The amount of cyanate decreased clearly when comparing the samples with lowest lignin content to the original liquor samples. The peak sulfur release occurred at 500°C for both kraft liquors. In almost all experiments, the share of sulfur released was highest for the original samples and lowest for the sample with lowest lignin content. These results provide new data on combustion properties for reduced-lignin black liquors and indicate that for lignin removal levels up to about 20%, no significant changes are expected in the combustion behavior.

Application: This work will help mills identify the effect of lignin precipitation on combustion properties of black liquor.

The pulp and paper industry is identifying possibilities in new value-added products from biomass to increase revenues. One possibility is the use of lignin that could be applied to various applications in the chemical industry [1-3]. The removal of lignin is also an option to increase the pulping capacity, if the recovery boiler is the bottleneck of the pulp mill. The separated lignin can be used in the pulp mill to replace fossil fuels used in the lime kiln [4,5] as a first step until new markets open up for lignin as a biomaterial.

Up to 70% of lignin from low dry solids (<30% dry solids) kraft black liquor can be separated by lowering the pH of the black liquor with carbon dioxide (CO_2) to pH 10 [6-8]. One such process based on this concept is the LignoBoost process (**Fig. 1**). Carbon dioxide is added to a stream of black liquor (30-45 wt% dry solids) taken from the evaporation plant. The precipitated lignin is then filtered off and the filtrate is pumped back to the evaporation plant. The precipitated lignin is dispersed in a solution acidified with sulfuric acid (H_2SO_4) and the lignin is filtered off a second time. The filter cake is washed with warm water acidified with H_2SO_4; part of the filtrate is pumped back to the early stages of evaporation and part is used to disperse lignin from the first filtration. The amount of lignin removed from the black liquor sent to the process is approximately 70%. By treating a larger stream of black liquor, more filtrate is produced and then blended back in with the liquor to the recovery boiler. This results in as-fired black liquor with lower lignin content.

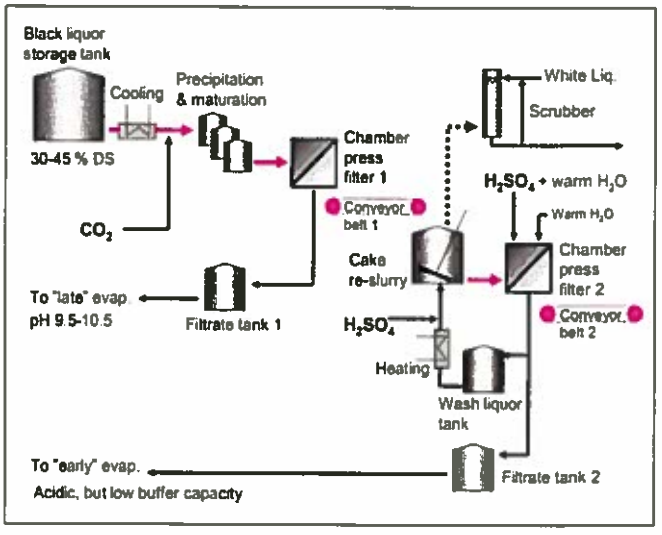

1. General layout of the LignoBoost lignin removal process.

Lignin is 30%-45% of the dry solids in black liquor [9].

Hardwood and softwood kraft lignins have higher heating values (i.e., 23-27 MJ/kg), while kraft black liquor has a much lower high heating value (i.e., 13-15 MJ/kg) [10,11]. Therefore, the removal of lignin from black liquor will decrease the high heating value of black liquor. On the basis of the changes in black liquor composition with varying levels of lignin removal, mathematical calculations estimate that up to 20% lignin removal is possible without any considerable changes in recovery boiler operation. Also, the estimated minimum load at which the recovery boiler can operate without support fuel is 40%-50% lignin removal [11,12].

Recovery boiler NO_x emissions come from nitrogen (N) in the black liquor [13]. The N content of lignin is higher than black liquor so black liquor N will be reduced with lignin reduction [10,11]. Thus, one of the questions is whether lignin removal will affect nitric oxide (NO) emissions from black liquor. Lignin is the primary source of organic N in the char [14] and may affect char N more than pyrolysis N. Char N forms the inorganic compound cyanate during char conversion [15,16]; for this reason cyanate formation was studied for different levels of lignin removal.

Roughly 65% of the sulfur (S) in black liquor is present as inorganic compounds (i.e., sulfide, thiosulfate, sulfite, and sulfide) [9,17] and the remaining 35% as a wide variety of organic bound sulfur compounds [18]. With lignin removal, a fraction of the organic bound sulfur is removed from black liquor, meaning that the ratio between inorganic and organic sulfur will be changed.

The S content of the reduced-lignin black liquor increases slightly with increased lignin removal [11,12] because the removed lignin has lower S content than the original black liquor from which it is precipitated. The partial recycling of used acidified solution to black liquor evaporation will further increase the total S content of the black liquor and the share of inorganic S in black liquor.

The S in black liquor is released during pyrolysis mainly as methyl mercaptans, dimethly sulfide, dimethly disulfide, or hydrogen sulfide (H_2S) [19-22]. The main contributors to volatile sulfur compound formation are sulfide, thiosulfate, and organic sulfur compounds found in black liquor, while sulfite and sulfate do not result in volatile sulfur formation [23,24]. Lignin methoxyl groups reacting with HS- have been hypothesized as a route to mercaptan formation [20,25].

	Soda	
	Lignin Content mg / g d.s.	**Kjeldahl N (wt-% d.s.)**
Black liquor	391	0.071%
8.4% lower lignin	358	0.066%
30% lower lignin	274	0.063%

I. Lignin and nitrogen content of the soda liquor samples.

Thus, the impact of lignin removal on S release during the devolatilization stage of black liquor combustion was of interest in this work.

A single-particle reactor was used to determine the impact of lignin removal on the combustion properties of black liquor. The properties studied were maximum swollen volume, combustion times, NO formation during combustion, amount of cyanate in smelt, and release of S during pyrolysis. Intermediate levels of lignin reduction were obtained by mixing the weak black liquors and filtrates.

EXPERIMENTAL

The lignin removal of the soda liquor from hardwood pulping was conducted at Chalmers University of Technology, and the removal of lignin from kraft black liquors from softwood and eucalyptus pulping was conducted at Innventia AB. One original soda liquor sample and two samples with levels of lignin reduction were obtained from Metso Power Oy. The soda liquor was generated in a laboratory cook. The received soda samples had dry solids content of <41% and were dried to >74% dry solids before the tests in the single-particle reactor. The lignin and N contents of the soda liquor samples are given in **Table I**. The lignin content of soda liquors was determined by UV spectrophotometry, and the total N content of samples was analyzed with a modified Kjeldahl method using the Devarda alloy (CAS No. 8049-11-4) based on Finnish Standards Association (SFS) 5505 "Wastewater inorganic and organic nitrogen determination."

Both the softwood and hardwood (*Eucalyptus globulus*) kraft black liquors used in this study were processed in bench-scale equipment, similar to what has been used earlier [6]. The process was operated as follows. Industrial kraft black liquors (~40% DS) were used and the pH was lowered to about 10 by addition of CO_2 (g), causing the lignin to precipitate (**Fig. 2**). The precipitated lignin was separated by filtration (chamber press filter), referred to as filtration 1. The lignin filter cake was then resuspended at pH 2-3, using sulfuric acid solution. The lignin slurry was filtered once more (filtration 2) and the separated lignin cake was washed with acidified water at pH 2-3. After washing, the lignin cake was dewatered by pressing and by blowing compressed air through the filter cake. All filtrates were collected and mixed. These mixtures were used to represent the filtrate mixture that would be obtained in a full-scale LignoBoost plant.

Two kraft liquor samples (one softwood and one eucalyptus) before lignin removal and two filtrates were obtained. The softwood filtrate had 54.6±5% lower lignin content than the softwood black liquor and the eucalyptus filtrate had 43.6±5% lower lignin content than the eucalyptus black liquor. The received samples had dry solids content of <25%. For both black liquors, the original sample and filtrate were mixed to obtain two more samples with different levels of lignin content. The lignin, S, and N contents of the obtained and mixed kraft liquor samples are shown in Table II. The samples were dried in an oven at 105°C to a dry solid content

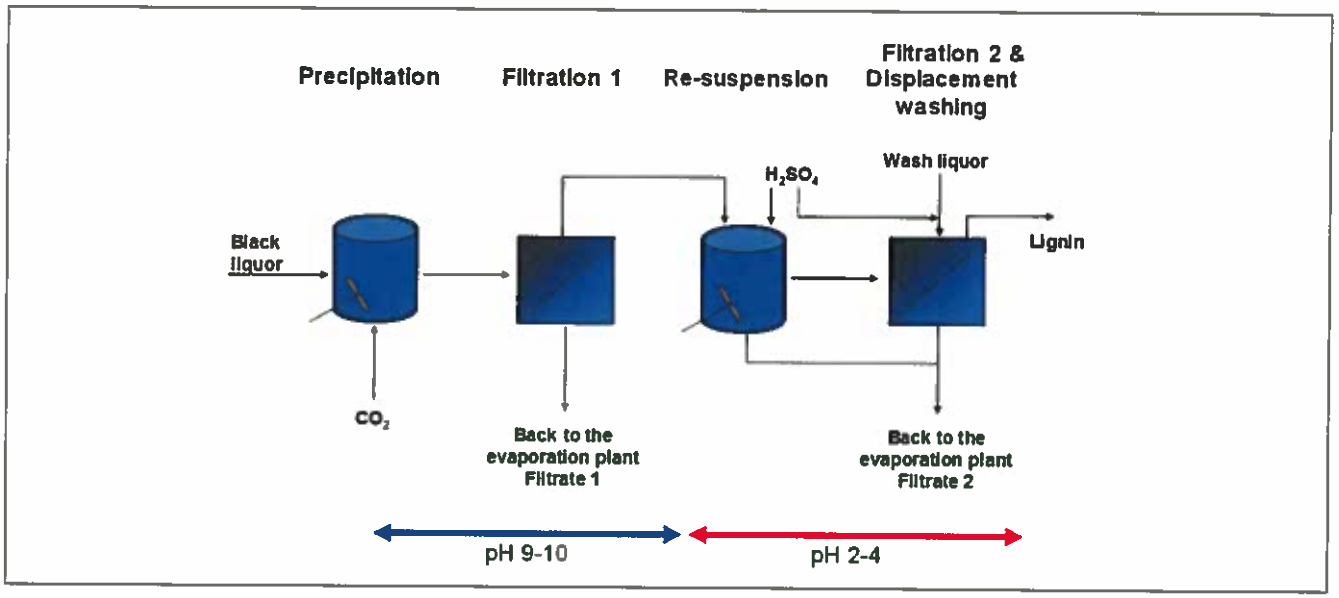

2. Schematic figure of the bench-scale equipment used for lignin removal.

of approximately 85% before the tests in the single-particle reactor.

The lignin content shown in **Table II** for the kraft liquors was analyzed using TAPPI T 222 om-02 "Gravimetric determination of acid-insoluble lignin" and UV spectrophotometry (acid soluble lignin). The total N content of selected samples was analyzed with a modified Kjeldahl method using the Devarda alloy (CAS No. 8049-11-4) based on SFS 5505; the S content was analyzed using SCAN-N 38:10 "Acid-soluble metals."

Combustion, cyanate formation, and S release experiments were conducted in a laboratory-scale quartz glass reactor as illustrated in **Fig. 3** [26]. The temperature and the atmosphere in the quartz glass reactor can be adjusted. Six droplets weighing 10±0.5 mg of each sample were suspended on platinum hooks and combusted at 900°C in a 10% O_2/90% N_2 atmosphere. The formed NO emissions were measured with a Model 200EM chemilumenescence analyzer (Teledyne Technologies; Thousand Oaks, CA, USA). The combustion was recorded with a video camera to determine the maximum swollen volume and the combustion times.

The maximum swollen volume of the droplet is estimated by capturing an image from the recorded video. The captured two-dimensional image is compared to an area of a circle or

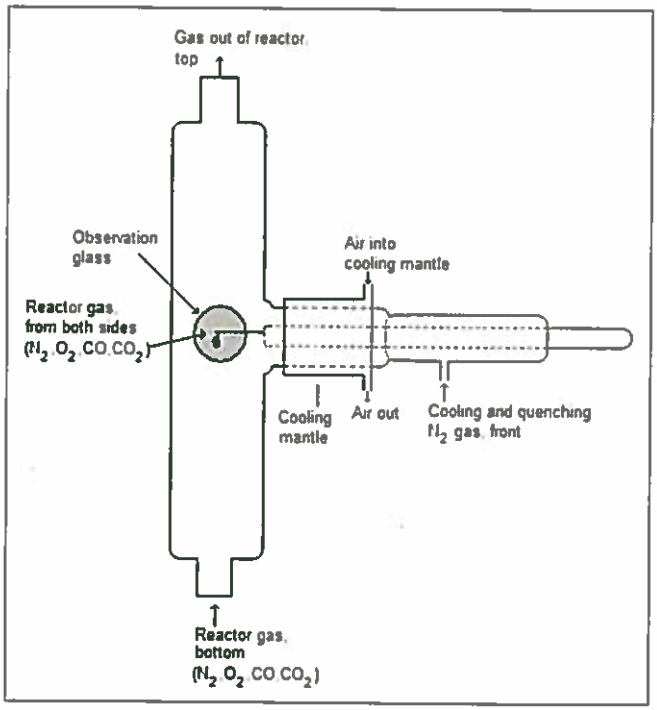

3. Schematic drawing of the quartz glass reactor used in the experiments.

	Lignin Content mg/ g d.s.	Softwood Sulfur Content wt-% d.s.	Kjeldahl N (wt-% d.s.)	Lignin Content mg / g d.s.	Eucalyptus Sulfur Content wt-% d.s.	Kjeldahl N (wt-% d.s.)
Black liquor	366	6.11%	0.062%	429	5.10%	0.086%
10% lower lignin	329.4*	6.56%*	0.060%*	386.1*	5.76%*	0.082%*
25% lower lignin	274.5*	7.25%*	0.057%*	312.75*	6.76%*	0.077%*
Filtrate	166	8.58%	0.052%	242	7.99%	0.070%
* Calculated based on the analysis of black liquor and filtrate.						

II. Lignin and sulfur content of the kraft black liquor samples before evaporation.

an ellipse, which is then used to calculate the volume of a corresponding sphere or ellipsoid. In this work, the maximum swollen volume is represented as cm^3/g of dry solids.

The combustion of black liquor droplets can be divided into four stages: (1) drying, (2) devolatilization, (3) char burning, and (4) smelt coalescence [27]. The times for the different combustion stages were determined from the recorded video. The drying time was not determined in these experiments, because the sample dried before it entered the combustion chamber. Devolatilization time is defined as the time from the appearance of the flame to the disappearance of the flame. The droplets often ignited as they entered the combustion zone; thus, pyrolysis times can be slightly longer (by about 0.5 s) than what is observed. The char burning time is defined as the time from the point where the visible flame disappears to the point where smelt coalescence occurs.

The cyanate formation in the samples was determined by pyrolyzing six droplets (10±0.5 mg) of each sample in the quartz glass reactor at 800°C in 100% N_2 for 10 s to form a char. The chars were then gasified at 800°C in 13% CO_2/87% N_2 to obtain smelts. The formed smelts were dissolved in ion exchange water using a ratio of 1.25 mg smelt:1 mL ion exchange water and filtered. The filtrates were analyzed for cyanate with ion chromatography using a Metrosep Anion Dual 2 column and conductivity detector (Metrohm AG; Herisau, Switzerland) [28].

The S release for the kraft liquor samples was measured in the quartz glass reactor by pyrolyzing six droplets (10±0.5 mg) of each sample at 300°C, 500°C, 700°C, and 900°C in 100% N_2 atmosphere. After the quartz glass reactor a flow of pure oxygen was added to the flue gas. The oxygen content in the flue gas was around 4–5 vol% and was measured with a Servopro 4900 continuous emissions analyzer (Servomex; Crowborough, UK). The flue gas flow containing oxygen was then introduced to an SCC-K catalytic converter (ABB; Zurich, Switzerland) to oxidize released sulfur species to sulfur dioxide (SO_2). The released S was measured as SO_2 with an ABB AO2020 infrared analyzer. The total amount of S released was calculated based on the SO_2 measurement and the total flue gas flow before dilution with oxygen [26].

RESULTS AND DISCUSSION

Combustion characteristics of reduced-lignin black liquors

The combustion times; maximum swollen volume; and distribution between volatile matter, fixed carbon, and smelt for the softwood kraft liquor samples is shown in **Fig. 4** and for the eucalyptus samples in **Fig. 5**. The devolatilization time was around 1 s for all of the samples, and no clear difference between devolatilization time and the level of lignin content in the samples was detected. This was consistent with the idea that the dissolved hemicelluloses are the main source of volatile products in black liquor combustion [14]. For the softwood samples the char burning time and total combustion time decreased with increasing lignin removal, while the op-

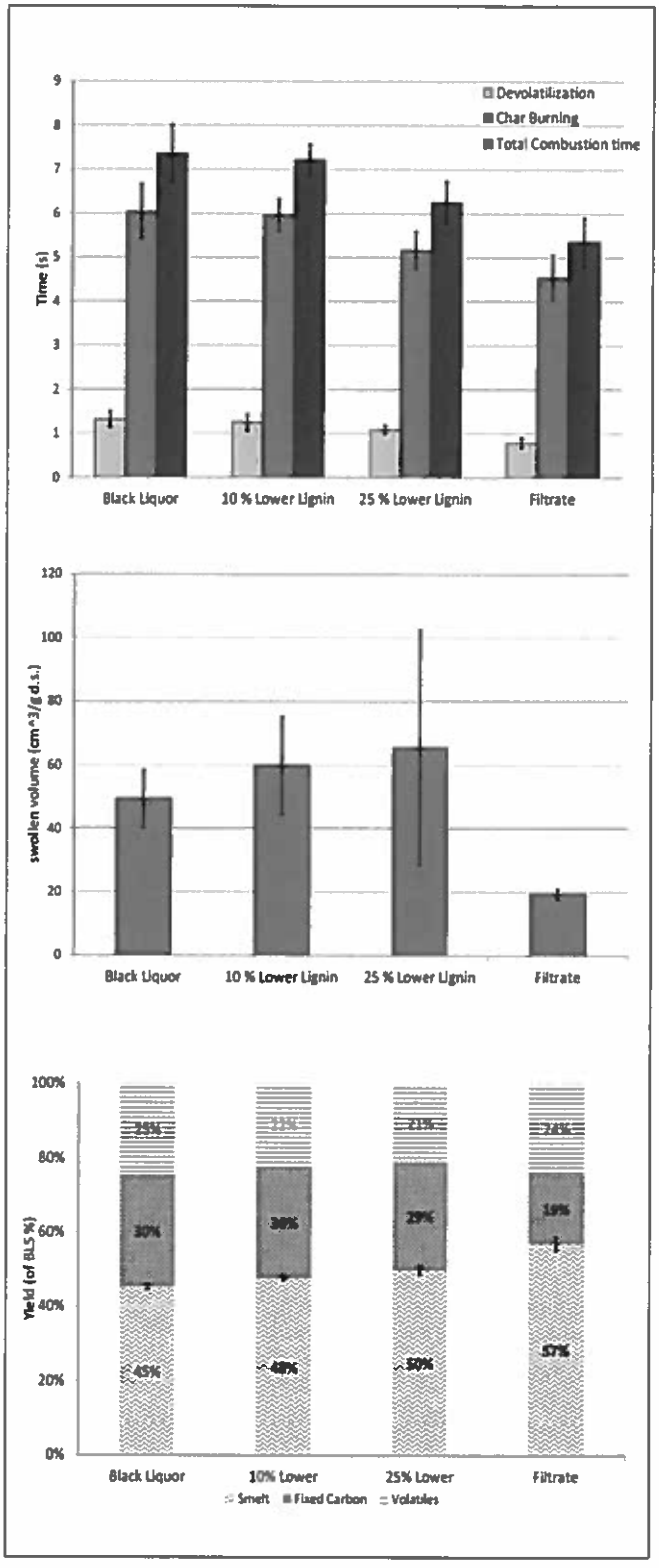

4. Combustion times (top) and maximum swollen volume (middle) from experiments conducted at 900°C at 10% oxygen/90% nitrogen. Distribution of volatile matter, fixed carbon, and smelt (bottom) calculated based in weighed initial samples, chars, and smelts from the cyanate formation experiments of softwood kraft liquor samples. Error bars represent one standard deviation of six droplets.

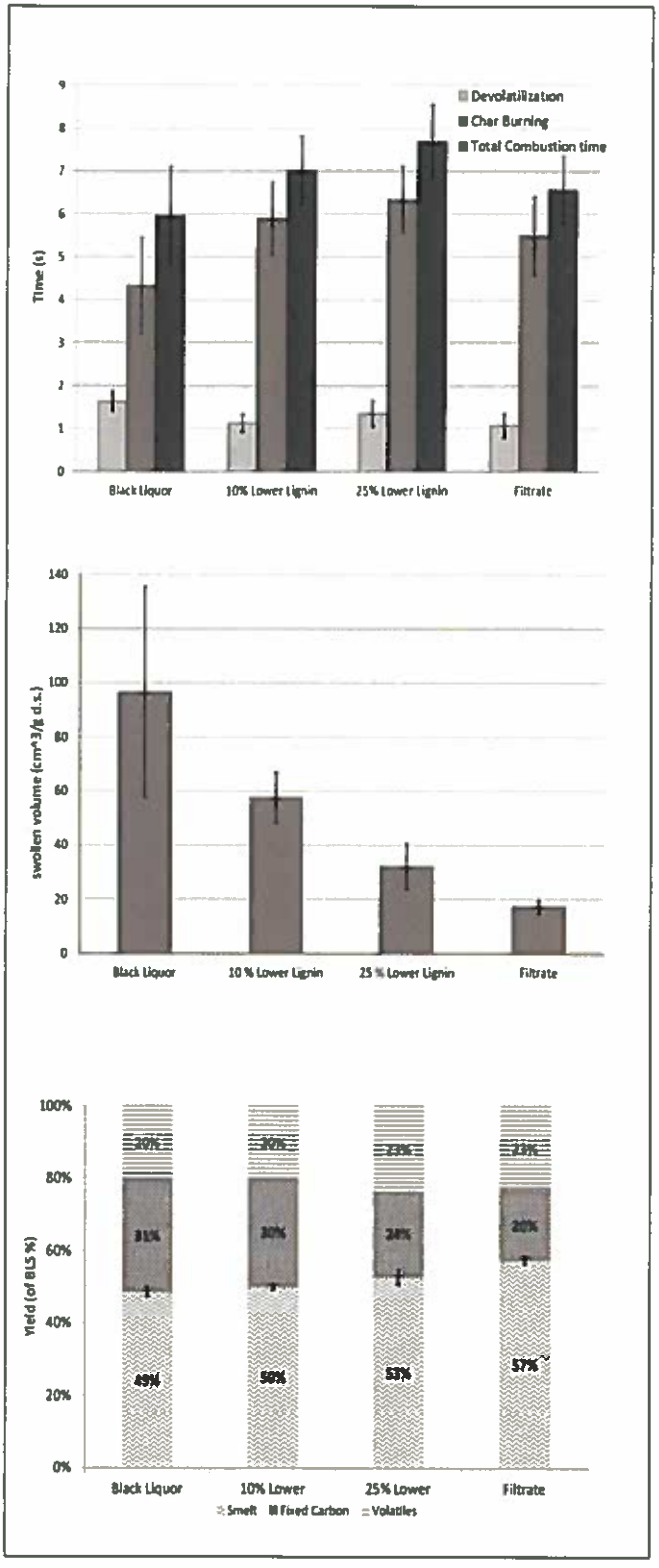

5. Combustion times (top) and maximum swollen volume (middle) from experiments conducted at 900°C at 10% oxygen/90% nitrogen. Distribution of volatile matter, fixed carbon, and smelt (bottom) calculated based in weighed initial samples, chars, and smelts from the cyanate formation experiments of eucalyptus kraft liquor samples. Error bars represent one standard deviation of six droplets.

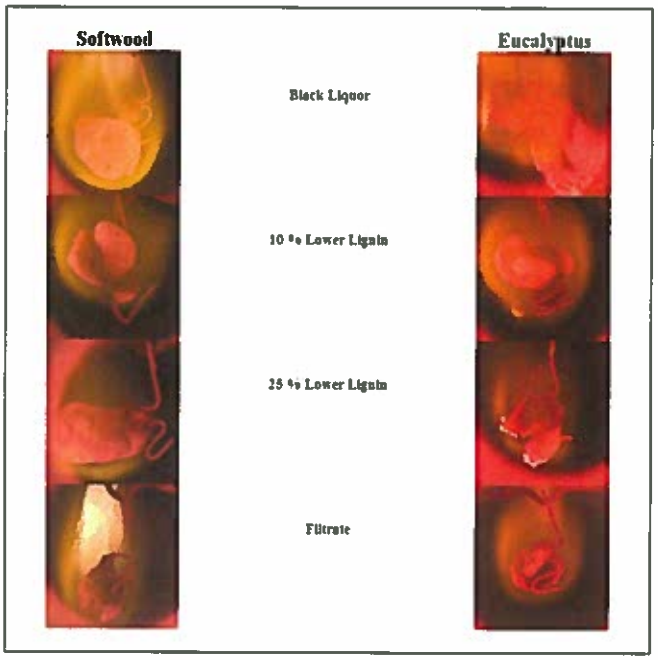

6. Maximum swollen volume images of the kraft liquor samples.

posite was observed for the eucalyptus sample. This reduced char burning time was most likely due to the combined effects of slightly increased swelling and the reduced organics in the black liquor, specifically the lignin that will contribute to char formation. Increased lignin removal decreased the share of fixed carbon and increased the share of smelt as seen in Figs. 4 and 5. The eucalyptus black liquor had considerably larger maximum swollen volume than the softwood black liquor. The swelling for the eucalyptus black liquor samples decreased with increasing lignin reduction, which may be the reason for slightly higher average char burning times despite lower organic content. Alén et al. [29] showed that hardwood lignin swelled more than softwood lignin because the presence of xylan increases swelling. The ratio between hemicelluloses and lignin affects the swelling, and at a certain ratio maximum swelling occurs. This could be one reason for the difference in the average maximum swollen volume pattern for the eucalyptus and softwood samples. In both cases, the filtrate swelled considerably less than the original sample. The high standard deviations seen in the maximum swollen volume can be explained by nonuniform swelling of black liquor and use of two-dimensional images for estimating volume. **Figure 6** shows captured maximum swollen volume images for different kraft black liquor samples.

The combustion times; maximum swollen volume; and distribution between volatile matter, fixed carbon, and smelt of soda liquor with different lignin content are shown in **Fig. 7**; the capture maximum swollen images are shown in **Fig. 8**.

The devolatilization time and the share of volatile matter slightly increased with increasing lignin removal. The char burning time and total combustion time increased and the maximum swollen volume decreased with increasing lignin

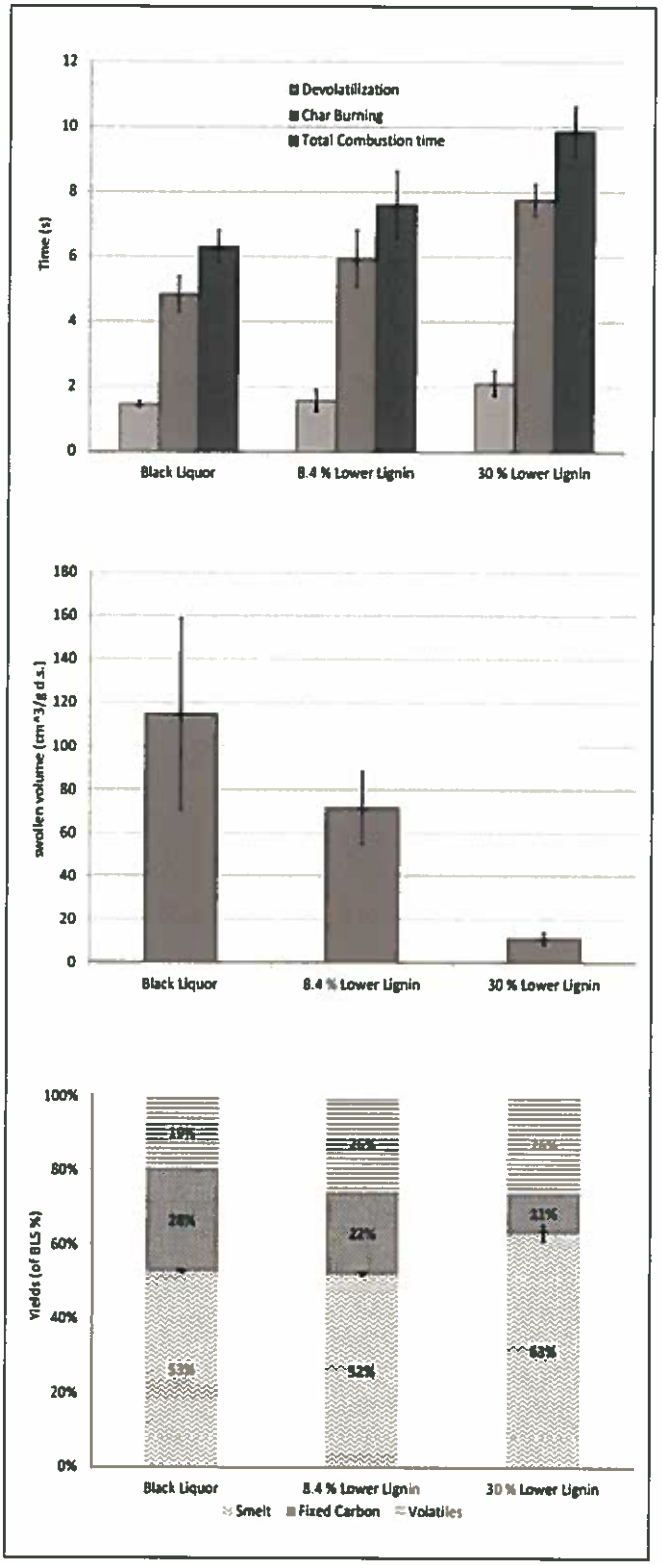

7. Combustion times (top) and maximum swollen volume (middle) from experiments conducted at 900°C at 10% oxygen/90% nitrogen. Distribution of volatile matter, fixed carbon, and smelt (bottom) calculated based in weighed initial samples, chars, and smelts from the cyanate formation experiments of soda liquor samples. Error bars represent one standard deviation of six droplets.

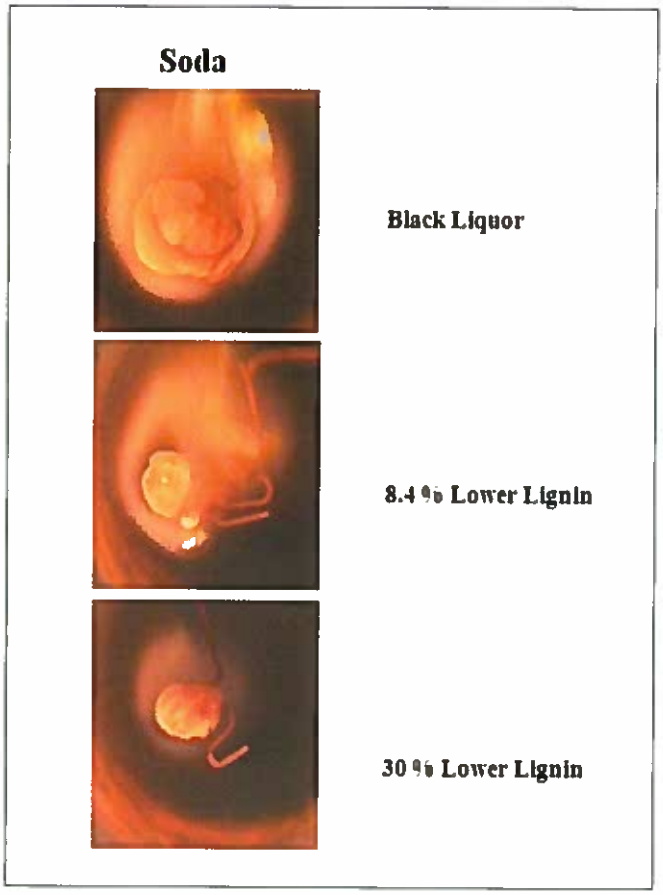

8. Maximum swollen volume images of the soda liquor samples.

removal for the soda liquor samples. The amount of smelt increased with increasing lignin removal, while the amount of fixed carbon decreased. The char burning times clearly depend on the maximum swollen volume and the amount of fixed carbon left in the char.

NO formation

The NO formation (as g N/kg dry black liquor) for the eucalyptus and softwood samples are shown in **Fig. 9**. For both black liquors, the NO formation decreased with increasing lignin removal. Part of the black liquor N is removed with lignin, which lowers the N content of the lignin-reduced black liquor compared with the original black liquor samples shown in Table II. The conversion of fuel N to NO was roughly 40% for the eucalyptus samples and roughly 45% for the softwood samples. This includes NO formed during pyrolysis and NO from char burning. In a recovery boiler, much of the char N will exit the recovery boiler as cyanate in the smelt.

The NO formation (as g N/kg dry black liquor) slightly increased for the soda liquor with 30% lower lignin content compared to the original soda liquor, as shown in **Fig. 10**. An equal amount of NO was formed from the 8.4% lower lignin sample and original sample. In the soda liquor samples, N content also decreased with increasing lignin removal, while the amount of formed NO increase remains unknown. The conversion of fuel N to NO was roughly 45% for the original

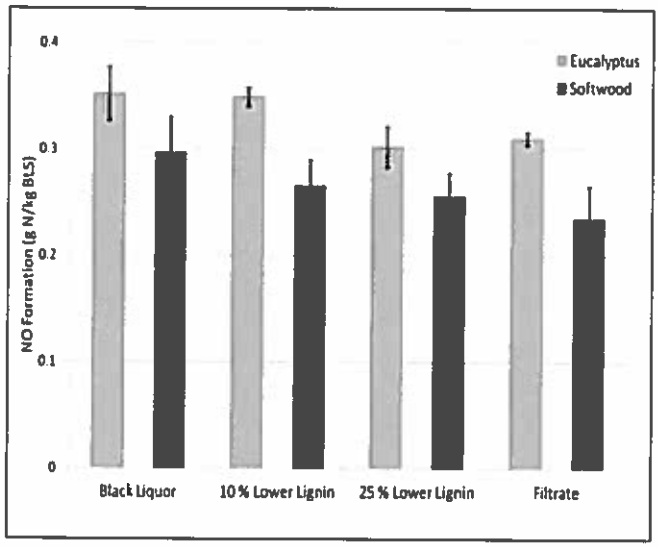

9. Average nitric oxide formation of softwood and eucalyptus kraft liquor samples. Experiments conducted at 900°C at 10% oxygen/90% nitrogen. Error bars represent one standard deviation of six droplets.

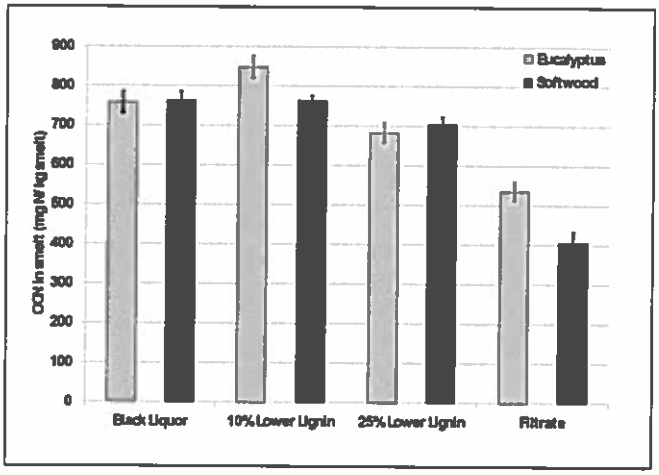

11. Cyanate formation after pyrolysis (10 s at 800°C at 100% nitrogen) and gasification (800°C in 13% carbon dioxide/87% nitrogen) to smelt for eucalyptus and softwood kraft liquor samples. Error bars represent one standard deviation of six ion chromatography analyses.

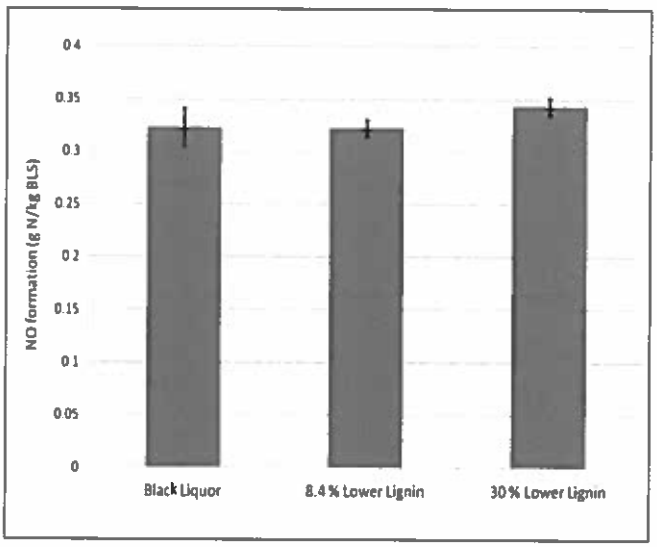

10. Average nitric oxide formation of soda liquor samples. Experiments conducted at 900°C at 10% oxygen/90% nitrogen. Error bars represent one standard deviation of six droplets.

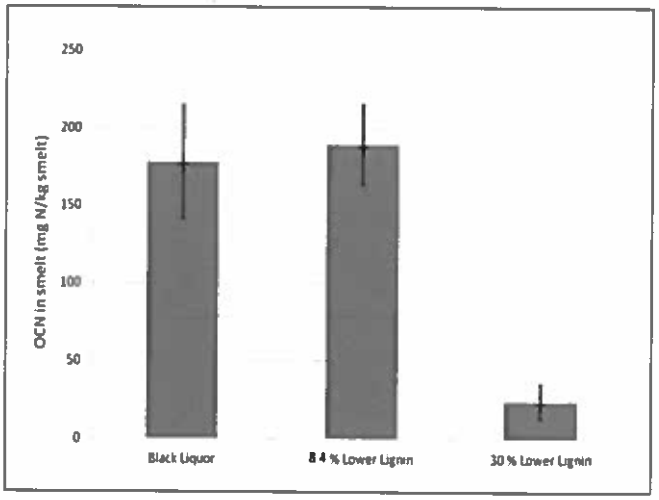

12. Cyanate formation after pyrolysis (10 s at 800°C at 100% nitrogen) and gasification (800°C in 13% carbon dioxide/87% nitrogen) to smelt for soda liquor samples. Error bars represent one standard deviation of six ion chromatography analyses.

soda sample and increased to approximately 55% for the 30% lower lignin sample.

Cyanate of reduced-lignin black liquors

Cyanate formation (as mg N/kg smelt) for the softwood and eucalyptus samples is shown in **Fig. 11**. The amount of formed cyanate from the 10% lower lignin eucalyptus sample slightly increased when compared with the original sample, while the amount of cyanate formed from the 10% lower lignin softwood sample and original sample are equal. In both kraft liquors, less cyanate was formed from the 25% lower lignin and filtrate samples compared with the original black liquor samples. The fuel N to cyanate conversion for the eucalyptus samples was between 40% and 50%, and the lowest conversion occurred for the original black liquor sample. Roughly 47% of the softwood filtrates N was converted to cyanate. For the rest of the softwood samples, the fuel N to cyanate conversion was between 57% and 62%. It has been shown that reaction between alkali salts (i.e., sodium and potassium carbonate) and the char N results in cyanate formation [30]. The reason for the increase in cyanate formation from the eucalyptus liquor sample with a 10% lower lignin content is not clear. The ratio between inorganic and organic compounds in the fuel and the amount of inorganic compounds in the char or simply a higher char N content may be possible explanations, but further work would be needed to clarify this question.

Figure 12 shows the cyanate formation (as mg N/kg smelt) for the soda liquor samples. The amount of formed

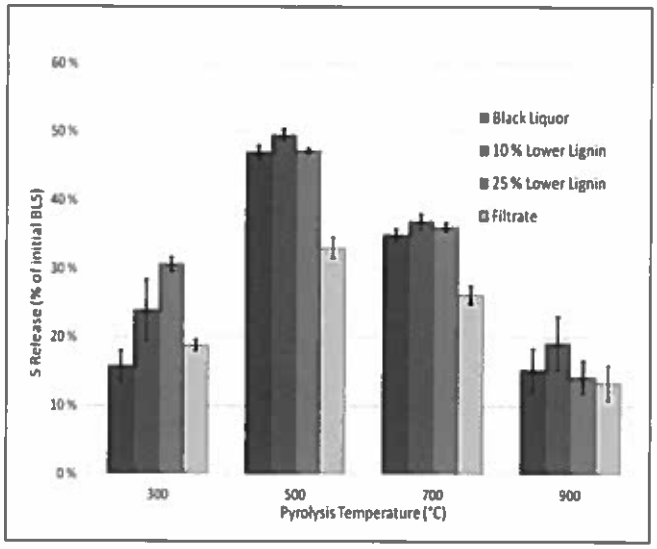

13. Sulfur release of softwood black liquor samples during pyrolysis (100% nitrogen) at different temperatures. Error bars represent one standard deviation of six droplets.

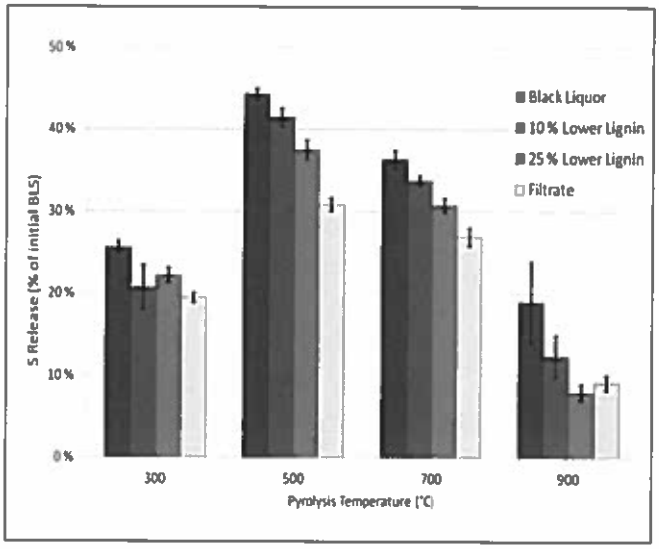

14. Sulfur release of eucalyptus black liquor samples during pyrolysis (100% nitrogen) at different temperatures. Error bars represent one standard deviation of six droplets.

cyanate slightly increased for the 8.4% lower lignin sample when compared with the original sample. Almost no cyanate was formed from the 30% lower lignin sample. One reason behind the low cyanate formation is that soda liquor samples did not form a smelt at these conditions. The remaining residue still looked partially swollen and thus the char was not fully converted to smelt. Previous studies show that when gasification is conducted at 800°C, maximum conversion occurs when almost 100% of the char is converted [16]. The levels of cyanate formed represent 14% of the fuel N converted to cyanate for the black liquor and the 8.4% lower lignin sample and only 2% for the 30% lower lignin sample.

Sulfur release of reduced-lignin black liquors

Sulfur release during pyrolysis was measured at different temperatures for the softwood samples (**Fig. 13**) and the eucalyptus samples (**Fig. 14**). Softwood and eucalyptus samples showed S release peaks at 500°C and decreases with increasing temperature. This has also been observed in previous studies [20,21]. For the softwood black liquor and the 10% and 25% lower lignin samples, the share of S released was quite similar when the pyrolysis was conducted at 500°C, 700°C, and 900°C. However, at 300°C, the share of S released was clearly higher for the 10% and 25% lower lignin samples than for the original black liquor sample. The share of S released from the softwood filtrate sample was clearly lowest of all the samples when the pyrolysis was conducted at 500°C and 700°C. For the eucalyptus samples, the share of S released was highest for the black liquor sample in all of the pyrolysis experiments and lowest for the filtrate sample, except when the pyrolysis was conducted at 900°C. For the S release experiments conducted for the eucalyptus samples, the share of S released was lower for the liquors with lower lignin content.

The removal of a portion of the organic sulfur with the precipitated lignin, along with the recycling of H_2SO_4 acidified washing solution back to the black liquor, affects the distribution of sulfur species found in black liquor. Previous studies have shown that at most only a very small fraction of the SO_4^{2-} results in S release during black liquor pyrolysis [23,24]. Therefore, the share of S released from lignin-reduced liquors was expected to be lower compared with the original black liquor before lignin removal. While this was observed for the eucalyptus liquors (Fig. 14), this was not the case for the softwood black liquor samples with 10% or 25% lower lignin where S release on black liquor dry solids was the same or increased slightly.

CONCLUSIONS

This research gives new information regarding the combustion properties of reduced-lignin black liquors. The removal of lignin decreased the N content of all of the liquor samples. The use of acidified warm-water H_2SO_4 solution in washing of lignin increased the sulfur content of kraft liquor samples. Lignin removal also reduced the organic content of the black liquor and can affect both swelling and char burning. In all samples, the char burning time was affected by lignin removal, while no clear difference could be seen in the devolatilization time. These changes in combustion time were small and will not result in any observable change in char burnout in a recovery boiler. The changes in maximum swollen volume were fairly significant and could slightly affect carryover, but sheet breakup and droplet formation from the liquor spray need to be studied before any predictions can be made about the effect of swelling changes on carryover.

The NO formation was not greatly affected by lignin removal, and NO emissions from the recovery boiler on a dry solids basis are not expected to be significantly affected by lignin removal. However, on a per ton of pulp basis, NO emis-

sions should go down as the flow of as-fired black liquor solids/ton of pulp will decrease. The concentration of cyanate in the smelt will likely be quite similar to the original black liquor, at least at 10% lignin reduction. The lower furnace temperature and air distribution are expected to influence cyanate decomposition; therefore, lignin reduction also may indirectly influence the amount of cyanate exiting the boiler with the smelt.

Assuming the temperature at which devolatilization happens in the recovery boiler is the same, S release from reduced lignin black liquor is expected to be the same or slightly lower than for the original black liquor. This clearly can be seen at all temperatures for the eucalyptus black liquor. For the softwood liquor this is less clear, but when looking at S release at 900°C for the softwood black liquor, there is little difference with lignin reduction. Older boilers with lower temperatures at the gun level and char bed will need to adjust firing with reduced-lignin black liquor to keep up the temperature; otherwise, S emissions could increase due to a cooler lower furnace, which can result in higher S release from black liquor. The influence of lignin removal on S release should be studied in more detail to better understand what role, if any, lignin has on the formation of volatile sulfur compounds.

On the basis of this work, the combustion of reduced-lignin black liquors in the recovery boiler furnace is possible without any major changes. Mill trials with reduced black liquor firing would provide more details on variables such as sheet formation and droplet formation during spraying. **TJ**

ACKNOWLEDGEMENTS

The authors acknowledge the Graduate School in Chemical Engineering (GSCE) for the scholarship supporting Niklas Vähä-Savo. This work has been carried out within the Future fuels for Sustainable Energy Conversion (FUSEC) project (2011–2014) as part of the activities of the Åbo Akademi Process Chemistry Centre. Support from the National Technology Agency of Finland (Tekes), Andritz Oy, Metso Power Oy, Foster Wheeler Energia Oy, UPM-Kymmene Oyj, Clyde Bergemann GmbH, International Paper Inc., and Top Analytica Oy Ab is gratefully acknowledged.

LITERATURE CITED

1. Kadla, J.F., Kubo, S., Venditti, R.A., et al., *Carbon* 40(15): 2913(2002).
2. Borges da Silva, E.A., Zabkova, M., Araujo, J.D., et al., *Chem. Eng. Res. Des.* 87(9): 1276(2009).
3. Gosselink, R., "Lignin as a renewable aromatic resource for the chemical industry," Ph.D. thesis, Wageningen University, Wageningen, Netherlands, 2011.
4. Richardson, B. and Uloth, V.C., *Tappi J.* 73(10): 191(1990).
5. Richardson, B., Watkinson, A.P., and Barr, P.V., *Tappi J.* 73(12): 133(1990).
6. Öhman, F., Wallmo, H., and Theliander, H., *Nord. Pulp Pap. Res. J.* 22(1): 9(2007).
7. Wallmo, H., Wimby, M., and Larsson, A., "Increase production in your recovery boiler with LignoBoost—extract valuable lignin for biorefinery production and replacement of fossil fuels," *TAPPI Eng., Pulping Environ. Conf.*, TAPPI PRESS, Atlanta, GA, USA, 2009.
8. Tomani, P., *Cellul. Chem. Technol.* 44(1–3): 53(2010).
9. Adams, T.N., in *Kraft Recovery Boilers*, TAPPI PRESS, Atlanta, 1997, p. 381.
10. Blunk, S.L., Jenkins, B.M., and Kadam, K.L., "Combustion properties of lignin residue from lignocellulose fermentation," National Renewable Energy Laboratory, Golden, CO, USA, 2000.
11. Vakkilainen, E. and Välimäki, E., "Effect of lignin separation to black liquor and recovery boiler operation," *TAPPI Eng., Pulping Environ. Conf.*, TAPPI PRESS, Atlanta, 2009.
12. Välimäki, E., Niemi, P., and Haaga, K., *Int. Chem. Recovery Conf.*, TAPPI PRESS, Atlanta, 2010, p. 148.
13. Forssen, H.M., Hupa, M., and Hellstrom, P., *TAPPI J.* 82(3): 221(1999).
14. Alen, R., *Bioresour. Technol.* 49(2): 99(1994).
15. Kymalainen, M., Forssen, M., Jansson, M., et al., *J. Pulp Pap. Sci.* 28(5): 151(2002).
16. Vähä-Savo, N., DeMartini, N., Hupa, M., *Energy Fuels* 25(11): 4944(2011).
17. Forssen, M., Frederick, W.J., Hupa, M., et al., *Proc. – For. Prod. Symp.*, TAPPI PRESS, Atlanta, 1992, p. 11.
18. Niemelä, K., "Low-molecular-weight organic compounds in birch kraft black liquor," Ph.D. thesis, Helsinki University of Technology, Helskinki, Finland, 1990.
19. Feuerstein, D.L., Thomas, J.F., and Brink, D.L., *Tappi* 50(6): 258(1997).
20. McKeough, P., Kurkela, M., Arpiainen, V., et al., *Int. Chem. Recovery Conf.*, TAPPI PRESS, Atlanta, 1995, p. A217.
21. Sricharoenchaikul, V., Frederick, W.J., and Grace, T.M., *J. Pulp Pap. Sci.* 23(8): J394(1997).
22. Vainio, E., Brink, A., Demartini, N., et al., *J. Pulp Pap. Sci.* 36(3–4): 135(2011).
23. Strohbeen, D.T. and Grace, T.M., *Tappi J.* 65(10): 125(1982).
24. Harper, F.D., "Sulfur release during the pyrolysis of kraft black liquor (combustion)," Ph.D. dissertation, Georgia Institute of Technology, Atlanta, Georgia, 1989.
25. McKeough, P., Kurkela, M., Kyllönen, H., et al., in *LIEKKI 2 Technical Review 1993–1998* (M. Hupa and J. Matinlinna, Eds.), Åbo Akademi University, Turku, Finland, 1998, p. 855.
26. Björkvik, T., "Measurement of sulfur release from black liquor droplets in a single particle reactor," M.S. thesis, Åbo Akademi University, Turku, Finland, 2010.
27. Hupa, M., Solin, P., and Hyoty, P., *J. Pulp Pap. Sci.* 13(2): J67(1987).
28. DeMartini, N., "Determination of cyanate in kraft green liquor," M.S. thesis, Åbo Akademi University, Turku, Finland, 2001.
29. Alen, R., Hupa, M., and Noopila, T., *Holzforschung* 46(4): 337(1992).
30. Vähä-Savo, N., DeMartini, N., and Hupa, M., *Energy Fuels* 25(11): 7108(2013).

LIITE 4

ÅA, Understanding Low Temperature Corrosion in BL Combustion – esitys

PROCESS CHEMISTRY CENTRE

ÅBO AKADEMI UNIVERSITY

Understanding Low Temperature Corrosion in Black Liquor Combustion

Niklas Vähä-Savo, Emil Vainio, Nikolai DeMartini, Patrik Yrjas & Mikko Hupa

Åbo Akademi

Overview

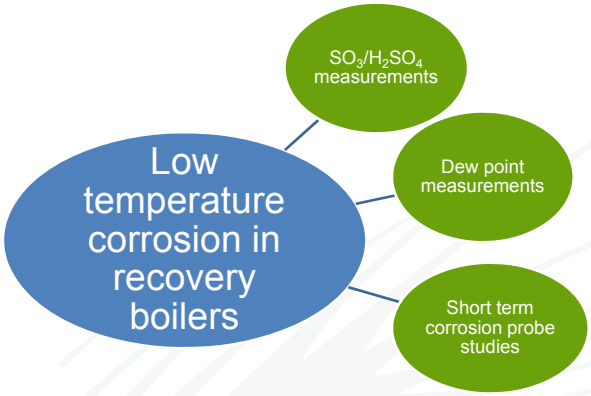

Measurement campaigns

Measurements
1. Kraft recovery boiler
2. Sulfite recovery boiler
3. During start-up with HFO

Measurements
1. $H_2SO_4(g)$
2. Dew point
3. Corrosion rate

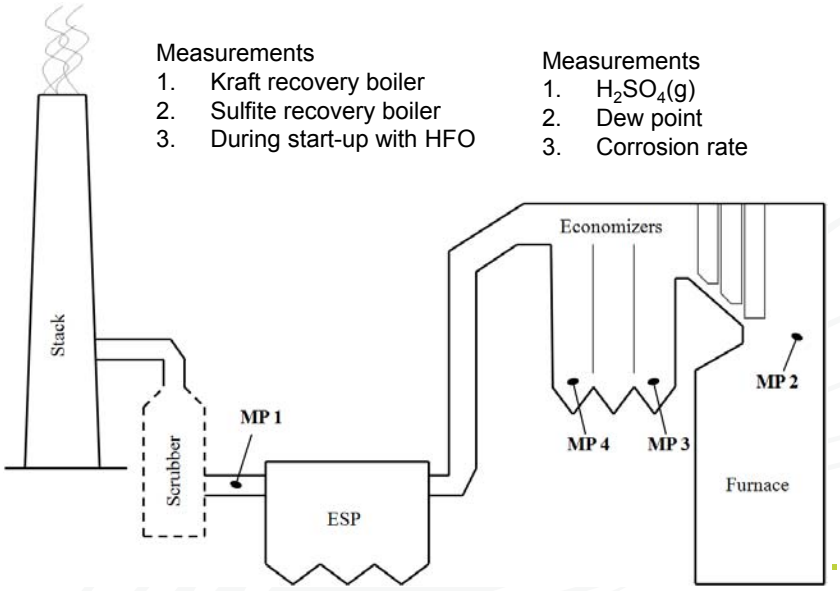

Conclusions

- The work showed that the studied boilers did not show any signs of potential to low temperature corrosion caused by the condensation of sulfuric acid during black liquor combustion
- During start-up with heavy fuel oil there might be a risk of condensing sulfuric acid
- An elevated dew point was observed due to hygroscopic salts

Dew point over salts

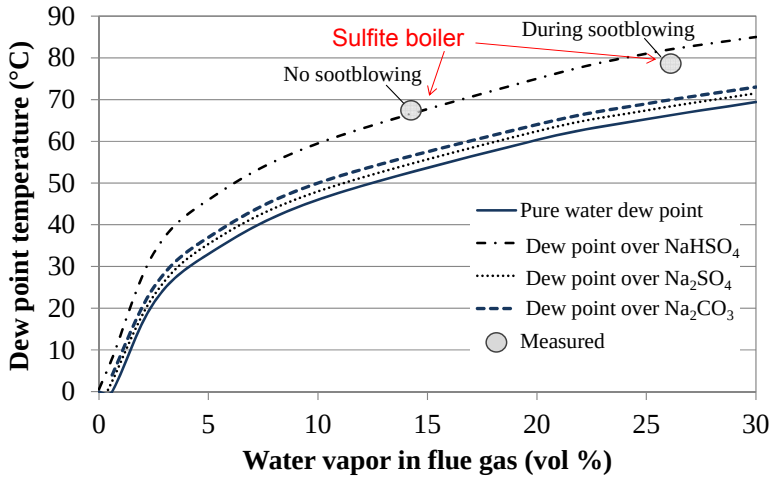

Overview

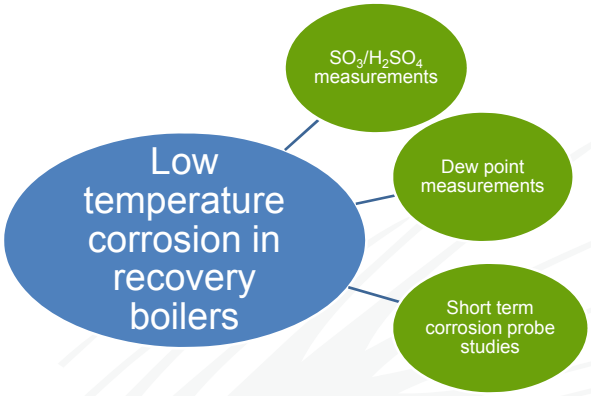

Overview

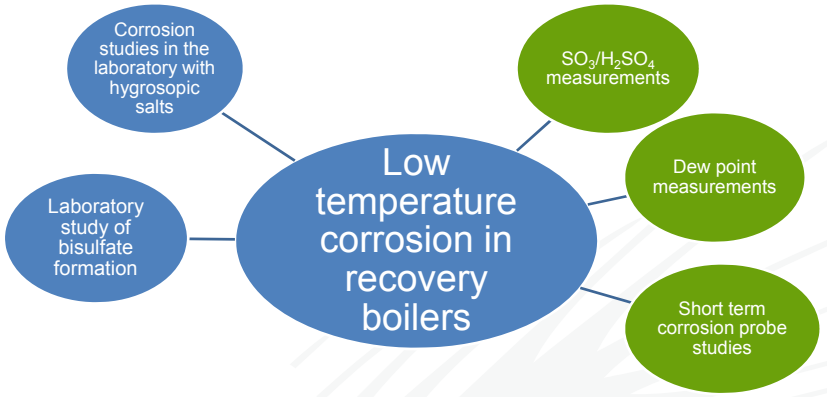

Overview

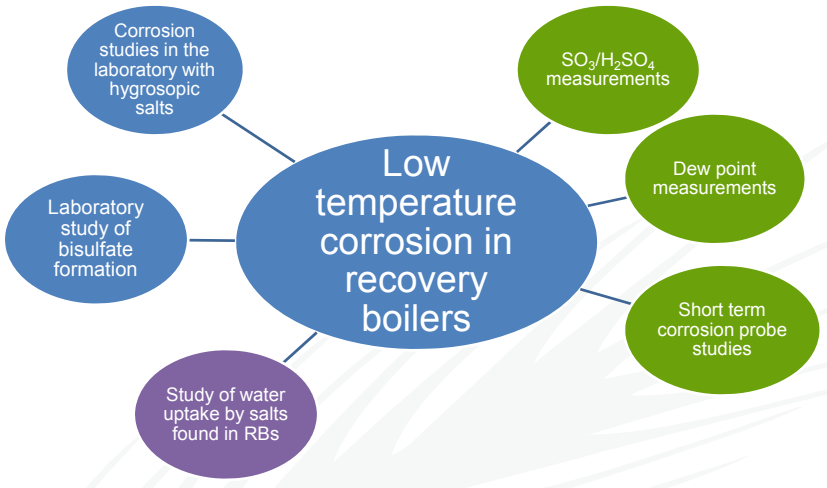

Water ”dew point” over salts

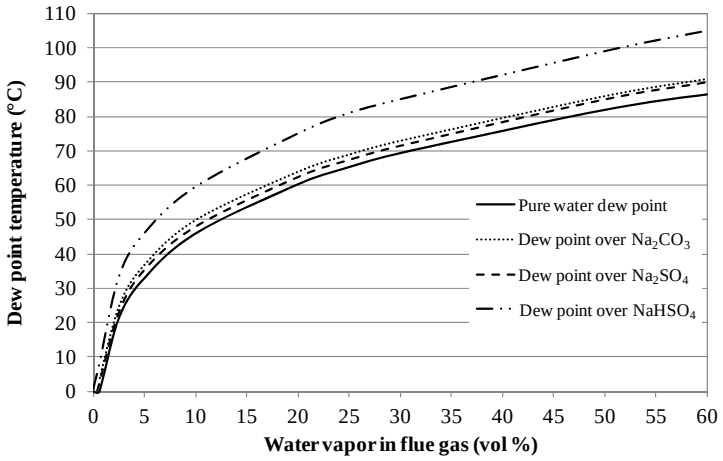

Objectives

- Understand the role of hygroscopic salts on low temperature corrosion for various water vapor concentrations
- Build a setup to study this with controlled conditions and with an even flow of water vapor (60 vol%) at 90-120°C

Experimental setup

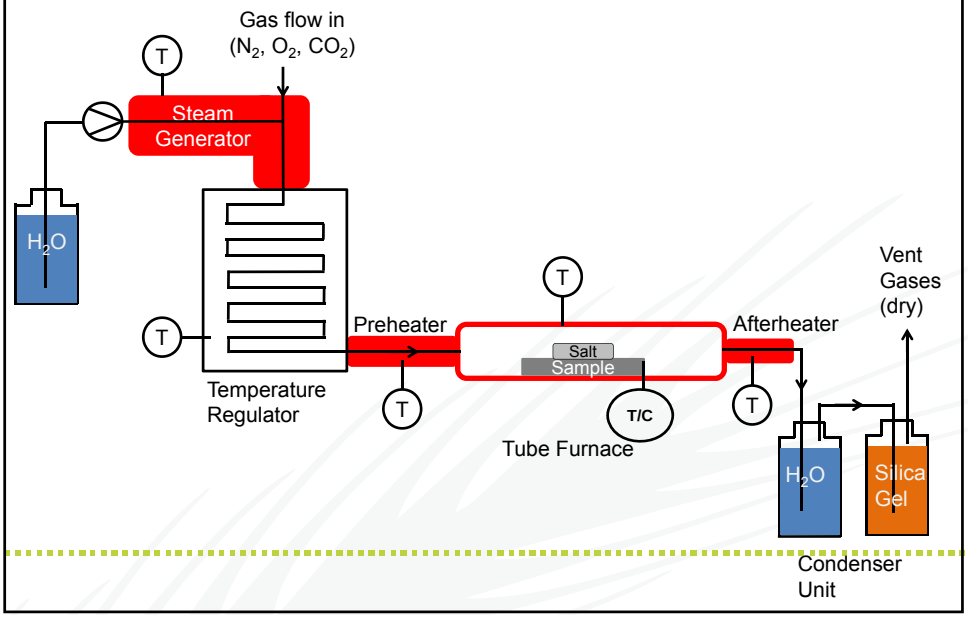

Experimental setup

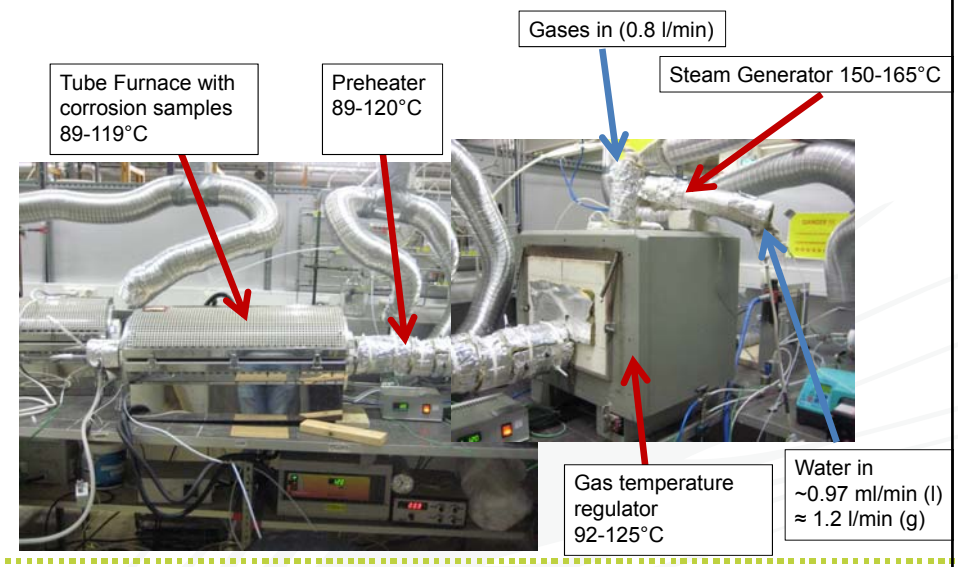

Experimental work

- corrosion sample:
  - 2x2 cm carbon steel coupon
  - 3-4 coupons per experiment
- ~0.1 g of salt on the corrosion sample
- Total gas flow 2 l/min
- Gas composition during experimental runs: 60% H_2O, 31% N_2, 7% CO_2 & 2% O_2
- Corrosion determined by:
  - Weight loss
  - Visual inspection
  - SEM analysis

Experimental setup

Experimental Plan

Run	Salt	Temperature (°C)	Water vapor content (%)	Time (h)	Steel
1	$NaHSO_4$	90	60	4	Carbon Steel
2	$NaHSO_4$	100	60	4	Carbon Steel
3	$NaHSO_4$	110	60	4	Carbon Steel
4	$NaHSO_4$	120	60	4	Carbon Steel
5	Na_2SO_4	90	60	4	Carbon Steel
6	Na_2SO_4	90	60	24	Carbon Steel
7	Na_2SO_4	100	60	4	Carbon Steel
8	Na_2SO_4	100	60	24	Carbon Steel
9	Na_2SO_4	110	60	24	Carbon Steel
10	Na_2SO_4	120	60	4	Carbon Steel

Results

(from the experimental setup)

Gas composition

	Target (vol %)	Average (vol%)	Highest (vol %)	Lowest (vol %)
H_2O	60	59.3	59.9	58.7
N_2	31	31.6	31.1	32
CO_2	7	7.1	7	7.2
O_2	2	2	2	2.1

Temperature

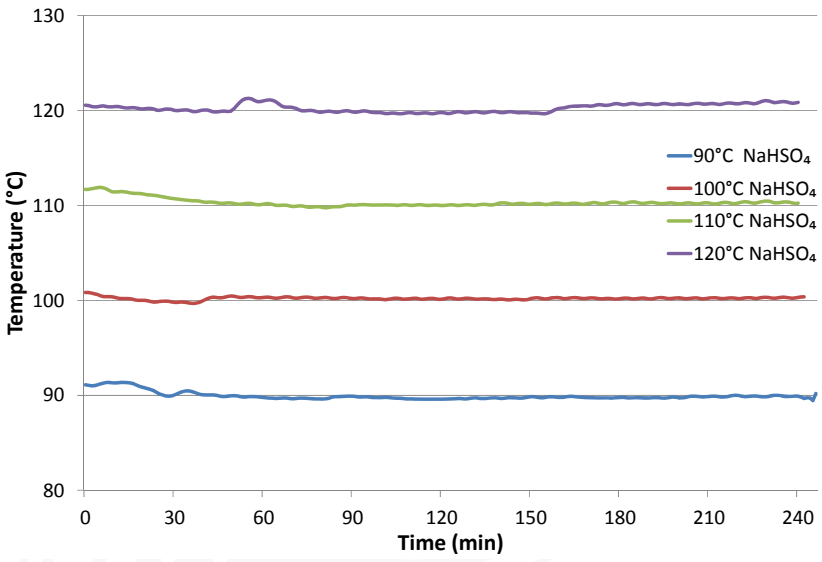

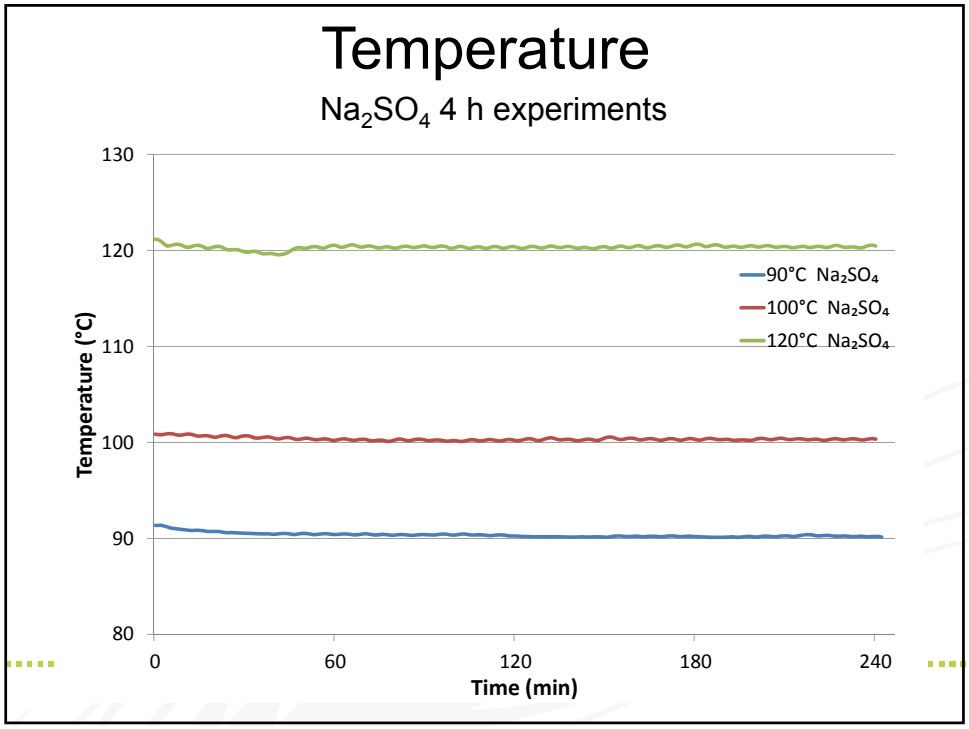
Temperature
Na2SO4 4 h experiments
130
120
110
100
90
80
Temperature (°C)
0
60
120
180
240
Time (min)
90°C Na2SO4
100°C Na2SO4
120°C Na2SO4

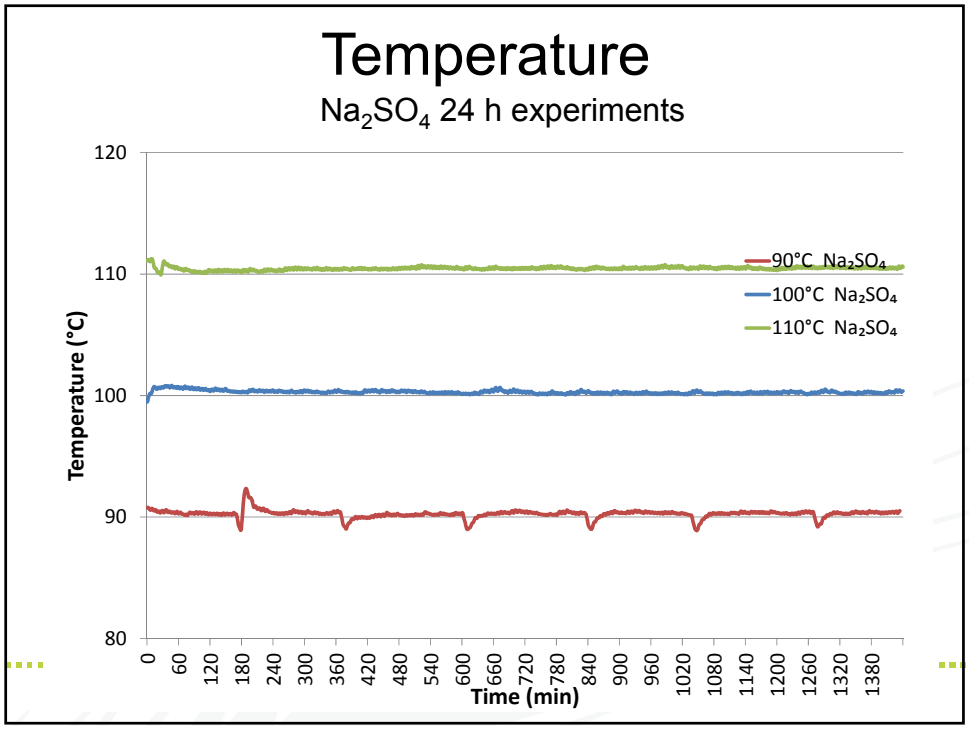
Temperature
Na2SO4 24 h experiments
120
110
100
90
80
Temperature (°C)
0
60
120
180
240
300
360
420
480
540
600
660
720
780
840
900
960
1020
1080
1140
1200
1260
1320
1380
Time (min)
90°C Na2SO4
100°C Na2SO4
110°C Na2SO4

Results

(from the corrosion experiments)

PROCESS CHEMISTRY CENTRE

ÅBO AKADEMI UNIVERSITY

$NaHSO_4$

Temperature: 90°C
Salt: $NaHSO_4$
Exposure: 4h

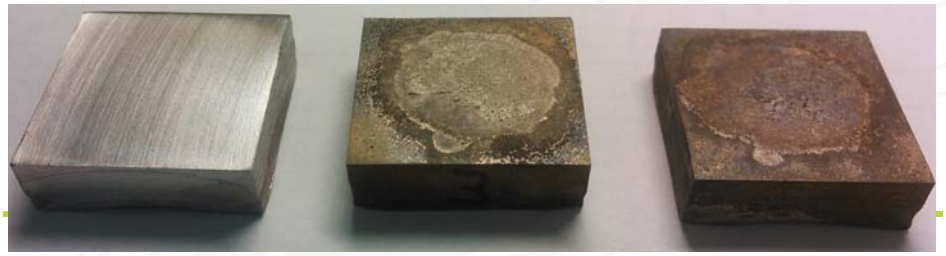

Temperature: 90°C
Salt: $NaHSO_4$
Exposure: 4h

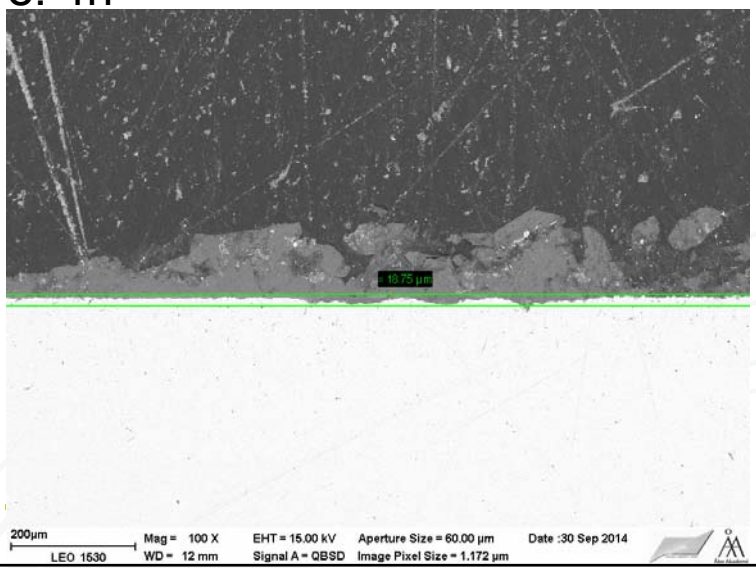

Temperature: 90°C
Salt: $NaHSO_4$
Exposure: 4h

	WT%			
	Fe	S	Na	O
1	17.4	19.6	16.7	46.2
2	98.7			
3	23.3	20.6	8.6	47.3
4	22.2	25.8	13.0	38.3
5	18.0	21.5	16.4	43.7
6	29.8	20.9		48.6

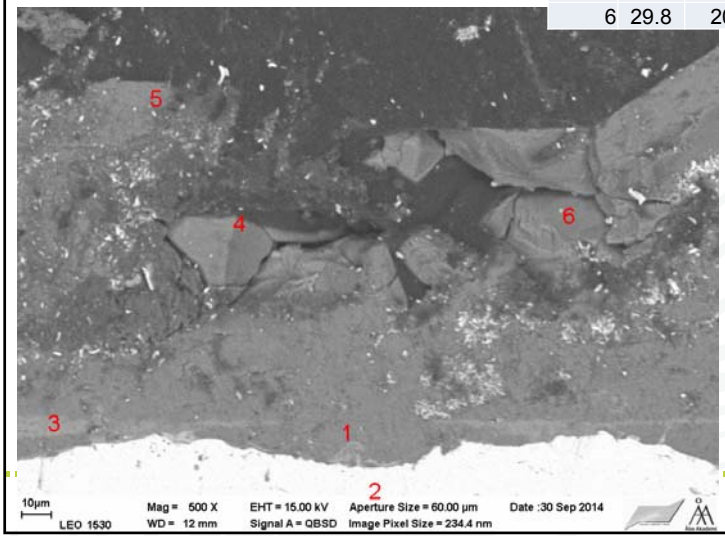

middle

Temperature: 90°C
Salt: NaH_2SO_4
Exposure: 4h

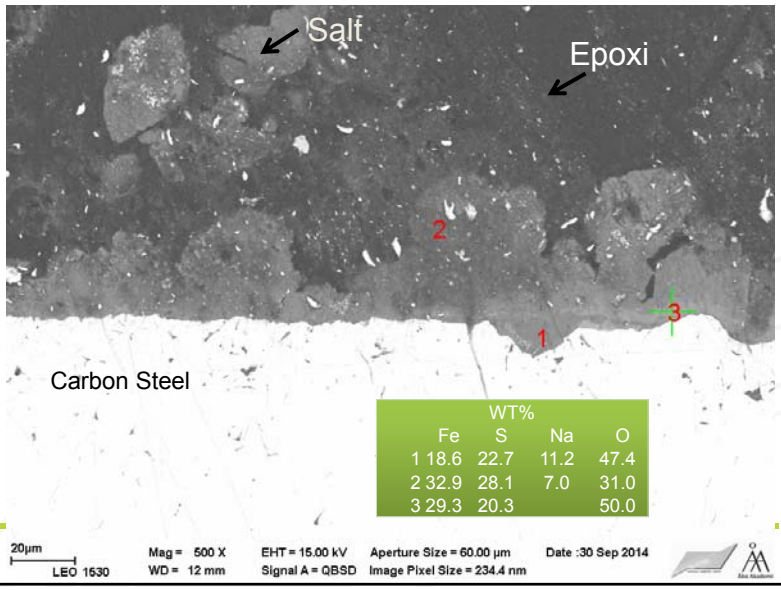

	WT%			
	Fe	S	Na	O
1	18.6	22.7	11.2	47.4
2	32.9	28.1	7.0	31.0
3	29.3	20.3		50.0

Temperature: 90°C
Salt: $NaHSO_4$
Exposure: 4h

	WT%			
	Fe	S	Na	O
1	33.4	20.1		45.1
2	95.9	0.3		2.4
3	97.0	0.3		1.3

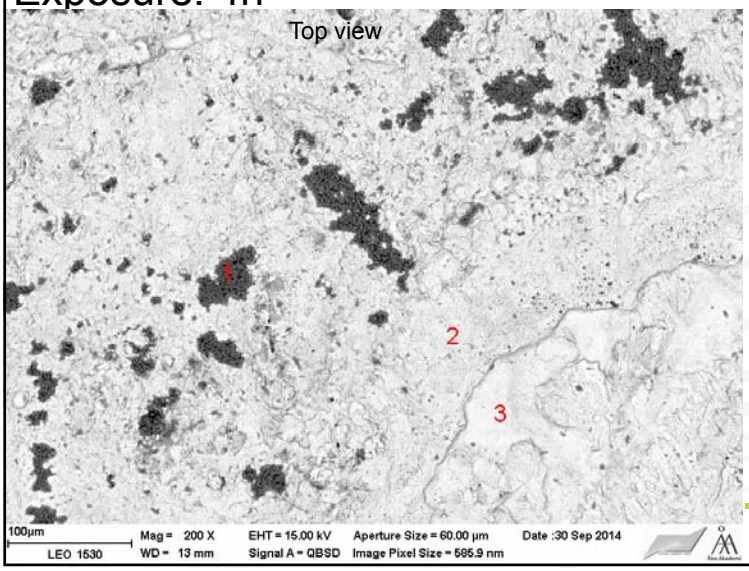

Temperature: 100°C
Salt: $NaHSO_4$
Exposure: 4h

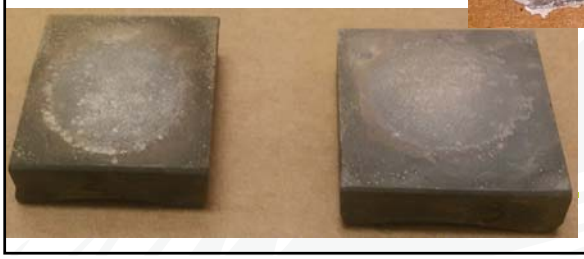

Temperature: 100°C
Salt: $NaHSO_4$
Exposure: 4h

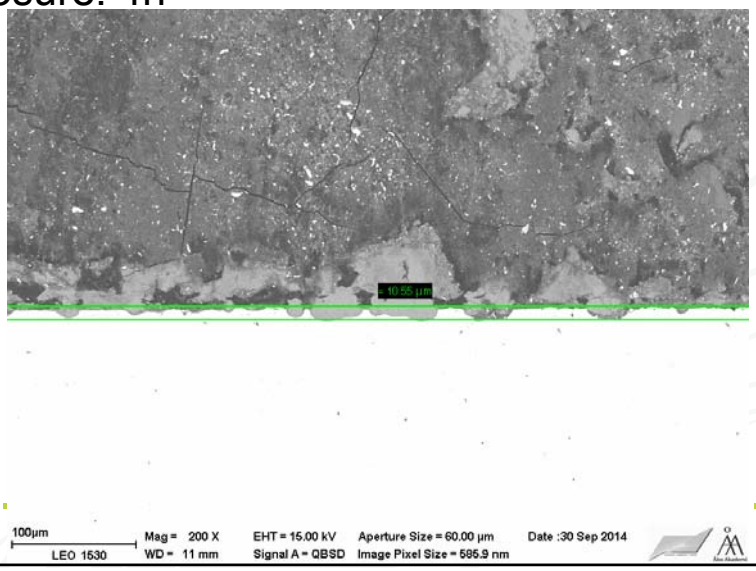

Temperature: 100°C
Salt: $NaHSO_4$
Exposure: 4h

	WT%			
	Fe	S	Na	O
1	15.3	23.7	14.7	46.1
2	32.2	21.9		45.6

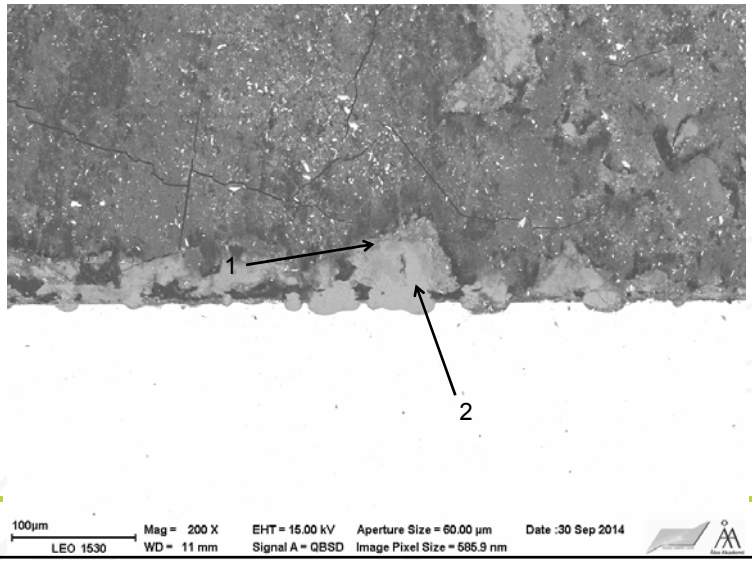

Temperature: 100°C
Salt: $NaHSO_4$
Exposure: 4h

Top view

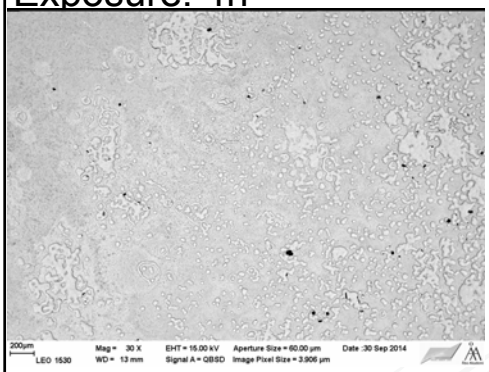

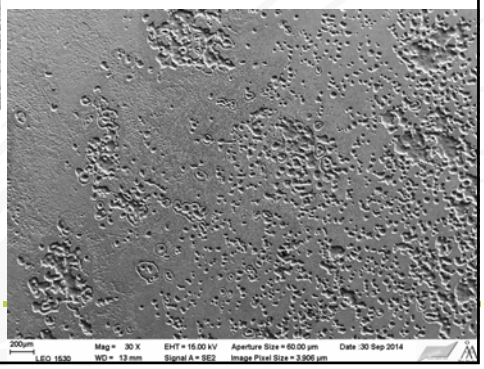

Temperature: 100°C
Salt: $NaHSO_4$
Exposure: 4h

Top view

	WT%			
	Fe	S	Na	O
1	97.0			
2	98.2			
3	18.6	1.2	2.3	31.9

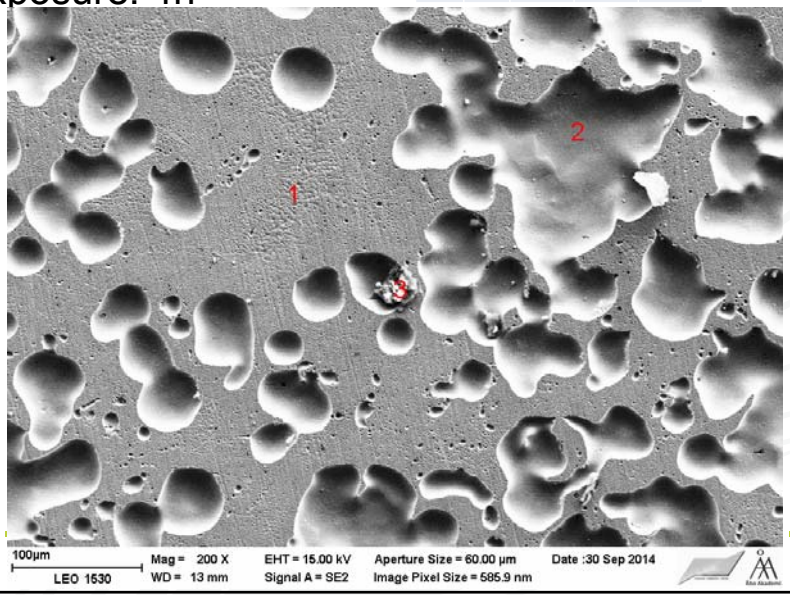

Temperature: 110°C
Salt: $NaHSO_4$
Exposure: 4h

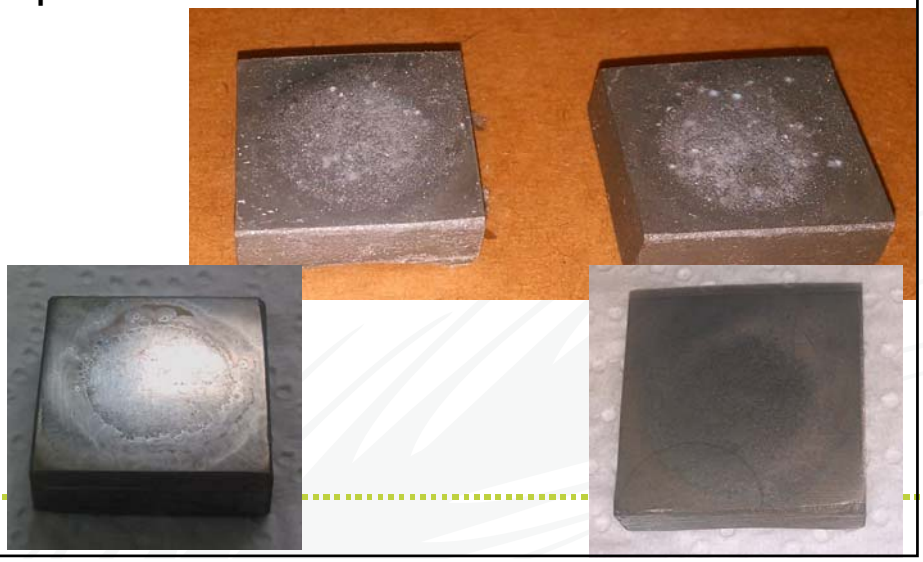

Temperature: 110°C
Salt: $NaHSO_4$
Exposure: 4h

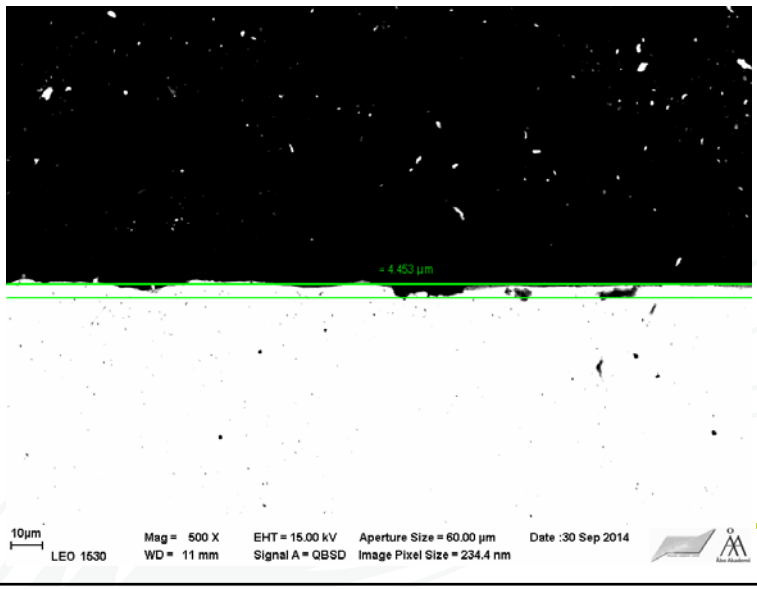

Temperature: 110°C
Salt: $NaHSO_4$
Exposure: 4h

Top view

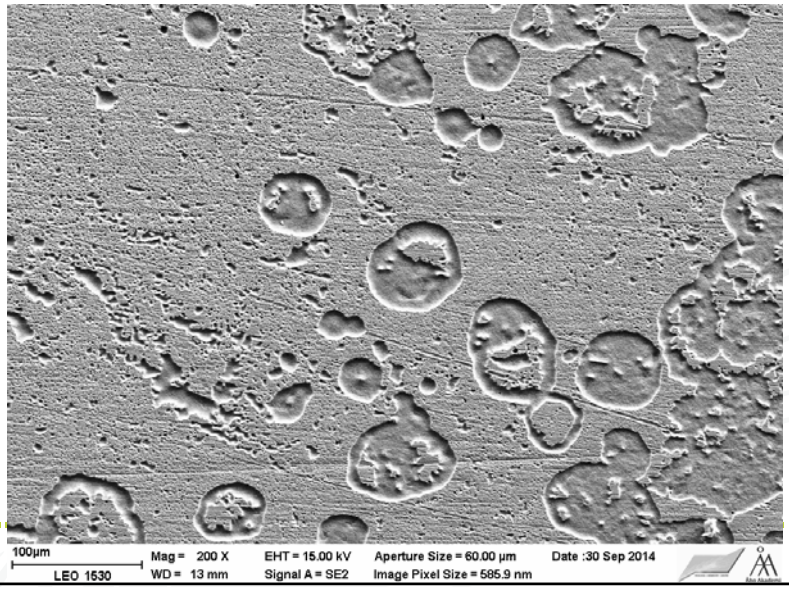

Temperature: 110°C
Salt: $NaHSO_4$
Exposure: 4h

Top view

	WT%			
	Fe	S	Na	O
1	98.0	0.1		0.4
2	98.4			
3	98.0	0.2		0.6

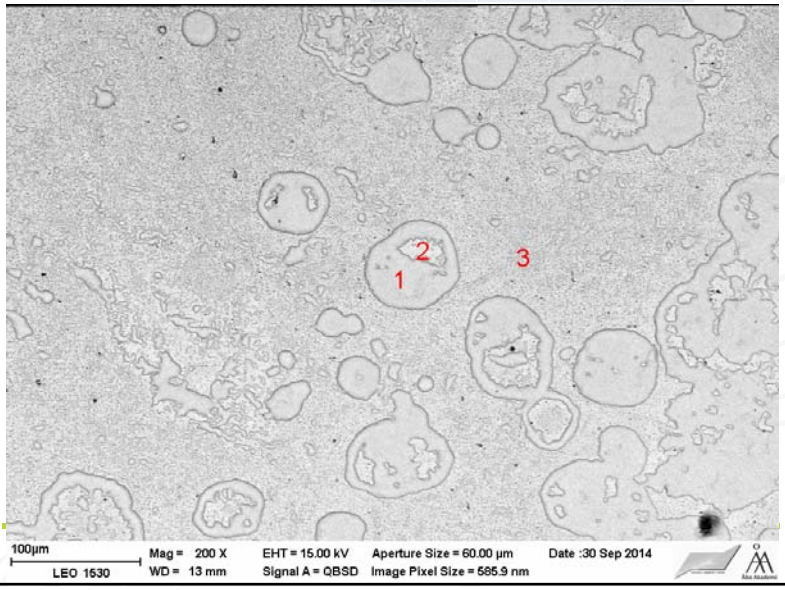

Temperature: 120°C
Salt: $NaHSO_4$
Exposure: 4h

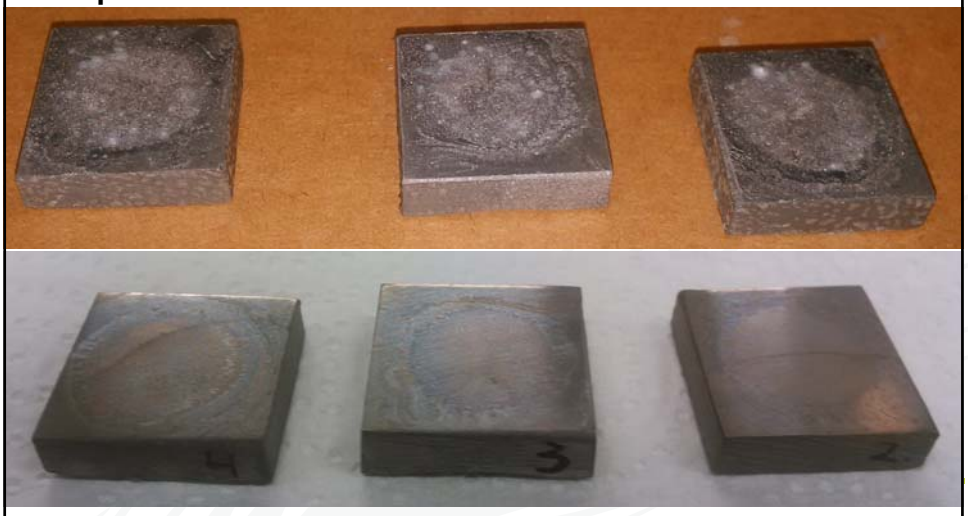

Temperature: 120°C
Salt: $NaHSO_4$
Exposure: 4h

Top view

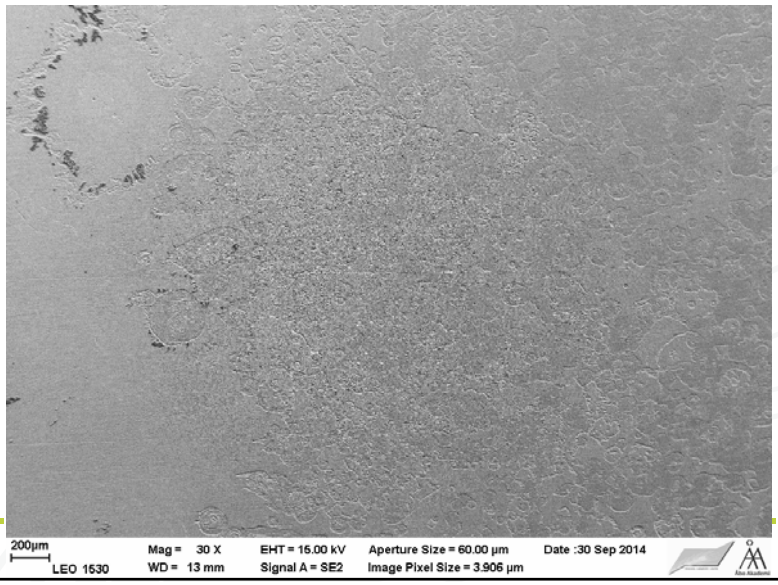

Temperature: 120°C
Salt: $NaHSO_4$
Exposure: 4h

Top view

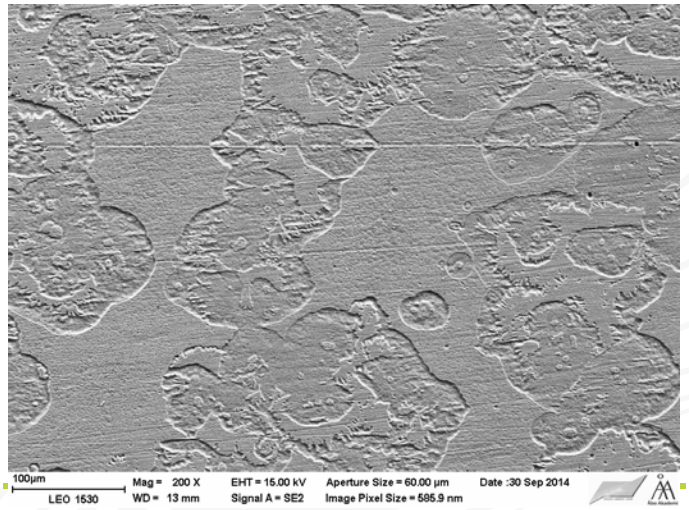

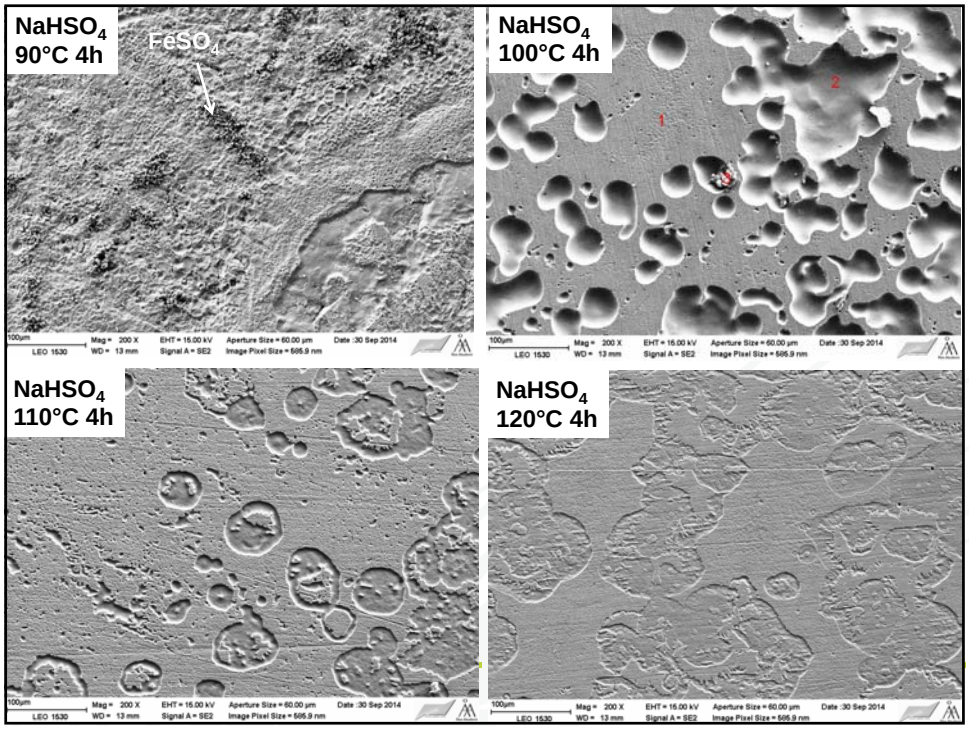

Na_2SO_4

Temperature: 90°C
Salt: Na_2SO_4
Exposure: 4h

Temperature: 90°C
Salt: Na_2SO_4
Exposure: 4h

Top view

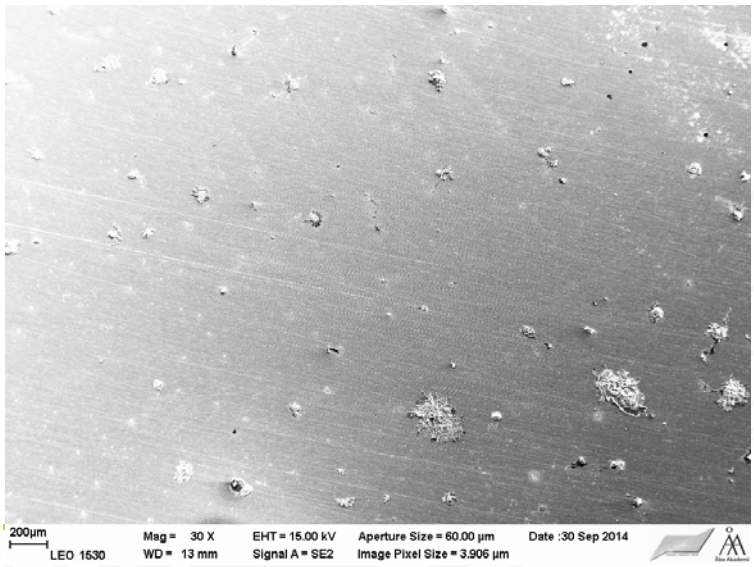

Temperature: 90°C
Salt: Na_2SO_4
Exposure: 4h

Top view

	WT%			
	Fe	S	Na	O
1	64.0	1.1	1.4	31.7
2	40.7	5.7	16.6	35.1
3	62.9	3.9	20.9	11.7

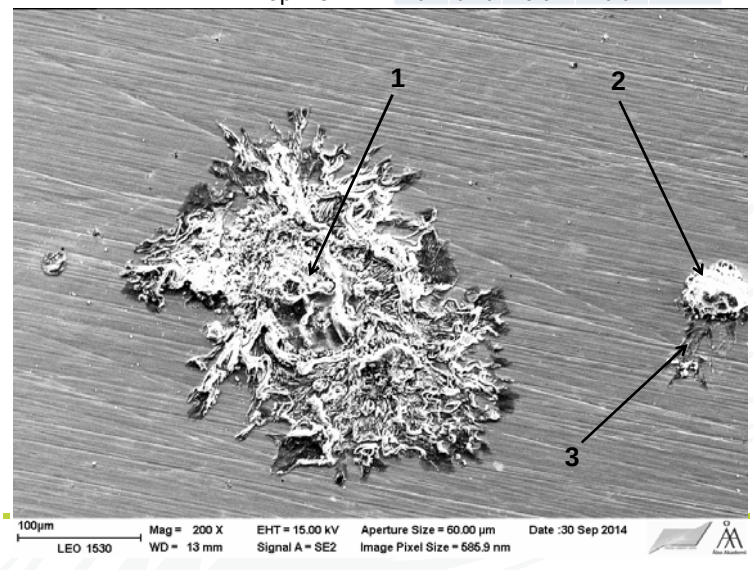

Temperature: 90°C
Salt: Na_2SO_4
Exposure: 24h

Temperature: 90°C
Salt: Na_2SO_4
Exposure: 24h

	WT%			
	Fe	S	Na	O
1	0.3	24.0	35.5	40.2
2	62.0	1.1	4.9	30.8

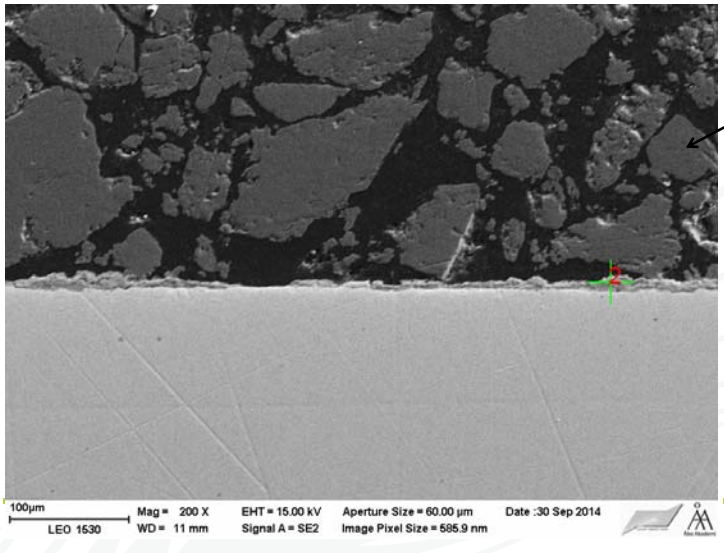

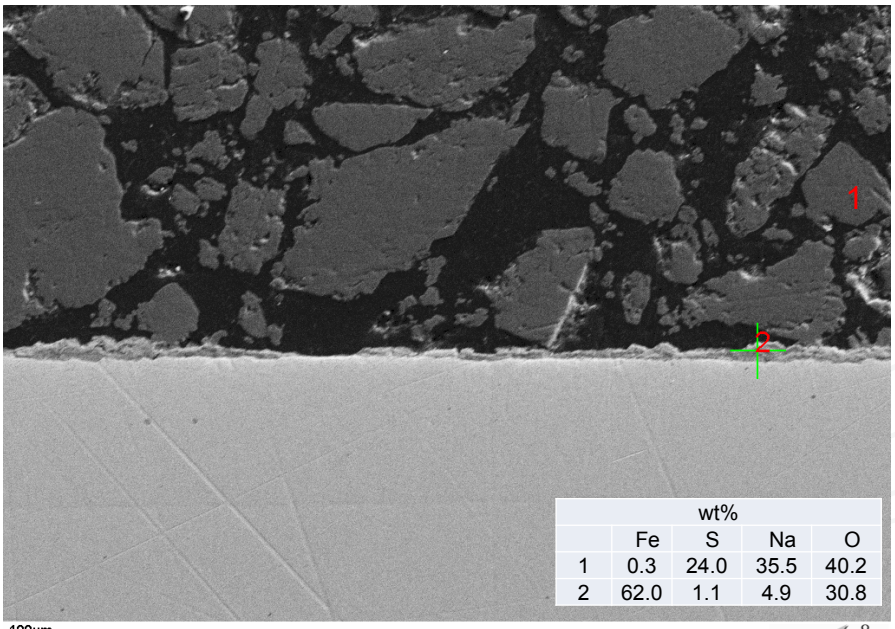

Temperature: 90°C
Salt: Na_2SO_4
Exposure: 24h

Top view

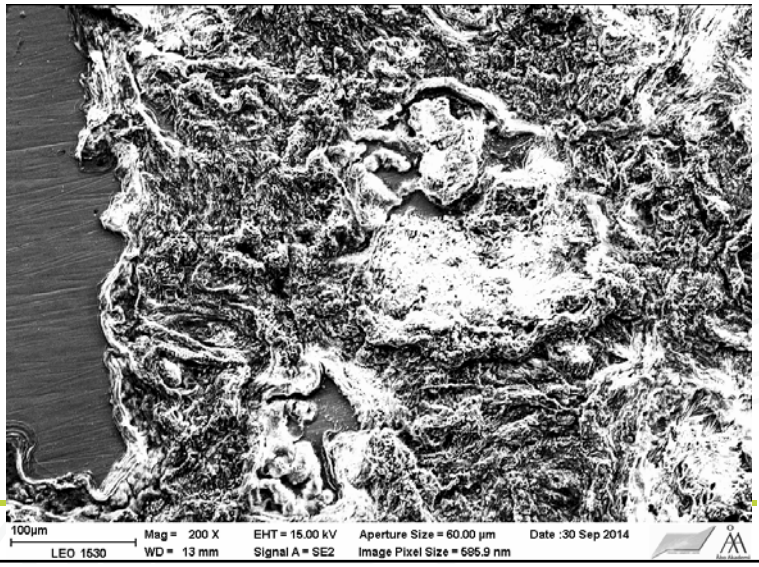

Temperature: 90°C
Salt: Na_2SO_4
Exposure: 24h

Top view

	WT%			
	Fe	S	Na	O
1	65.0	0.5	1.5	31.9
2	63.8	0.6		34.5
3	98.6			0.0

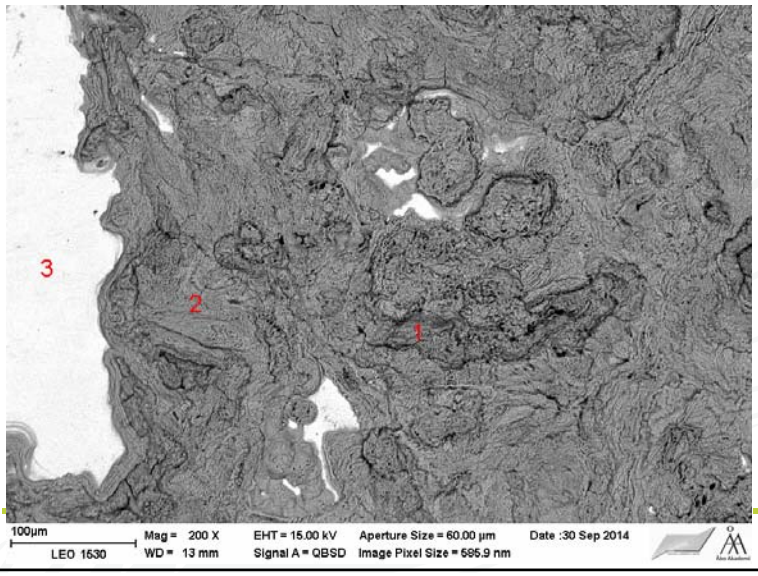

Temperature: 100°C
Salt: Na_2SO_4
Exposure: 4h

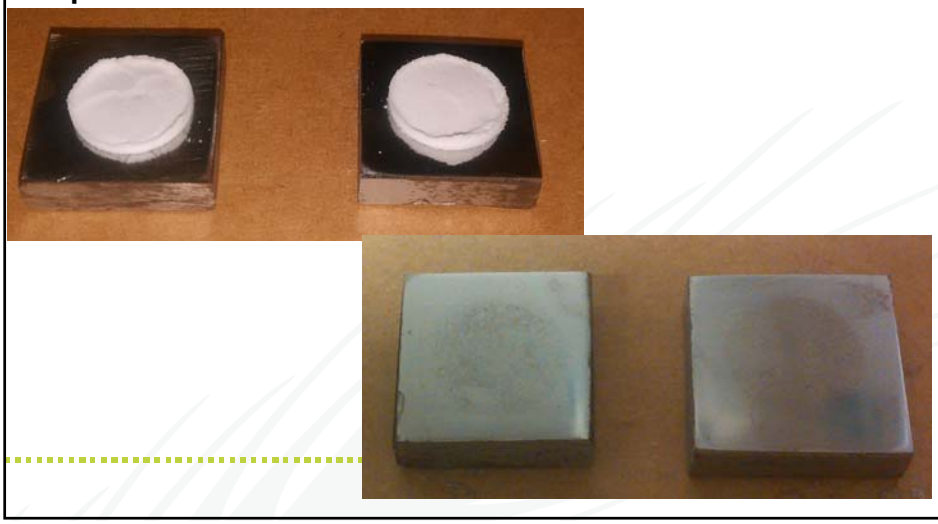

Temperature: 100°C
Salt: Na_2SO_4
Exposure: 4h

	WT%			
	Fe	S	Na	O
1	67.1	0.1		31.6

Top view

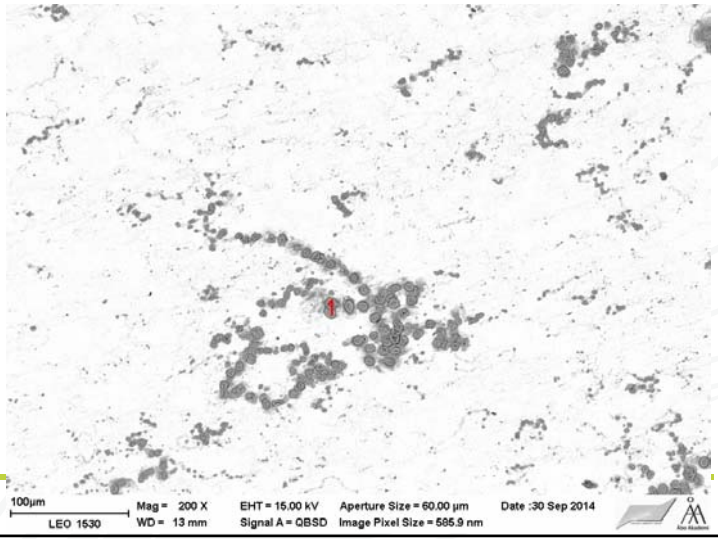

Temperature: 100°C
Salt: Na_2SO_4
Exposure: 24h

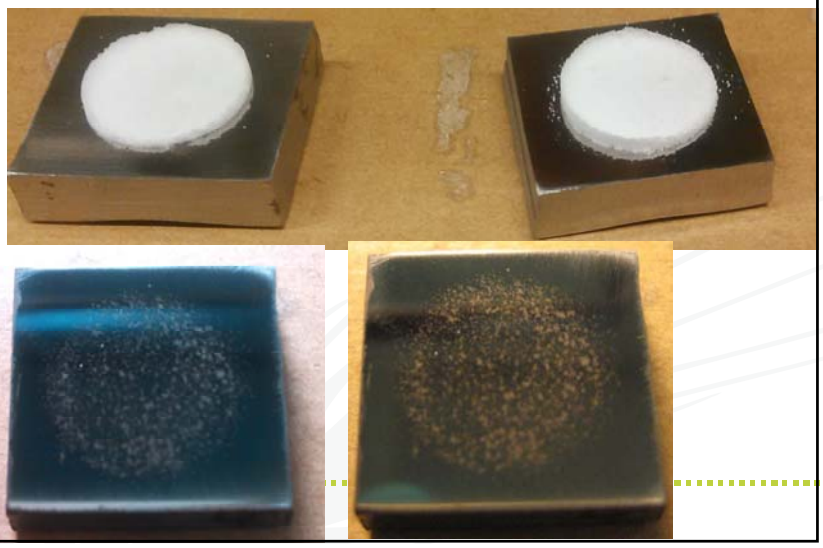

Temperature: 110°C
Salt: Na_2SO_4
Exposure: 24h

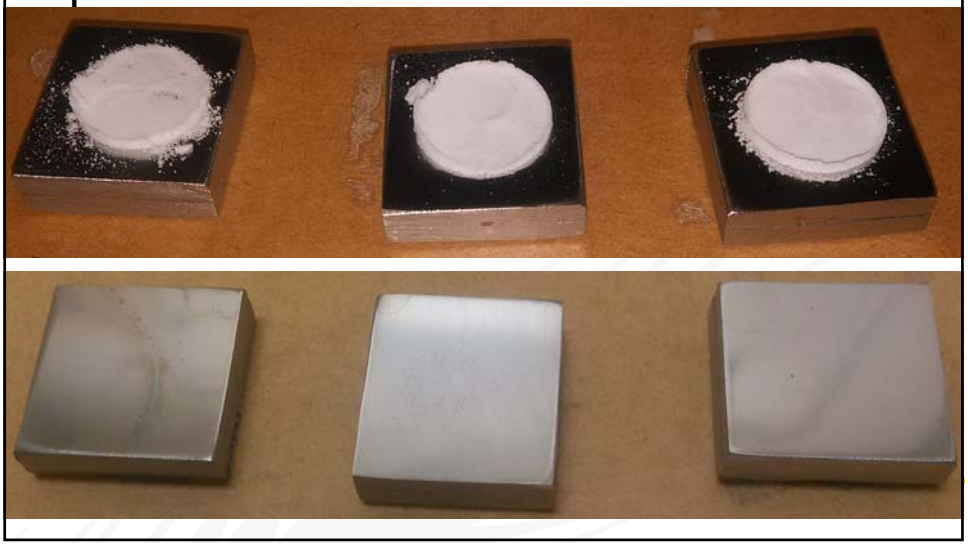

Temperature: 110°C
Salt: Na_2SO_4
Exposure: 24h

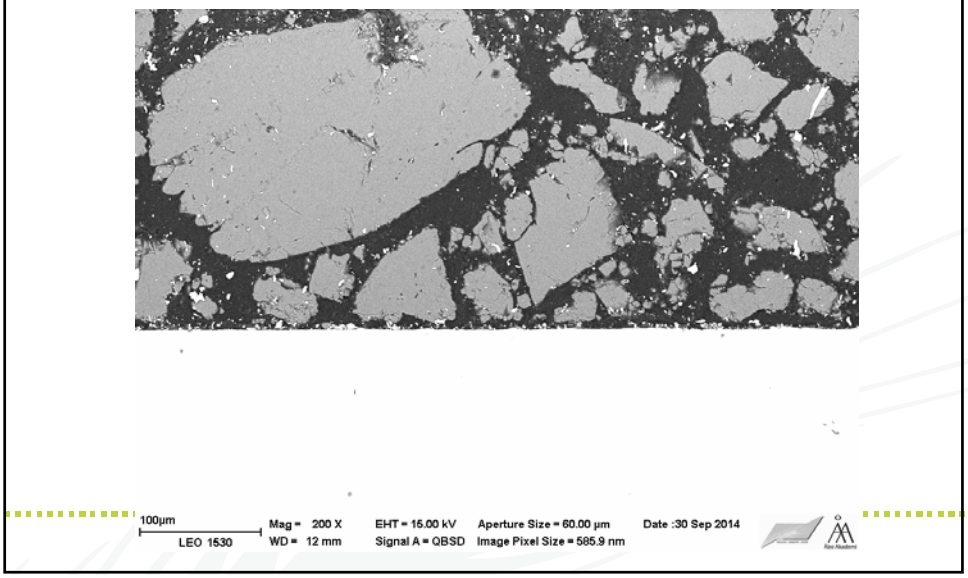

Temperature: 110°C
Salt: Na_2SO_4
Exposure: 24h

Top view

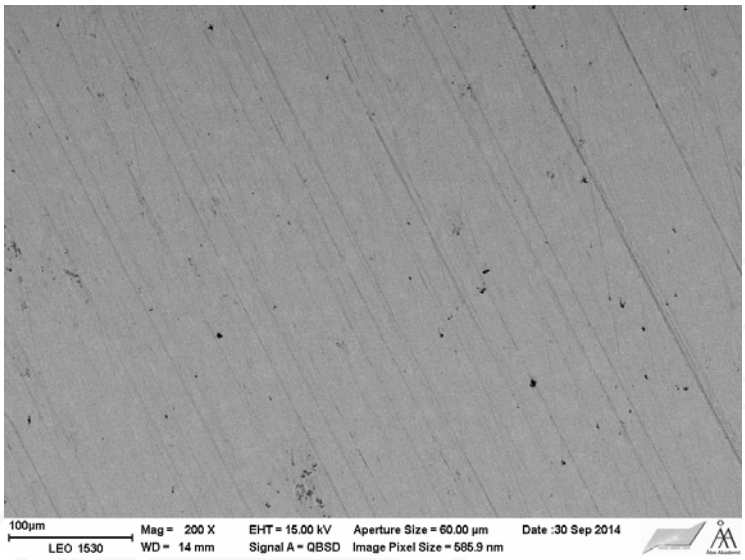

Temperature: 120°C
Salt: Na_2SO_4
Exposure: 4h

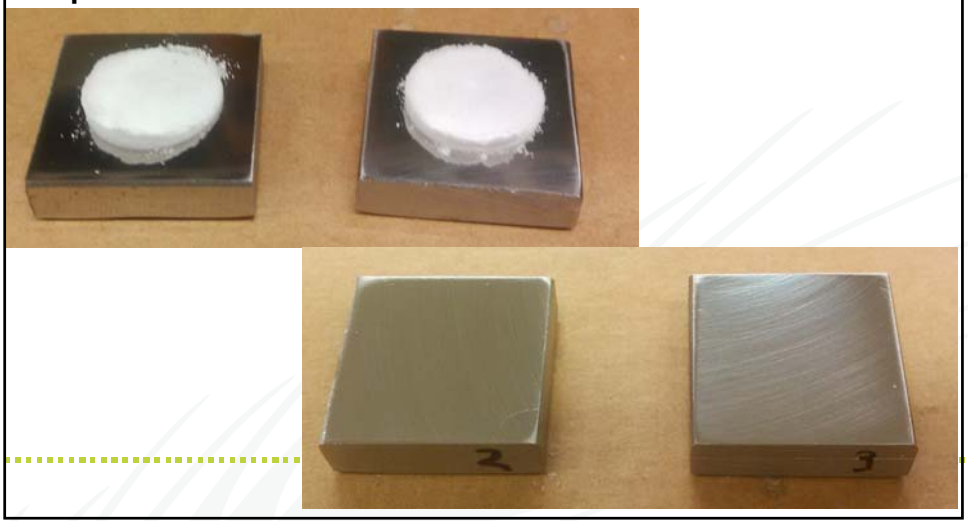

Temperature: 120°C
Salt: Na_2SO_4
Exposure: 4h

	WT%				
	Fe	S	Na	O	
1	3.3	23.1	34.0	39.1	Salt
2	56.8	0.9	0.3	33.5	Epoxi

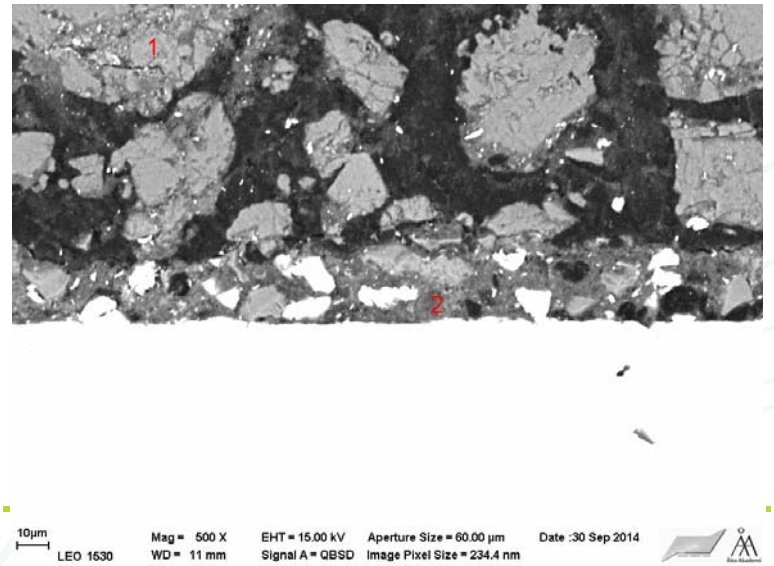

Temperature: 120°C
Salt: Na_2SO_4
Exposure: 4h

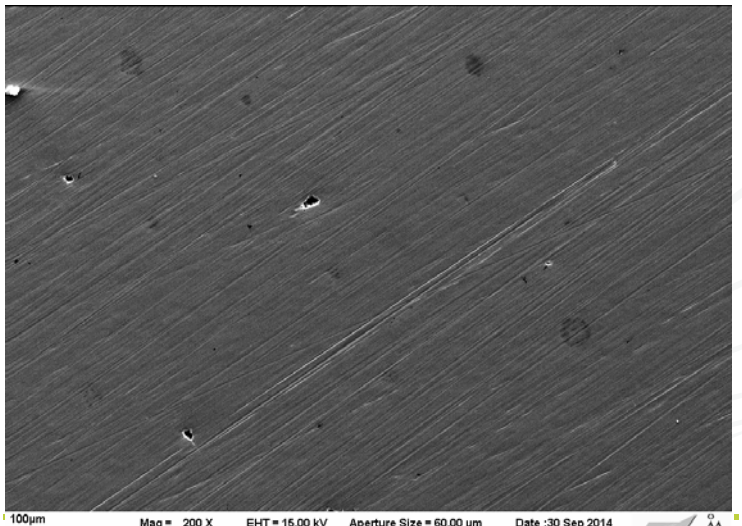

Wrap-up

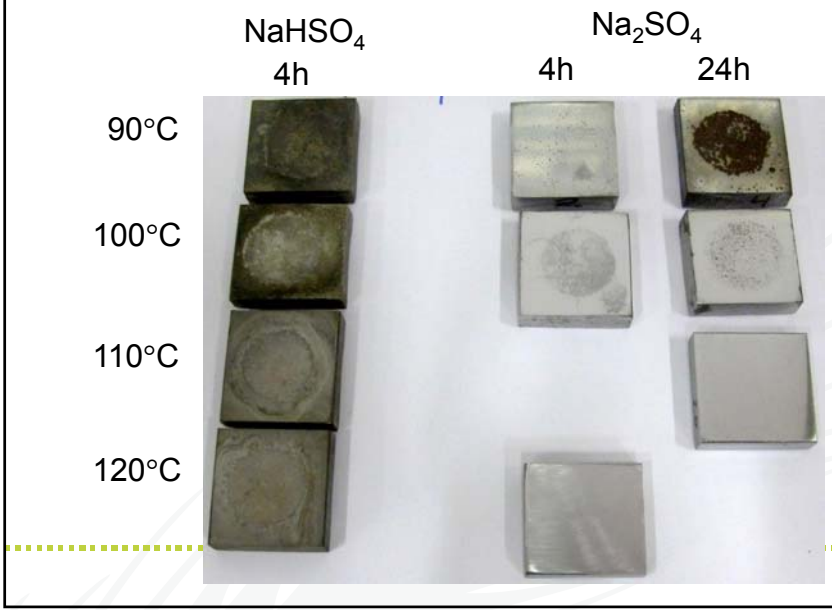

Weight loss

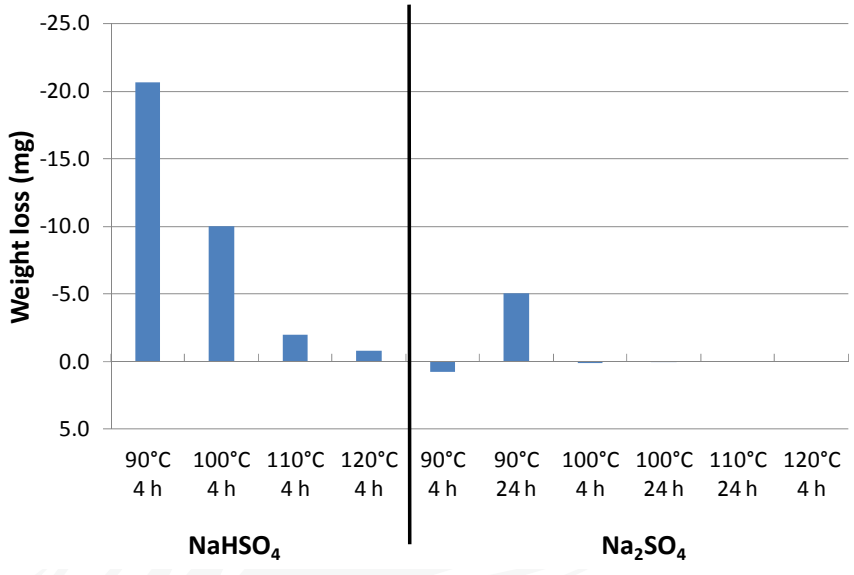

Corrosion rate

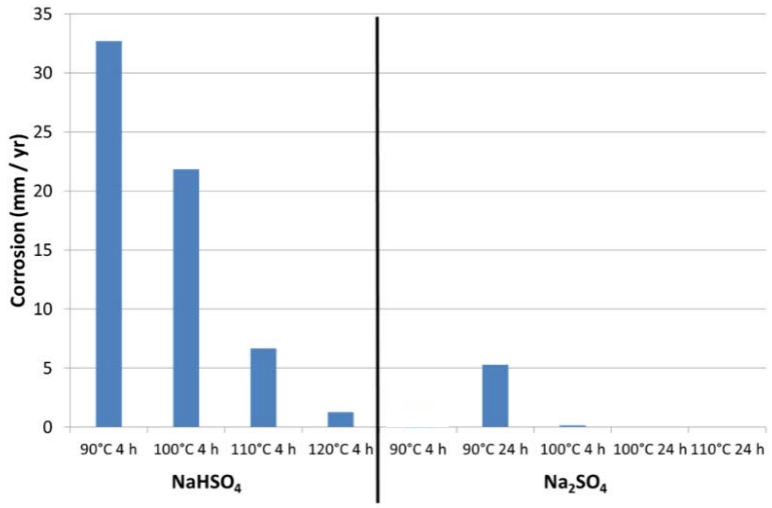

Conclusions

- Laboratory setup worked as planned
- For Na_2SO_4:
  - corrosion seen at 90°C and 100°C, but not at 110°C and 120°C
  - Iron oxide formation
- For $NaHSO_4$:
  - Increasing corrosion was seen at decreasing temperature
  - Clear acid corrosion
  - Iron sulfate in pits

Conclusions

- Salts seem to absorb moisture at a slightly higher temperature than the theoretical temperatures at 60vol% H_2O. The theoretical values are not from flue gas conditions (temperature gas composition)

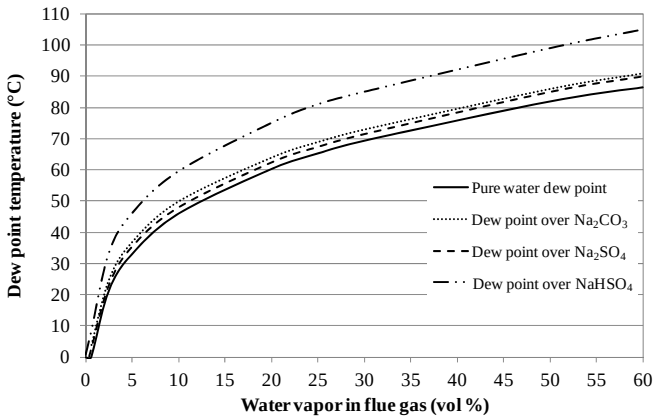

Suggested Future Work

- Larger matrix – DI work to look at the impact of different salts and salt mixtures
- Test apparatus to measure the temperature of deliquescence for salt mixtures relevant to recovery boilers

LIITE 5

ÅA, Understanding Low Temperature Corrosion in BL Combustion – raportti

PROCESS CHEMISTRY CENTRE

ÅBO AKADEMI UNIVERSITY

Understanding Low Temperature Corrosion in Black Liquor Combustion

Niklas Vähä-Savo, Emil Vainio, Nikolai DeMartini, Patrik Yrjas & Mikko Hupa

Åbo Akademi University

2 December 2014

Åbo Akademi Process Chemistry Centre, Inorganic Chemistry
FI - 20500 Turku / Åbo • Finland • Tel: +358 2 215 31 • Fax: +358 2 215 4962

1. Summary and Conclusions

A laboratory set-up to study low temperature corrosion was built and tested. The set-up worked as planned and stable water vapor concentrations were maintained. Corrosion of carbon steel coupons, measured as weight change, with either Na_2SO_4 or $NaHSO_4$ salt placed on top of the coupon was studied at the temperatures 90, 100, 110 and 120°C, Figure 1. The water vapor concentration was 60 vol% in the experiments, simulating the localized high humidity that can be seen near soot blowers. For the $NaHSO_4$ covered samples, pitting was found as well as an iron sulfate corrosion product, which is consistent with acid bisulfate solution corrosion. Corrosion increased with decreasing temperatures, with deeper pits at the lowest temperatures. For the Na_2SO_4 experiments, iron oxide formation was observed at 90°C and to a lesser extent at 100°C. No corrosion was observed at 110°C and 120°C under Na_2SO_4.

Hygroscopic salts will absorb water above the water dew point. At a given temperature, the humidity at which a salt absorbs water is called the humidity of deliquescence. Based on the data available from literature, at 60 vol-% water the temperature at which the salts were expected to absorb water was 91 °C for Na_2SO_4 and 106 °C for $NaHSO_4$. The corrosion seen is consistent with absorption of water by the salts, but this is occurring at a slightly higher temperature than would be expected based on predictions for the humidity of deliquescence based on the literature. Further research is needed both to map the conditions under which low temperature corrosion can occur and to measure the humidity of deliquescence for salts and salt mixtures at conditions relevant to recovery boilers.

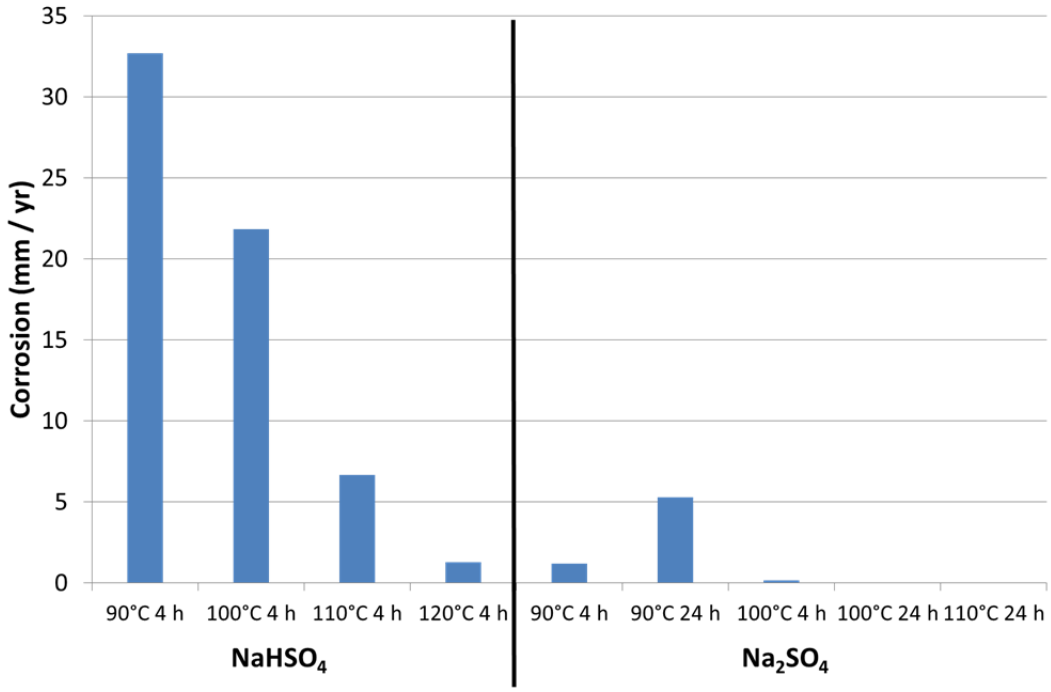

Figure 1. Calculated annual corrosion layer thickness based on mass loss after washing off corrosion layer in 4h and 24h tests.

Contents

1. Background 4

2. Experimental 4

3. Results 7

3.1. Experimental setup 7

3.2. Corrosion results 9

3.2.1. Visual inspection 9

3.2.2. Weight change 10

3.2.3. SEM analysis 11

3.2.3.1. Experiments with $NaHSO_4$ salt 11

3.2.3.2. Experiments with Na_2SO_4 salt 13

1. Background

Historically, some low temperature corrosion has been observed in recovery boilers. However, the underlying cause has not been clearly documented. One hypothesis had been the presence of a sulfuric acid dew point. This was the driving force for maintaining an elevated flue gas temperature. For companies to drop their flue gas temperatures lower and consider changing the construction materials of flue gas stacks, it is important to understand the cause of low temperature corrosion and map the conditions in which is can occur.

Corrosion probe studies and SO_3/H_2SO_4 measurements have shown that there is no H_2SO_4 and thus no acid dew point in modern recovery boilers. Furthermore, the measurements at Heinola, where there was high SO_2, indicate that even in a high SO_2 environment, there is no acid dew point. However, at Heinola, we did see an elevated dew point that was above the water dew point, but well below the acid dew point. The fly ash in recovery boilers contains hygroscopic salts, such as Na_2CO_3, Na_2SO_4, and NaHSO4 etc. These salts may have an impact on the corrosion of the heat exchangers in the flue gas duct. Hygroscopic salts will absorb moisture from the flue gas at a temperature higher than the pure water dew point. When the humidity in the flue gas reaches a critical level the solid salt particle transforms into an aqueous solution, which would lead to corrosion of the heat exchanger. Different salts have their own specific relative humidity at which the particle starts to absorb moisture. This is referred to as the relative humidity of deliquescence. A literature review found that salts can absorb water above the water dew point and that a salt such as $NaHSO_4$ can absorb water 10-20 °C above the water dew point depending on the relative humidity in the gas. Thus, one leading hypothesis is that if hygroscopic salts are present, water can be absorbed during periods of high humidity and form an aqueous solution at the steel surface, resulting in corrosion.

This initial study is focused around setting up and testing a reactor system for these low temperature corrosion studies and to make the first runs with $NaHSO_4$ and Na_2SO_4 salts and varying reactor temperature (90-120°C).

2. Experimental

The first part of this study was to set up a reactor system with stable temperature and water vapor concentration. Maintaining stable conditions throughout the experiment is crucial when studying low temperature corrosion due to water uptake by salts. Fluctuations in the water vapor concentration or temperature could lead to false interpretation of the results.

A schematic picture of the final experimental setup is shown in Figure 1. To create a constant feed of water vapor, the water is pumped with a Masterflex L/S pump at a constant flow to the steam generator. The steam generator consists of a thin pipe with heating. The temperature in the steam generator was set to 165°C in order to insure that water was vaporized at a constant rate. The hot steam was mixed with N_2, O_2 and CO_2, and the temperature of the wet gas

mixture flowed to a temperature regulator in which the temperature of the wet gas mixtures was cooled to the desired temperature. After the temperature regulator unit the wet gases flowed through a preheater before entering the quartz reactor, where the corrosion samples were placed, located in a tube furnace. The back end of the quartz reactor was heated to minimize water condensation and water from flowing back into the reactor. The wet gases exited the tube furnace to a water condenser unit where water was condensed and finally dry gases were vented out. With this setup the gas composition, gas flow, water vapor content and temperature can be easily adjusted.

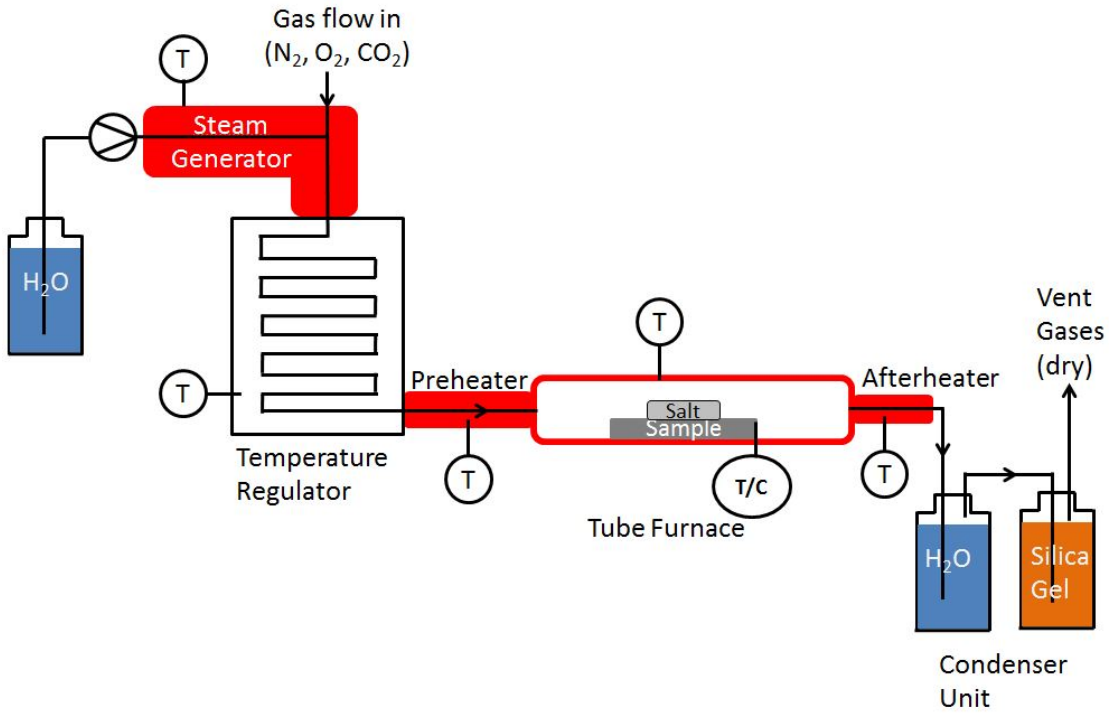

Figure 1. Schematic picture of the experimental setup.

The experimental plan for this work is shown in Table I. The corrosion of carbon steel (ST45) coupons was measured. The gas composition used during the experiments was 60% H_2O, 31% N_2, 7% CO_2, and 2% O_2 and the flow of wet gases was 2 Nl/min. This represents a gas composition near the soot blowers, i.e. a flue gas that is diluted with water vapor. The salts studied were sodium sulfate (Na_2SO_4) and sodium bisulfate ($NaHSO_4$) and the exposure time was 4 hours with some runs 24 hours to validate the 4 hour test results. The temperatures used during the experiments were between 90, 100, 110 and 120°C.

Table I. Experimental plan

Run	Salt	Temperature (°C)	Water vapor content (%)	Time (h)	Steel
1	$NaHSO_4$	90	60	4	Carbon Steel
2	$NaHSO_4$	100	60	4	Carbon Steel
3	$NaHSO_4$	110	60	4	Carbon Steel
4	$NaHSO_4$	120	60	4	Carbon Steel
5	Na_2SO_4	90	60	4	Carbon Steel
6	Na_2SO_4	90	60	24	Carbon Steel
7	Na_2SO_4	100	60	4	Carbon Steel
8	Na_2SO_4	100	60	24	Carbon Steel
9	Na_2SO_4	110	60	24	Carbon Steel
10	Na_2SO_4	120	60	4	Carbon Steel

The corrosion samples were 2x2 cm coupons of carbon steel and between 3-4 coupons were used during one experiment. The coupons were weighed before salt addition and roughly 0.1 g of the studied salt was added on top of the coupon. The carbon steel coupons with salts on top placed on the sample tray are shown in Figure 2. A thermocouple is located at the tip of the sample tray to record the temperature close to the samples during the experiments.

Figure 2. Carbon steel coupons with salt in top placed on the sample tray.

After the experiment one coupon was molded in epoxy and the cross section of the coupon was analyzed with scanning electron microscope (SEM). The remaining 2-3 coupons were washed with ultrapure water to remove the salt residue and then dried with acetone. The cleaned coupons were photographed and weighed in order to determine the weight change. The surface of one cleaned coupon was also analyzed with SEM.

3. Results

3.1. Experimental setup

The water pump was calibrated to obtain the desired water flow to the steam generator, and thus the desired vapor concentration during the experiments. After the experiments the weight difference in the water container was determined in order to calculate the exact water vapor concentration during the experiment. The target gas composition, gas composition with the measured highest water vapor concentration, lowest water vapor concentration and the average gas composition of all of the experiments are shown in Table II. From Table II it can be seen that with the experimental setup the water vapor concentration was within 1.3% of the desired water vapor concentration.

Table II. Target gas composition and gas composition at the measured highest, lowest, and average water flows during the experiments.

	Target (vol %)	Average (vol%)	Highest (vol %)	Lowest (vol %)
H_2O	60	59.3	59.9	58.7
N_2	31	31.6	31.1	32
CO_2	7	7.1	7	7.2
O_2	2	2	2	2.1

The recorded temperatures at the sample tray for the 4 hour $NaHSO_4$ experiments are shown in Figure 3, 4 hour Na_2SO_4 experiments in Figure 4, and the 24 hour Na_2SO_4 experiments in Figure 5. When the experiments started it took roughly 30 minutes for the temperature inside the tube furnace to stabilize. This is because the steam exits the generator at 165 C and the other temperature controllers have to adjust to get the system temperature down to the target temperature. However, the key is that the temperature is only very slightly above the target temperature for those approximately 30 minutes and won't affect the corrosion results. The temperature was stable during the experiments and the tube furnace was suitable for running experiments in low temperatures. For some reason during the 24 hour 90°C Na_2SO_4 experiment every 4 hours a small decrease in temperature was detected. The reason behind this regular decrease remained unknown.

Based on the observations during the experiments and the measured temperature and water vapor concentration, the experimental setup worked well. The temperature was stable during the experiments and the desired water vapor content was obtained with the experimental setup.

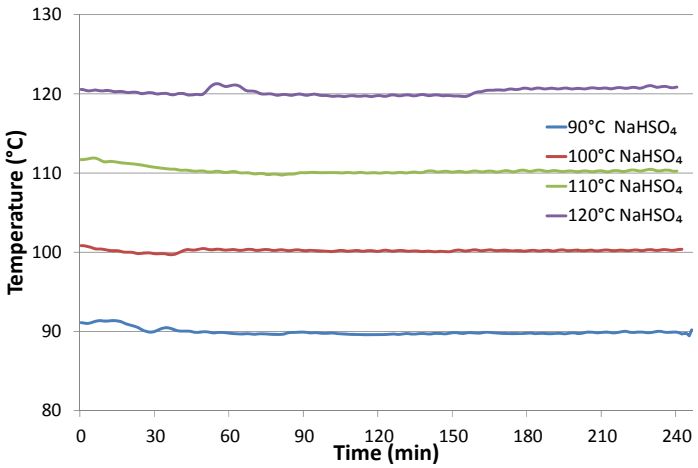

Figure 3. Temperature during 4 hour $NaHSO_4$ experiments.

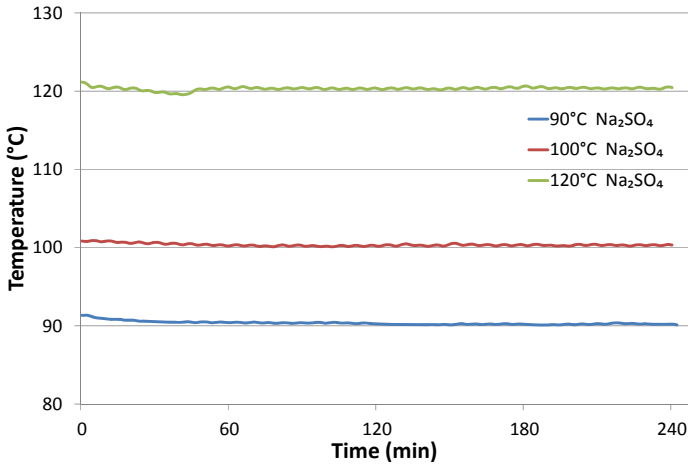

Figure 4. Temperature during 4 hour Na_2SO_4 experiments.

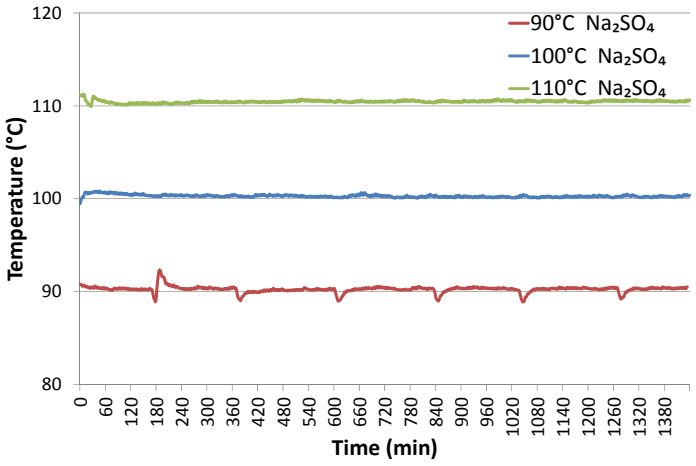

Figure 5. Temperature during 24 hour Na_2SO_4 experiments.

3.2. Corrosion results

3.2.1. Visual inspection

A photograph of the carbon steel coupons after the experiments before washing is shown in Figure 6. Sodium bisulfate was extremely hygroscopic, and absorbed moisture from the wet gas flow in all conditions. This can be seen as there was little to no salt remaining on the coupon after the experiments. This was not expected. Based on literature data for the humidity of deliquescence, it was expected that the temperature at which water would no longer be absorbed was ___ °C. Sodium sulfate is much less hygroscopic, and the salt was only slightly moist at the lower temperatures. It can be seen that the salt cake for the Na_2SO_4 experiments are more intact.

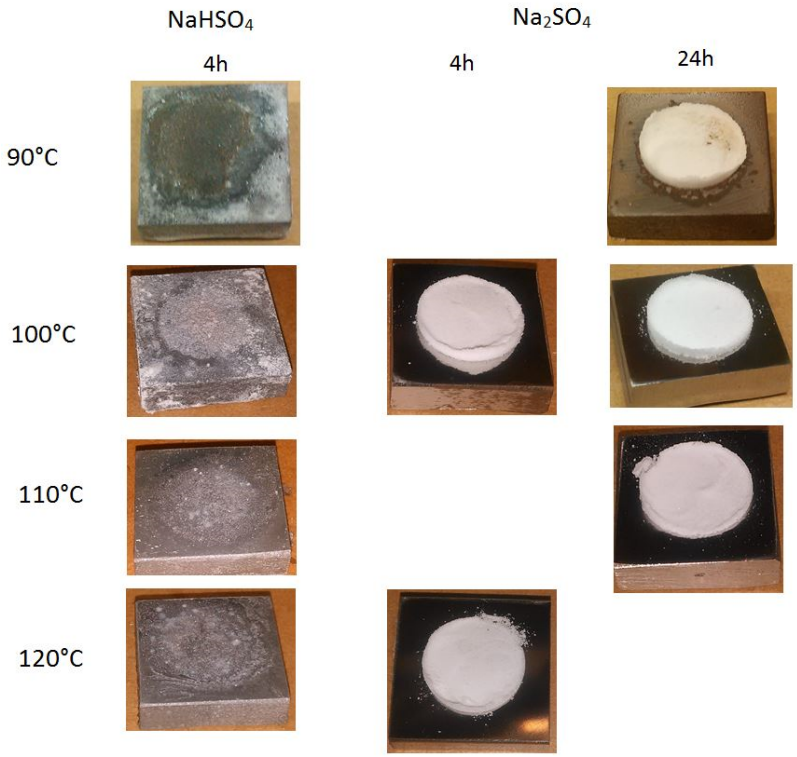

Figure 6. Corrosion samples after the experiments.

Figure 7 shows the carbon steel coupons after the salt residue was washed off. After the visual inspection it was clear that $NaHSO_4$ caused corrosion of the carbon steel at all temperatures with the corrosion being more severe the lower the temperature. This is due to the formation of an acidic bisulfate solution on the coupon. In the experiments with Na_2SO_4, no corrosion was visible after the 110°C and 120°C. After the 4 h experiments at 90°C and 100°C small spots of corrosion could be observed. To these results, 24h runs were made. These runs showed the same, that corrosion occurs at 90°C and 100°C, with more corrosion at 90°C than 100 °C. The corrosion experiment with Na2SO4 at 110 °C was run for 24 hours since if corrosion were to occur at 4 hours it would have been very slight. The coupon from the 24 hour run at 110 °C, however, showed no corrosion.

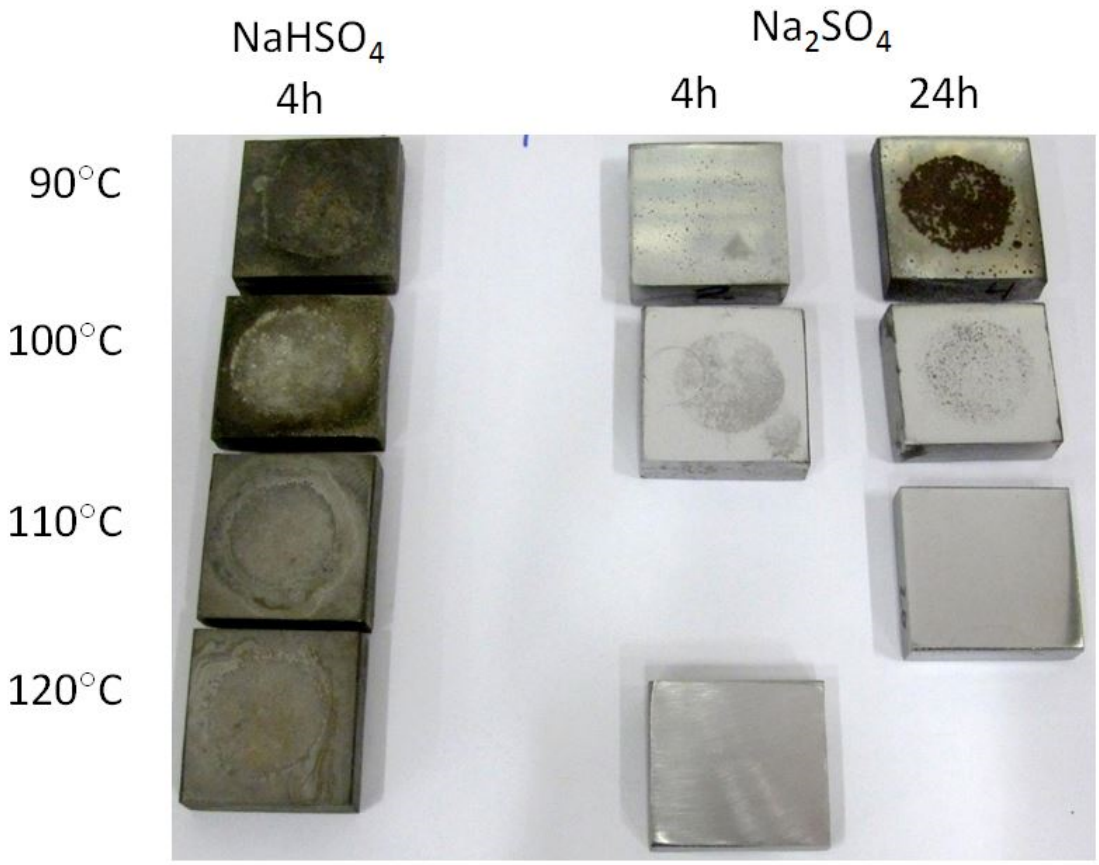

Figure 7. Visual inspection of the corrosion samples after washing

3.2.2. Weight change

After the experiment the carbon steel coupons were washed to remove the salt residue and then weighed in order to determine the weight change due to corrosion. Generally, the corrosion layer is removed during the washing process and the weight loss is due to the removal of the corrosion product. This weight was compared to the initial coupon weight, Figure 8. The results clearly show that the corrosion was more severe for the $NaHSO_4$ covered carbon steel samples at lower temperature than at higher temperatures. The 4 h 90°C Na_2SO_4 experiment showed a slight increase in weight after the experiments because the iron oxide was not removed by the washing process. The coupon from the 24 h 90°C Na_2SO_4 experiment, in which the corrosion was more severe, showed a decrease in weight. The formation of iron oxide during the 100°C Na_2SO_4 experiments was so low that no weight change was recorded. At higher temperatures no corrosion product was formed with Na_2SO_4.

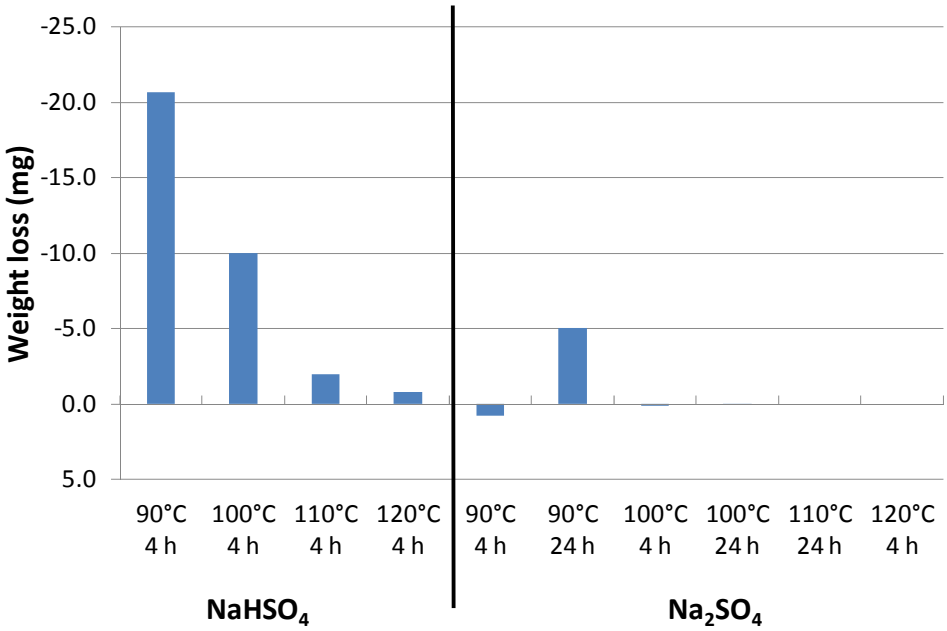

Figure 8. Material loss of the carbon steel samples due to corrosion.

3.2.3. SEM analysis

3.2.3.1. Experiments with $NaHSO_4$ salt

Figure shows the cross section SEM image of the carbon steel covered with $NaHSO_4$ after the 4h exposure at 90°C. The white flakes are pieces of metal originating from the cutting and polishing of the cross section sample. The dark grey areas are the epoxy mold and the light grey is either salt or salt mixed with the corrosion product. From the SEM image clear pitting corrosion can be observed. This is consistent with acidic corrosion due to the acid bisulfate solution produced when $NaHSO_4$ absorbed water from the gas. The corrosion products consisted of a mixture of iron, sodium, sulfur and oxygen (analysis spots 1 and 2 on the figure). The spot analysis (spot 3) showed clearly that $FeSO_4$ is formed as a corrosion product.

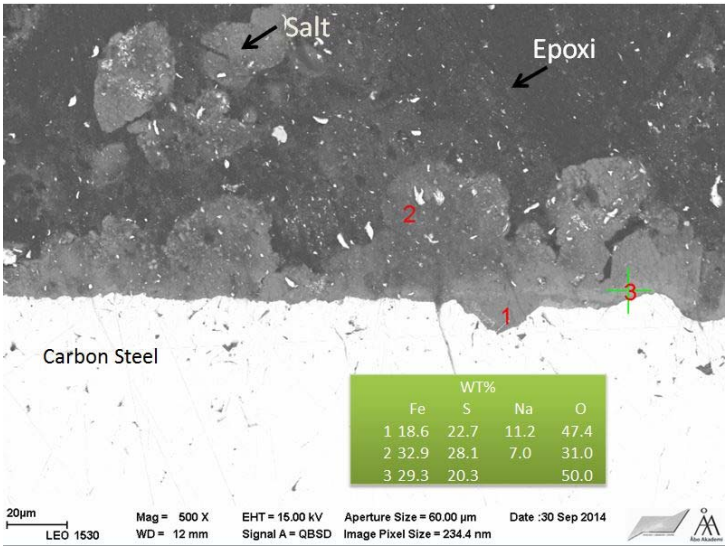

Figure 9. Cross section SEM image of the $NaHSO_4$ covered carbon steel after 4 h and 90°C experiment.

Figure clearly shows the pits formed from the acid corrosion after exposure with $NaHSO_4$ for 4h and 100°C. The pits are about 10µm deep and are filled with $FeSO_4$. Increasingly deep pits were observed with decreasing temperature.

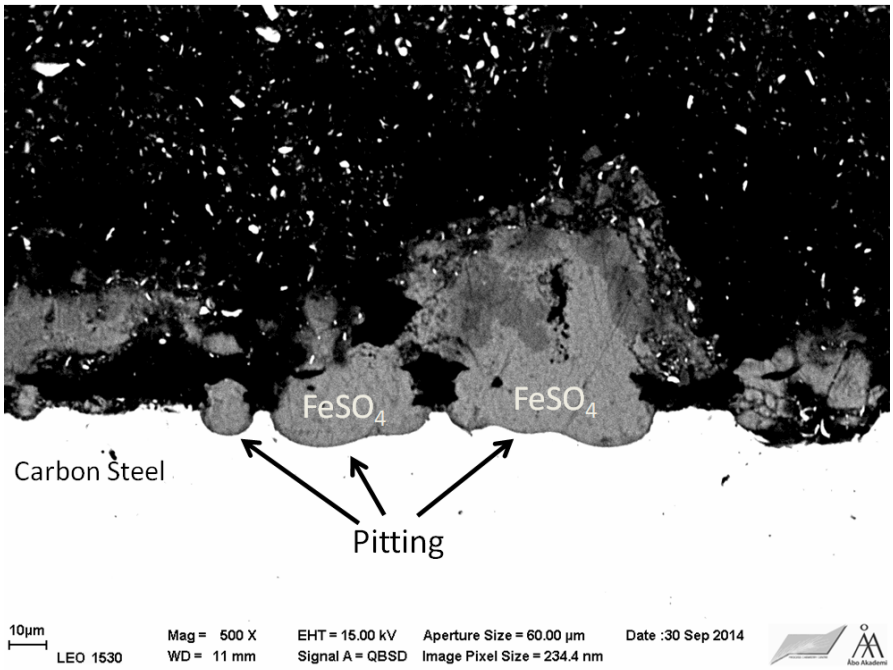

Figure 10. Cross section SEM image of the $NaHSO_4$ covered carbon steel after 4 h and 100°C experiment.

Figure 9 shows the top surface of the washed carbon steel coupons after the experiments with $NaHSO_4$ at different temperatures. After washing, some corrosion product ($FeSO_4$) remained on the surface of the carbon steel sample used in the 90°C experiment. The corrosion was more severe at lower temperatures than at higher. At the lowest temperature the whole sample was corroded, while at higher temperatures pit corrosion was only detected on the surface of the carbon steel sample. The cross section SEM images of the $NaHSO_4$ covered carbon steel samples showed increasingly deep pits at decreasing temperature; for the 90°C case the pits were around 19 µm deep, for 100°C 10 µm deep, and for 110°C the pits were approximately 4 µm deep. The pit depth for the 120°C $NaHSO_4$ corrosion sample was not measured.

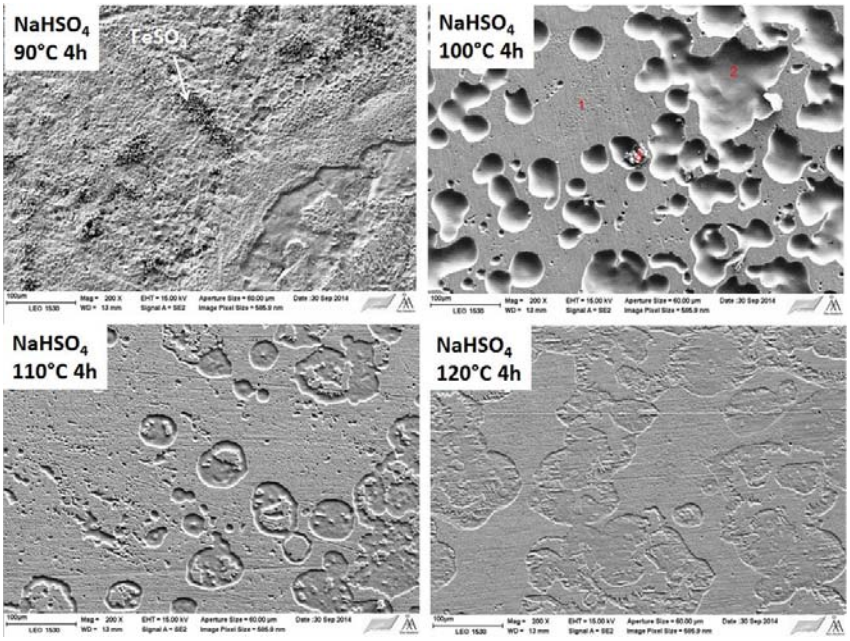

Figure 9. SEM surface image using 200x magnification with secondary electron detector of the washed $NaHSO_4$ corrosion coupons.

3.2.3.2. Experiments with Na_2SO_4 salt

Figure 10 shows the SEM cross section image of the carbon steel sample covered with Na_2SO_4 after 24h exposure at 90°C. The black in the Figure is the epoxy, lightest grey is the steel and the darkest grey is the salt crystals. There was a clear corrosion layer on top of the carbon steel which consisted of iron oxide (spot 2 in Figure 10) and had an average thickness of roughly 10 µm. Unlike with the $NaHSO_4$ samples, there is not pitting. This is characteristic of water dew point corrosion.

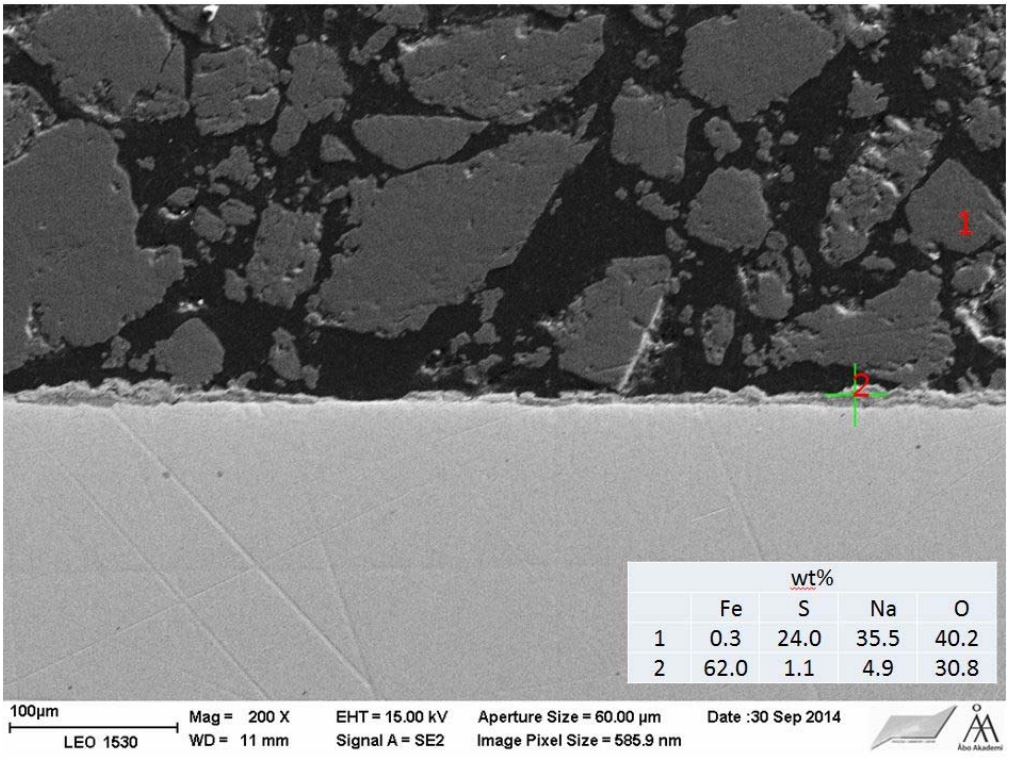

Figure 10. Cross section SEM image of the Na_2SO4 covered carbon steel after 24 h 90°C experiment.

Figure 11 shows the surface SEM images of the washed carbon steel samples after the 4 hour experiments at different temperatures. At 90 °C, there are clear areas of iron oxide on the surface. At 100 °C, there has been significantly less corrosion of the surface, but iron oxide is still detected. No visible corrosion was seen in the corrosion coupon after the 4 hour experiment at 120°C.

Figure 12 shows the SEM images of the surfaces of the washed carbon steel samples after the 24 hour experiments at different temperatures. The same trend with the carbon steel samples was noted after the 4 h experiments as after the 24h experiments. The severest corrosion was seen at 90 °C, some corrosion at 100 °C and no corrosion at 110 °C.

The fact that corrosion is seen at 100 °C, indicates that more work needs to be done to measure the humidity of deliquesce for sodium sulfate at conditions relevant to the recovery boiler.

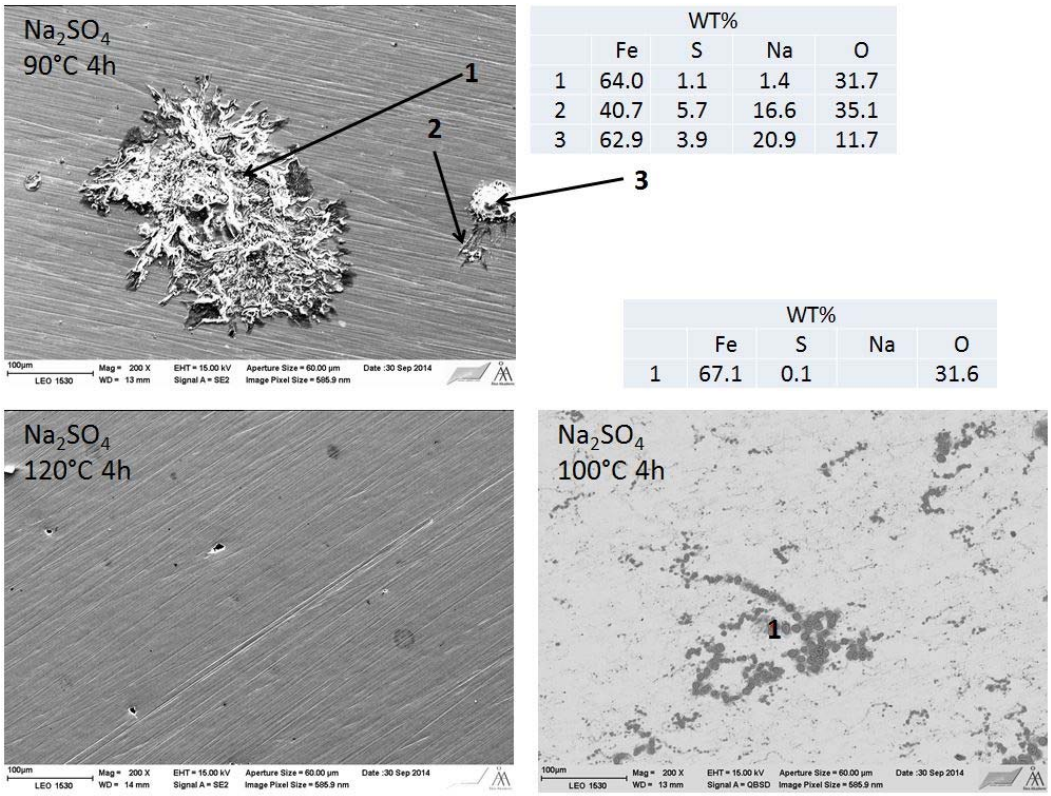

Figure 11. SEM surface image using 200x magnification of the washed Na_2SO_4 corrosion coupons after 4 hour exposure.

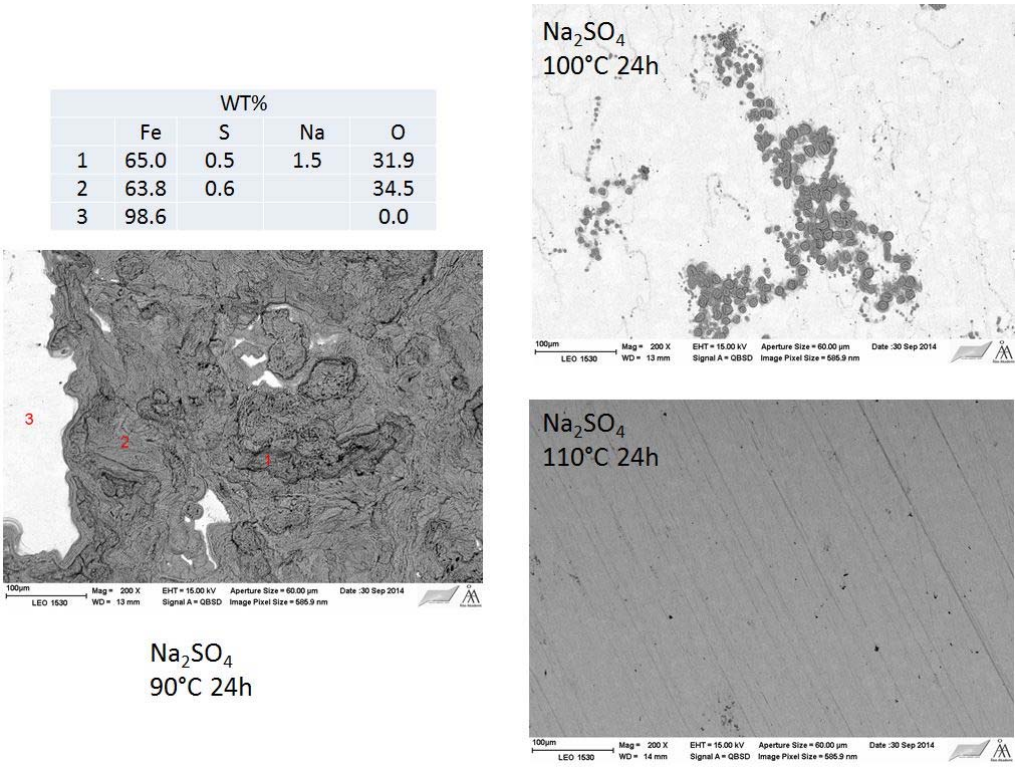

Figure 12. SEM surface image using 200x magnification of the washed Na_2SO_4 corrosion coupons after 24 hour exposure.

LIITE 6

ÅA, Understanding Low Temperature Corrosion in BL Combustion, Phase 2 – tarjous

Proposal: Understanding Low Temperature Corrosion in BL Combustion – Phase 2

Prepared by: Nikolai DeMartini; Emil Vainio; Patrik Yrjas & Mikko Hupa

3 December 2014

Historically, some low temperature corrosion has been observed in recovery boilers. However, the underlying cause has not been clearly documented. One previously held hypothesis was the presence of a sulfuric acid dew point. This was the driving force for maintaining an elevated flue gas temperature. For companies to drop their flue gas temperatures lower and consider changing the construction materials of flue gas stacks, it is important to understand the cause of low temperature corrosion. This proposal is for a DI thesis study of the influence of salt composition, humidity and temperature on low temperature corrosion.

This work would build on the first year study in which a system was built and tested with the salts Na_2SO_4 and $NaHSO_4$ at one steam concentration (60 v0l-%) and four different temperatures (90, 100, 110 and 120 °C). Those initial results have now been reported to SKY. The system worked very well; there was good stability in both steam flow and temperature and 4 hours was found to offer sufficient time to measure corrosion. In this initial study, water dew point corrosion was seen for Na_2SO_4 up to 100 °C, although the level of corrosion was very low, while corrosion was seen up to 120 °C when the salt was $NaHSO_4$. This is due to the difference in the hygroscopic nature of the two salts.

What is now needed is to test a number of salts, both alone and as mixtures at different humidities and temperatures to map out the influence of deposit chemistry, temperature and humidity on low temperature corrosion. This is an excellent topic for a DI Thesis as it is both scientifically and commercially relevant and the scope is sufficiently large to make for a quality thesis. All tests would be run with 2x2 cm carbon steel coupons. Corrosion will be measured using SEM-EDX and by measuring the weight loss after cleaning the corroded sample.

The salts suggested for testing are Na_2SO_4, Na_2CO_3, NaCl, KCl, mixtures of pure salts representative of upper furnace deposits and at least 2 deposits taken from the upper furnace of a recovery boiler. The salt mixtures will be melted, cooled and then crushed. The steam concentrations to be tested are between 20 and 80 vol-% and the temperatures will be chosen in 10 °C increments so that there is at least one temperature where there is no corrosion and one temperature where there is corrosion. These temperatures will vary according to the concentration of steam in the gas. The corrosion is expected to closely follow the humidity of deliquescence, illustrated in Figure 1 below.

The matrix will not be able to cover all salt humidity combinations, but the matrix will be sent to SKY for comments before initiating the thesis.

Deliverables.

- A DI thesis with an initial mapping of the influence of salt composition, humidity and temperature on low temperature corrosion of carbon steel
- The planned matrix will be send to SKY for comments before starting the project

The cost for the work planned here is **25 000€** + VAT.

_____ _____

Nikolai DeMartini, Senior Researcher Mikko Hupa, Professor

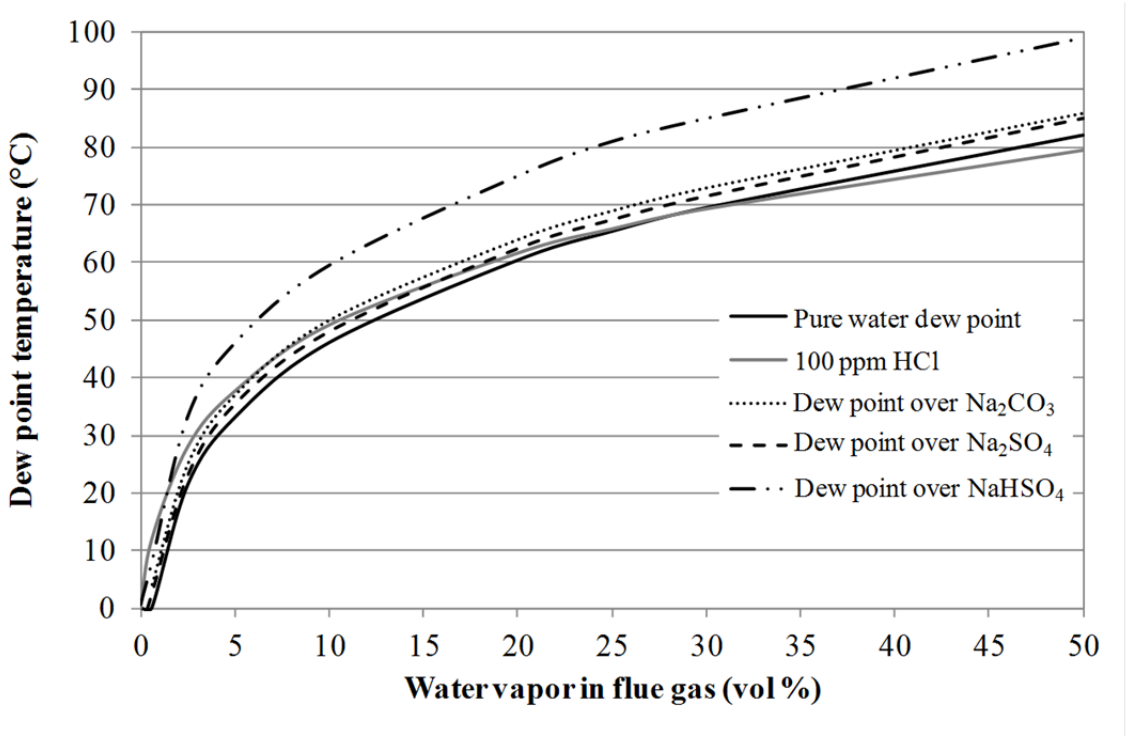

Figure 1. Pure water dew point, HCl dew point, and dew point over hygroscopic salts (Na_2CO_3, Na_2SO_4 and $NaHSO_4$) as a function of water vapor concentration.

LIITE 7

ÅA, Test apparatus to measure the temperature of deliquescence for salt mixtures relevant to recovery boilers – tarjous

Proposal: Test apparatus to measure the temperature of deliquescence for salt mixtures relevant to recovery boilers

Prepared by: Nikolai DeMartini; Emil Vainio; Patrik Yrjas & Mikko Hupa

3 December 2014

We have prepared a method to map the corrosion of carbon steel at low temperatures relevant to recovery boilers. One hypothesis is that this low temperature corrosion is related to the humidity of deliquescence of the salt deposits in recovery boilers. The humidity of deliquescence is the humidity at which a salt at a given temperature will absorb water from the gas. Hygroscopic salts will absorb water above the water dew point. This property of salts has been studied in the atmospheric sciences, but has not been studied in relationship to deposits and boilers. Therefore there are important gaps in the knowledge as it relates to boilers, both recovery and biomass fired power boilers.

This is a proposal to develop a method to measure the humidity of deliquescence of salts. The plan is to use an electrochemical cell to measure the resistance of a current passing through a salt. The temperature can be slowly increased while the humidity is kept constant. When the salt absorbs water, the resistance should decrease significantly resulting in a clear signal for the dew point temperature. This method would have added benefits for future applications. It would be possible to pulse the water in the gas so that we could measure both the absorption of water and the time it takes to dry at different temperatures. This has implications for salts that are not removed during soot blowing, but which could absorb water and thus for a short time there would be a solution in contact with the steel surface.

This capability is an important complement to the proposed study to map the influence of salt composition, temperature and humidity on low temperature corrosion. In addition to building the system, we would measure the dew point temperature at 20, 40, 60 and 80 vol-% H_2O, for $NaHSO_4$, Na_2SO_4, and a deposit collected in the upper furnace of a recovery boiler. These salts have a significantly different humidity of deliquescence, Figure 1, and would therefore be a good test of the system.

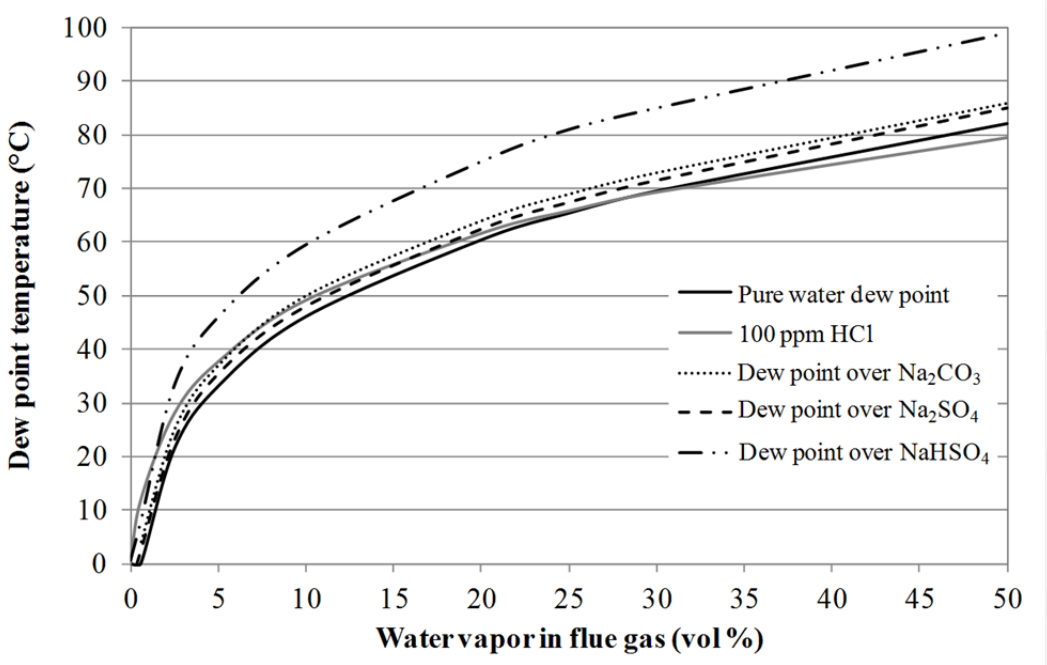

Figure 1. Pure water dew point, HCl dew point, and dew point over hygroscopic salts (Na_2CO_3, Na_2SO_4 and $NaHSO_4$) as a function of water vapor concentration.

Deliverables.

- A system to measure the humidity of deliquescence
- Measurement of the dew point temperature for $NaHSO_4$, Na_2SO_4, and a salt sample from the upper furnace of a recovery boiler at 20, 40, 60 and 80 vol-% H_2O

The cost for the work planned here is **15 000€** + VAT.

_____	_____
Nikolai DeMartini, Senior Researcher	Mikko Hupa, Professor

LIITE 8

Muiden työryhmien kuulumiset

Muut työryhmät

SUOMEN SOODAKATTILAYHDISTYS
FINNISH RECOVERY BOILER COMMITTEE

YTR: Hajukaasusuosituksen päivitys

- Päivitystyö valmis
  - Suomenkielinen suositus julkaistu 30.10.2013 -> esitelty Konemestaripäivillä 2014
  - Englanninkielisen käännös julkaistu 17.6.2014 -> esitelty ICRC 2014
- Päivitystä tekstiin tulossa Skoghallin tapauksen johdosta

YTR, BAT-dokumentin kommentointi

- Toukokuu 2014: BREFin BAT-päätelmät hyväksyttiin (adoptoitiin) IED artiklan 75 mukaisessa komiteamenettelyssä
- Syksy 2014: 26.9 komissio julkaissut toimialan BREFin yhteenvedon eri kielillä -> voimaantulo
  - Dokumentissa annetut BAT-rajat ovat lupaehtojen minimirajat, pakollisuus ei koske dokumentissa mainittuja kulutusarvoja, tarkkailuvaatimuksia eikä BAT- tekniikoita
  - Lupaehdoissa viimeistään 4 vuoden sisällä julkaisusta -> 2018
  - BAT-päästötasoista poikkeaminen vain tietyin ehdoin, esim. paikalliset ympäristöolot, maantieteellinen sijainti, tekniset ominaisuudet

Main BAT conclusions

BATs for Recovery Boilers (kraft pulping)

	Daily average		Yearly average	
SO_2 DS<75% DS 75-83%	10-70 mg/Nm³ - 6% O_2 10-50 mg/Nm³- 6% O_2		5-50 mg/Nm³- 6% O_2 5-25 mg/Nm³- 6% O_2	
Total reduced sulphur (TRS)	1-10 mg/Nm³- 6% O_2		1-5 mg/Nm³- 6% O_2	
Gaseous S (TRS-S + SO_2-S) DS<75% DS 75-83%			0,03-0,17 kgS/Adt 0,03-0,13 kgS/Adt	
NO_x Softwood Hardwood	120-200 mg/Nm³- 6% O_2		DS<75% : 0,8-1,4 – DS 75-83% : 1,0 -1,6 kg/Adt DS<75% : 0,8-1,4 – DS 75-83% : 1,0-1,7 kg/Adt	
PM	Existing	New/Refurb.	Existing	New/Refurb.
	10-40mg/Nm³- 6% O_2 Up to 50 mg/Nm3 for an ESP approaching the end of its operational life	10-25mg/Nm³- 6% O_2	0,02-0,3 kg/Adt Up to 0,4 kg/t for an ESP approaching the end of its operational life	0,02-0,2 kg/Adt

✓ BAT AEPL for effluent volume : 25-50 m³/ADT

YTR: TEKES-hanke, Polttoperäisten päästöjen ja nanohiukkasten haitallisuuden määrittäminen uudella tutkimusmenetelmällä, Itä-Suomen yliopisto

- TAVOITE:
  - Projektissa tutkittiin soodakattilan, hakevoimalaitoksen, pienpolton (tulisija ja arinakattila) päästöjä ja jälkikäsittelytekniikoiden vaikutusta ja verrattiin niitä dieselajoneuvon päästöihin sekä päästöjen fysikaalis-kemiallisia ja toksikologisia ominaisuuksia
- TILANNE:
  - Mittaukset tehty 12/2012, loppuraportti julkaistu 08/2014
  - Meesauunimittausta ei tehty -> UEF (University of Eastern Finland) omalla päätöksellä (ajanpuute / budjettikysymys)
- JOHTOPÄÄTÖKSET:
  - Mittaukset sekä pesurin että sähkösuodattimen jälkeen, näytteistä analysoitiin hiukkaspitoisuudet, kokojakaumat ja kemiallinen koostumus sekä toksikologiset vasteet.
  - Tärkeimpänä johtopäätöksenä mittauksista on soodakattilan hiukkaset eivät ole merkittävästi toksisia. Savukaasupesuri vähentää hiukkasten määrää mutta lisää toksisuutta, soodakattilaprosessi ei vaikuta tähän vaan syy on pesurissa.

SUOMEN SOODAKATTILAYHDISTYS
FINNISH RECOVERY BOILER COMMITTEE

YTR: TEKES-hanke, Polttoperäisten päästöjen ja nanohiukkasten haitallisuuden määrittäminen uudella tutkimusmenetelmällä, Itä-Suomen yliopisto

- JOHTOPÄÄTÖKSET JATKUU:
  - PAH-yhdisteiden pitoisuudet sähkösuodattimen jälkeen otetuissa näytteissä olivat UPM A 29,8 ng/mg, UPM B 22,9 ng/mg ja pesurin jälkeen hieman korkeampi 52,9 ng/mg.
  - Luvut ovat hieman suuremmat kuin esimerkiksi pellettitakan poltossa (~5 ng/mg), mutta mutta huomattavasti pienemmät kuin esimerkiksi puutakan (18 000 ng/mg) ja raskaan polttoöljyn (10 000 ng/mg) poltossa.
  - Vaikka savukaasupesuri vähensi hiukkaspäästön määrää, oli se massayksikköä kohti toksisempaa kuin pääosin alkalisuoloista koostuva hiukkaspäästö sähkösuodattimen jälkeen.
  - On mahdollista että suurempi toksisuus aiheutuu maaperä- tai bakteeriperäisten komponenttien joutumisesta hiukkasmassaan esimerkiksi pesurissa käytetyn jokiveden mukana tai pesurin vesikierrossa syntyvästä bakteerikontaminaatiosta. -> teoria on vielä varmistamatta.
- JATKOTUTKIMUS
  - Tarjous saatu kahden kattilan/meesauunin mittaamisesta, kustannus ~100 000 EUR +ALV

YTR: Soodakattilan käynnistys-, pysäytys- ja häiriöjaksojen määrittely

TAVOITE

- Dokumentti jossa määritellään soodakattilan käynnistys-, pysäytys ja häiriöjaksot.
- Uuden BAT/BREF dokumentin päästöarvot koskevat vain normaaliajoa -> jaksojen määrittely tulee ajankohtaiseksi ympäristölupakierroksella -> hyvä muodostaa yhteinen käsitys
- Direktiivin 2010/75/EU III luvun soveltamisalaan kuuluvien polttolaitosten käynnistys- ja pysäytysjaksot on määritelty

• TILANNE

- Kysely tehtaille lähetty 1.9.2014 -> Yhteenveto tekeillä vastauksista

SUOMEN SOODAKATTILAYHDISTYS
FINNISH RECOVERY BOILER COMMITTEE

Projekti	KTR: Vauriot
Tavoite	Vaurioinformaation keräys, analysointi ja tiedon levittäminen. Tarkoituksena olisi oppia muiden vaurioista ja välttää niitä.
Tekijä	KTR
Tilanne / Aikataulu	Edellisen kokouksen jälkeen raportoidut vauriot: • 8/2014 MF, Kemi – venttiilivuoto syöttövesiputken tyhjennyslinjassa • 9/2014 MF, Kemi – primääri-ilmaaukkojen ohiheittoputkissa piikkausjälkiä • 10/2014 SE Oulu – LHK järjestelmän vesitykset tukossa • 11/2014 MF Äänekoski – Vuoto höyrynjäähdyttimessä • 12/2014 MF Äänekoski – Vuoto konvektio-osassa • 13/2014 MF Äänekoski – Vuoto konvektio-osassa
Johtopäätökset Toimenpiteet	

Projekti	KTR: Suojaussuosituksen päivitys
Tavoite	Päivittää vuonna 1997 tehty soodakattilan suojaussuositus vastaamaan nykytilannetta ja -tarvetta
Tekijä	KTR/Inspecta/VTT
Kustannus (bud. / tot.)	5000 eur / 780 eur (+alv)
Tilanne / Aikataulu	Valmet päivittänyt päällehitsaus-osuuden standardit nykypäivään. Puuttuu vastaukset kysymyksiin: • Päällehitsauksen edellytykset • Mitä asioita tulisi ottaa huomioon
Johtopäätökset Toimenpiteet	Seuraavassa KTR kokouksessa 28.1 SHK:n vastaavan ohjeen läpikäynti -> ohjetta ei vielä SHK:n toimesta julkaistu

SUOMEN SOODAKATTILAYHDISTYS
FINNISH RECOVERY BOILER COMMITTEE

Projekti	ATR: Valvomohälytykset – hyvät käytännöt hälytysten laatimiseksi
Tavoite	Laatia ohje johon kerätään hyvät käytännöt hälytysten laatimiseksi ja jossa kuvataan menetelmä turhien hälytysten karsimiseksi.
Tekijä	ATR
Kustannus (bud. / tot.)	- eur (+alv)
Tilanne / Aikataulu	Sihteeri / Taneli Mutikainen tekevät yhteenvedon olemassa olevista oppaista seuraavaan ATR:n kokoukseen 12.3.2015
Johtopäätökset Toimenpiteet	

SUOMEN SOODAKATTILAYHDISTYS
FINNISH RECOVERY BOILER COMMITTEE

Projekti	OTR: Konemestaripäivä-seminaari
Tavoite	
Tekijä	SKY
Kustannus (bud. / tot.)	25 000 eur (+alv)
Pääsymaksut (bud. / tot.)	25 000 eur (+alv)
Tilanne / aikataulu	28-29.1.2015 Cumulus Rauma sekä vierailu Metsä Fibren tehtaalle.
Johtopäätökset	Alustava ohjelma
Toimenpiteet	Paneelikeskustelu suovan erottumisesta?
Päätökset	

SUOMEN SOODAKATTILAYHDISTYS
FINNISH RECOVERY BOILER COMMITTEE

Projekti	OTR: Vuosikokous
Tavoite	
Tekijä	SKY
Kustannus (bud. / tot.)	12 000 eur (+alv)
Tilanne / aikataulu	Kokouspäivä 23.4.2015 Helsingissä
Johtopäätökset	
Toimenpiteet	

SKY Historiikki

- Risto Valkeapää on aloittanut projektin maaliskuun 2014 alussa. Haastatteluihin ja arkistomateriaaliin perustuva kovakantinen kirja valmis .
  - Kevät-Kesä Tehdasvierailut,Varkaus siirtyi syksyyn
  - Kevät-Kesä Viirihenkilöiden haastatteluja
  - Elokuu: arkistokäynnit UPM Valkeakoski, Elinkeinoelämän keskusarkisto, haastattelujen puhtaaksikirjoitusta.
  - Syyskuu: haastattelujen täydennystä, puhtaaksikirjoitusta ja tarkistusta.
  - Lokakuu 2014 haastattelujen puhtaaksikirjoitusta, täydennystä ja tarkistuksia. Esitelmä soodakattilapäiville.
  - Marraskuu/joulukuu2014: kirjatekstien viimeistelyä ja taittoa
  - Tammi-helmikuu 2015: kommentit ja painoon valmistelua

SUOMEN SOODAKATTILAYHDISTYS
FINNISH RECOVERY BOILER COMMITTEE

Konemestaripäivä 2015

- Raumalla, Cumulus-hotellissa 28.- 29.1.2015
- Tehdasvierailu Metsä Fibren Rauman tehtaalle
- Ohjelma: http://www.soodakattilayhdistys.fi/toiminta6.html